Electronic Journal of Applied Multivariate Statistics *Volume 9 · 2018*

Contents

Article	1	**The climate sensitivity of water quality in the Pacific Northwest: Linking anticipated shifts in hydrologic regime to riverine nitrogen sources in Puget Sound watersheds** Elizabeth Elmstrom
Article	11	**The influence of interference competition and foraging conditions on partial prey consumption** Alex Lincoln
Article	24	**Effects of parental low pH exposure on gonadal and larval gene expression in the Olympia oyster (Ostrea lurida)** Laura H. Spencer
Article	40	**Characterization of Pacific oyster *Crassostrea gigas* proteomic response to natural environmental differences** Yaamini R. Venkataraman
Article	51	**Regional Steller sea lion (Eumetopias jubatus) population structure varies with oceanographic conditions on rookeries and haul-outs in Alaska** Amanda Warlick

Electronic Journal of Applied Multivariate Statistics
Volume 9, 2018

Article

The climate sensitivity of water quality in the Pacific Northwest: Linking anticipated shifts in hydrologic regime to riverine nitrogen sources in Puget Sound watersheds

Elizabeth Elmstrom
School of Aquatic and Fishery Sciences, University of Washington
E-mail: elmstrom@uw.edu

Received March 2019; accepted in revised form April 2019; published June 2019

Abstract

Regional climate is the primary determinant of in-stream hydrologic regime in the Pacific Northwest. This, in turn, governs multiple critical ecosystem functions, such as ecosystem productivity through habitation formation processes and the supply and transfer of nutrients. Sources of nitrogen (N) to rivers in the Puget Sound watershed of the Northwestern U.S.A. are affected by hydrologic regime, as well as a variety of other land-use characteristics and physical drivers at both regional and local scales. However, little is known of the interactions between drivers and how this interaction relates to water quality. We used principal component regression, a multivariate technique incorporating dimensionality reduction, to quantify the influence of these drivers on riverine N source (using nitrate triple isotopes), synthesizing fine-scale land cover data, local flow classification, and two highly contrasting hydrologic water years. We found that relative sources of N shift along gradients of watershed land-use, and this shift can also be visualized in riverine flow classification. High variation in isotopic signatures was seen between years of drought and years representing normal hydrologic conditions. Our results suggest that anticipated changes to hydrologic flow class under future climate change may dictate the seasonality and source of riverine N inputs to the Puget Sound.

Introduction

The productivity of freshwater and marine environments is largely determined by the magnitude of external nitrogen (N) loads delivered to rivers and receiving coastal waters (Howarth 1988, Valiela 2006, Valiela et al. 2016). The role of N in aquatic ecosystem function is multifaceted. N is a critical nutrient for primary and secondary productivity in streams and estuaries (Nixon et al 1986). However, in excess, N becomes a regulated pollutant, driving eutrophication, declines in dissolved oxygen, and increasing ocean acidification (Mohamedali et al. 2011, Washington State Blue Ribbon Panel on Ocean Acidification 2012). Atmospheric, fertilizer, and wastewater sources contribute to riverine and estuarine N loads, and the relative contributions of each source shift across watersheds of contrasting land use and physical characteristics (Valiela et al 2016). While the impacts of excess N on aquatic ecosystems have been researched for decades, anthropogenic sources of N continue to have significant environmental impacts on freshwater and coastal ecosystems (Rabalais et al. 2002, Galloway et al. 2003, Galloway et al. 2008, Elser et al. 2009, Holtgrieve et al. 2011).

In the case of the Puget Sound in Washington state, riverine N loads represent a significant source of N to the estuary, as they deliver both anthropogenic and natural sources from the watershed to the marine environment (Mohamedali et al. 2011). Surface water nitrate (NO_3) concentrations have increased by approximately 15% per decade since 1999 in the Puget Sound (Mohamedali et al. 2011, Banas et al. 2015). Riverine inputs of N appear to be exacerbating ocean acidification. In some locations within the Puget Sound, riverine N

inputs are thought to be creating localized hypoxia to levels not previous observed (Washington State Blue Ribbon Panel on Ocean Acidification 2012). As such, N loads to rivers is included in the composite set of ecosystem health indicators for the Puget Sound and thought to be one of several factors potentially limiting the recovery of ESA listed Puget Sound salmon (Wong and Rylko 2014). At present, there is no direct information connecting N loading from Puget Sound rivers to specific watershed sources. Increasing concentrations of NO_3 in the Puget Sound highlight the need to quantify the sources of riverine N loads and to understand the underlying watershed characteristics that drive N contributions from river to coastal waters.

Previous research on sources of N to rivers and the Puget Sound has focused on watershed and landscape characteristics as the driving factors of N loads (e.g., land-use change and non-point sources, Barnes et al. 2008). The role of watershed hydrologic conditions and climate have received a fair amount of attention, but this has typically been in the context of individual storms or short-term events such as spring freshets (e.g., Brooks and Williams 1999, Divers et al. 2014). Relatively little attention has been paid to hydrologic classification and/or recurrent drought or floods, yet understanding N sources in the context of hydrology in the Pacific Northwest is critical to anticipate future effects of climate change on water quality. In the Puget Sound, watersheds can be classified broadly into three categories by flow source and hydrograph shape (Beechie et al. 2006, Reidy Liermann et al. 2012, Mauger et al. 2015). Rain-dominated (RD) rivers receive little or no input from snowmelt, and peak in discharge during the rainy season, usually between October and February. Snow-dominated (SD) rivers instead see peak flow during spring snowmelt, often in April, May, or June. Between these extremes lies a third class of rain-and-snow-driven (RS) rivers, which have appreciable peaks at both times (Reidy Liermann et al. 2012). Contrasting responses of these different hydrologic river types to altered precipitation are likely to impact relative contributions of N from different sources and seasonality of N loads due to changing peak flows. With little existing information on the sources of N in Puget Sound rivers, understanding how both *watershed characteristics* and projected *hydroclimatic conditions* will affect riverine N sources is essential for the management of freshwater and estuarine ecosystems.

We sought to determine how sources of NO_3 change seasonally and during extreme drought across rivers of varying watershed characteristics and hydrologic type (snow-fed vs. rain-snow-fed vs. rain-fed) using the triple isotopes of NO_3 ($\delta^{15}N$, $\delta^{17}O$, and $\delta^{18}O$) as an indicator of N source. Variations in the ratio of 15N to 14N ($\delta^{15}N$) and 18O to 16O ($\delta^{18}O$) of NO_3 can provide information on physical or landscape controls of non-atmospheric N sources. For example, values of $\delta^{15}N$ are relatively depleted in ammonia-based fertilizers compared to atmospheric or forest soil N sources (i.e., N derived from biological N fixation). Alternatively, $\delta^{15}N$ signatures of sources of N from manure and septic system are generally enriched. $\delta^{18}O$ values are informative for tracing NO_3 based fertilizer as it is usually enriched relative to natural sources or ammonia-based fertilizer (Kendall et al. 2007). Together, $\delta^{17}O$ and $\delta^{18}O$ are informative for atmospheric N budgets. This is due to a consistent relationship in all oxygen bearing terrestrial materials where $\delta^{17}O$ tracks $\delta^{18}O$ by a factor of 0.52. NO_3 oxidized in the atmosphere, however, incorporates atmospheric O which is highly enriched in 17O. Thus, samples with atmospheric NO_3 will fall off this line proportionally to the amount of atmospheric N present (Kendall et al. 2007). This offset (termed $\Delta^{17}O$) provides an unambiguous tracer of atmospheric N. Looking at $\Delta^{17}O$ across rivers with varying elevation and presence of snowpack/glaciers, and between drought and normal years, will identify and quantify snow pack and glaciers as an N source to these systems.

The initial focus of this study was to identify watershed features that correlate with variation in sensitivity, i.e. coupling between climatic forces and river N sources, and thus to provide a more nuanced basis for predicting impacts on aquatic biodiversity and fishery health. The expectation is that watershed physical features (e.g., slope, elevation) and land-use patterns (e.g., % forest or agriculture) would control the isotopic composition of river NO_3, and this effect will be variable across season and hydrologic year. From this it will likely be possible to infer the most probable sources of N to these systems and their relative influence. We hypothesized that rivers with relatively enriched $\delta^{15}N$, and $\delta^{18}O$ of NO_3 will be strongly associated with human-modified land use at the urban fringe. Conversely, relatively depleted signatures will be associated with forest landscapes. Patterns in N sources will be much more prominent in the normal water year compared to the drought year, and the relative

effect will be pronounced different across season. We additionally anticipated that the amount of atmospheric N in Puget Sound rivers, both proportionally and as a mass flux, would be greater in river systems with higher watershed elevation, snow-driven hydrologies, and presence of glaciers, indicating a link between watershed ice and snow cover and supply of atmospheric Nr to rivers.

Methods

Water and climate data

Study sites include 23 different river sites in Puget Sound watersheds of varying landscape and watershed characteristics and hydrologic regime. These sites represent 19 separate watersheds across 9 counties, and range from 4 to 775 m in elevation. River order (Strahler number) at the mouth ranges from 5 to 8. Monthly water samples for isotopes were obtained for each site by the Washington Department of Ecology's River and Stream Water Quality Monitoring program (von Prause 2017). By chance, the two years sampled covered an exceptionally large difference in regional precipitation and hydrologic conditions compared to historical records, with the 2014-15 water year as a record drought and the 2015-16 water year representative of average conditions. Landscape predictors were compiled individually for each of the watersheds corresponding to our 24 river sites, using the EPA's StreamCat data library and the National Hydrography dataset as described in Vlah and Holtgrieve (submitted). The hydrologic class of each river site (i.e. hydrologic regime) was assigned based on the flow classification of Washington rivers done by Reidy Liermann et al. (2012).

Stable isotopic analysis

$\delta^{15}N$, $\delta^{18}O$, and $\delta\ ^{17}O$ values of NO_3 were determined via coupled gas chromatography, pyrolysis, and mass spectrometry using the bacterial denitrifier method (Sigman et al. 2001) at the University of Washington's Δ*IsoLab. Briefly, NO_3 and NO_2 are converted quantitatively to N_2O by a strain of bacterial denitrifier that lacks nitrous oxide reductase activity, and the product N_2O is extracted, purified, and analyzed by continuous flow isotope ratio mass spectrometry. Isotope measurements are reported in the delta notation in per mil (‰), relative to atmospheric N2 (AIR) for $\delta^{15}N$ and VSMOW for $\delta^{18}O$. Variations in isotope ratios are expressed using the delta notation as follows:

$\delta^{15}N$, $\delta^{17}O$, and $\delta\ ^{18}O$ (‰) = [(Rsample – Rstandard)-1] × 1000,

where R is 15N/14N, 17O/16O or 18O/16O.

$\Delta^{17}O$ was quantified using the $\delta^{17}O$ and $\delta^{18}O$ values. $\delta^{17}O$ tracks $\delta^{18}O$ by a factor of 0.52, thus giving the following equation:

$$\Delta^{17}O = \delta^{17}O - 0.52 * \delta^{18}O$$

Four international reference materials, USGS32: $\delta^{15}N$ = 180‰, $\delta^{18}O$ = 25.4‰, USGS34: $\delta^{15}N$ = −1.8‰, $\delta^{18}O$ = −27.9‰, USGS35: $\delta^{15}N$ = 2.7‰, $\delta^{18}O$ = −56.8‰ and IAEA-N3: $\delta^{15}N$ = +4.7‰, $\delta^{18}O$ = +25.6‰ (Sigman et al. 2001) were used. Blanks consisted of vials that had no injected water samples or microbes. Samples were analyzed for stable isotopes using a GasBench II coupled to a continuous flow isotope ratio mass spectrometer (IRMS, Thermo Delta V Advantage). Analytical precision based on replicate analysis of isotopically homogeneous NIST Standard reference materials was ±0.1-0.2‰ for $\delta^{15}N$, $\delta^{17}O$, and $\delta^{18}O$ measurements.

Statistics and model fitting

Principal component analysis

Using a combination of multivariate statistics and linear regression models, we sought to explore the associations between the sources of NO_3 and broad-scale watershed characteristics and hydroclimate. First, to summarize dominant gradients of variability among stream watershed characteristics, principal component analysis (PCA; Pearson, 1901) was used to reduce the dimensionality of landscape attributes used as predictors in the consequent regressions. Variables included elevation (m), total area (km2), soil permeability (cm hr-1), water table depth (cm), bedrock depth (cm), Base Flow Index (BFI; %), runoff (mm mo-1), percent perennial ice and snow coverage (National Land Cover Database [NLDC] 2011), riparian population density (people km-2 within 100m of streams; 2010 census), riparian road density (km km-2; 2010 census), and percent riparian urban land (NLCD 2011). Monitoring site elevation (m) was also included. Finally, we calculated area above 1000 m (as % watershed area), mean slope (% rise), and mean aspect (degree from true north) by delineating and summarizing watersheds from a digital elevation model in ArcMap v. 10.4 (ESRI 2016). Data constrained to irregular, restricted ranges were scaled to [0-1] and arcsine-square root transformed, along with all proportional

data (the logit transform was avoided to prevent generation of infinite values.). All multivariate data analyses were conducted using the *vegan* (Oksanen et al. 2010) and *biostats* (McGarigal 2009) packages in the program R (R Development Core Team, 2011).

Principal component regression

To evaluate how variation among NO_3 triple isotopes co-varied with watershed characteristics, seasonality and hydrologic conditions of drought, we applied principal component regression analyses to the isotopic dataset. River site scores on principal component axes 1 and 2 were regressed (using ordinary least-squares linear regression) against each of the NO_3 triple isotopes ($\delta^{15}N$, $\delta^{18}O$, and $\Delta\ ^{17}O$). Additional fixed effects of season and year (normal vs. drought) were included in each of the regression models to assess the effects of drought and projections of altered hydroclimate regimes on relative N source contributions. This led us to create three different regression models with raw isotopic $\delta^{15}N$, $\delta^{18}O$, and $\Delta^{17}O$ data as the response variable for each. We then used Akaike's information criterion (AIC; Burnham and Anderson, 2002) to compare correlations with the NO_3 triple isotopes against three linear models according to a global model equation: $y = \beta0 + \beta1 * X1 + \beta2 * X2 + \beta3 * X3 + \beta4 * X4$, where $\beta0$ = the intercept, $\beta1$, $\beta2$, $\beta3$, and $\beta4$ = the slopes, and ε = the residual error.

(1) $\delta^{15}N \sim \beta0 + \beta1*PC1 + \beta2*PC2 + \beta3*Season + \beta4*WaterYear + \varepsilon$

(2) $\delta^{18}O \sim \beta0 + \beta1*PC1 + \beta2*PC2 + \beta3*Season + \beta4*WaterYear + \varepsilon$

(3) $\Delta^{17}O \sim \beta0 + \beta1*PC1 + \beta2*PC2 + \beta3*Season + \beta4*WaterYear + \varepsilon$

We also plotted and regressed the PC1 scores against each NO3 triple isotope dataset to visualize how variation among $\delta^{15}N$, $\delta^{18}O$, and $\Delta\ ^{17}O$ signatures was explained by composite variation in watershed land-use characteristics, hydrologic regime, and drought (Figure 2).

Variable contributions of PCs to principal component regressions

To strengthen the interpretation of each principal component axis (PC1 and PC2) in our principal component regression (PRC), we quantified the relative variable contribution of each landscape predictor following the methods described in Olden and Peres-Neto (2003). This method moves past the qualitative interpretation of PC1 and PC2 by quantifying the different contributions of the explanatory variables (landscape predictors) to the principal components and, in turn, the relative contribution of each predictor in the principal component regression model. The squared eigenvectors of the PCA represent the proportion of the variance contributed by each variable to each principal component. To quantify the relative variable contribution of each landscape predictor described by the original PCA analysis, we then multiplied the squared eigenvectors by the squared semi-partial correlation coefficients for the principal components. The row sums of the first two principal components used in the PCR, therefore, represent the relative total amount of variation explained by each of the original explanatory variables (Olden and Peres-Neto 2003).

Results

River sites in this study correspond to a wide range of watershed land-use and physical characteristics, ranging from low-gradient urban or agricultural areas to steeper gradient forested areas at higher elevations. PCA was initially used to determine which exploratory watershed characteristics or variables explained the greatest amount of variation in the data set (Table 1). The first two axes of the PCA summarized a large proportion (57.6%) of the variance in watershed characteristics (PC1 = 40.1%, PC2 = 17.5%). Both axes were found to be statistically significant using a Monte Carlo randomization test (PC1, p=0.00, PC2, p=0.008). The first principal component axis primarily captured differences among river sites in the dominant landcover and land-use characteristics of the watershed, representing a range from high population, urban or agricultural sites to more forested, natural sites at higher elevations. The second principal component axis was driven by differences in sites characterized by runoff, baseflow, and other features that vary along elevational gradients, including snow (% area > 1000 m), ice and watershed slope and watershed elevation itself. The three hydrologic regimes of rivers in western Washington were separated in ordination space by watershed characteristics. Plotting the flow classification from Reidy-Liermann et al. in Figure 1 allowed us to visualize hydrologic regime of watershed characteristics in ordination space. River sites classified into rain-driven hydrologic regime were described by low elevations, high population densities and large urban and agricultural areas by the PCA. River sites classified into rain-snow or snow-driven hydrologic regime shifted to the right along the

first principal component axis, representing forested areas with higher elevations and larger areas of snow and ice cover.

Table 1. *Structure correlations of the variables from the principal component analysis.*

	Variance explained (%)	Environmental variable	r
PC axis 1	40.1%	Site elevation	0.49
		Watershed elevation	0.73
		Soil permeability	-0.79
		Aspect	-0.46
		Riparian population density	-0.87
		Impervious surface	-0.96
		% Urban	-0.93
		% Natural vegetation	0.95
		% Agriculture	-0.65
		% Perennial ice and snow	0.60
PC axis 2	17.5%	Watershed elevation	-0.51
		% area over 1000 m	-0.64
		Slope	-0.60
		Watershed runoff	0.56
		BFI	-0.85

As expected, principal component regression analysis showed the effect of human-modified land use vs. natural vegetation or forested areas on the signatures of $\delta^{15}N$ in rivers. The best model identified included the effects of PC1, season, and year, with an AIC of 2817, a delta AIC of 0 and a model weight of 0.68. However, considering the statistical significance of PC2 in the original PCA, we opted to move forward with the second-best model, with an AIC of 2819, a delta AIC of 1.55, and a model weight of 0.3. This was our original global model (1) described above. The relative effect sizes of the potential drivers of $\delta^{15}N$ isotope variation are included in Table 2. To understand best these parameter estimates, it is important to note that the intercept represents the fall season and the 2015 drought year. The relative effect of season varied, with the largest effect seen in the spring ($p = 0.0$) and the summer ($p = 0.0$). PC1 had a statistically significant ($p = 0.0002$), negative effect on the signatures of $\delta^{15}N$, whereas PC2 was not a significant predictor. The top panel of Figure 2 shows a simple regression of $\delta^{15}N$ and PC1, where we can see how $\delta^{15}N$ varies along the PC1 axis. The relative effect of drought on $\delta^{15}N$ signatures is mostly seen in rain and rain-snow driven systems that are characterized by human-modified land-use and lower elevations.

Figure 2. *Nitrate triple isotopes ($\delta^{15}N$, $\delta^{18}O$, and $\Delta^{17}O$) regressed again the PC1 axis ($p = 0.0001$, 0.000, and 0.000 respectively). Black points represent rain-driven hydrologic regime. Grey points represent rain-snow-driven hydrologic regime. White points represent snow-driven hydrologic regime. Circles represent the 2015 drought. Triangles represent normal hydrologic conditions.*

Figure 1. *Ordination of landscape predictors by principal coordinates analysis. Length and direction of arrows are proportional to loading of landscape predictors onto each principal axis of their variation. "Imperv." refers to artificial impervious surfaces, "Soil perm." refers to soil permeability, and "% area > 1000 m" is a proxy for snow load. Black points represent rain-driven hydrologic regime. Grey points represent rain-snow-driven hydrologic regime. White points represent snow-driven hydrologic regime.*

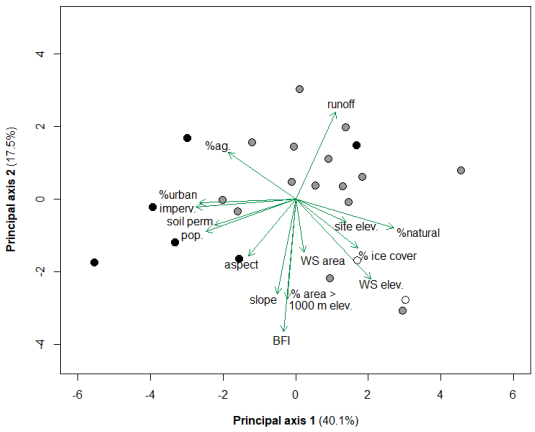

The relative contribution of each explanatory variable is visualized in Figure 3. Land-use characteristics explained the largest variance in the principal components, with elevation falling

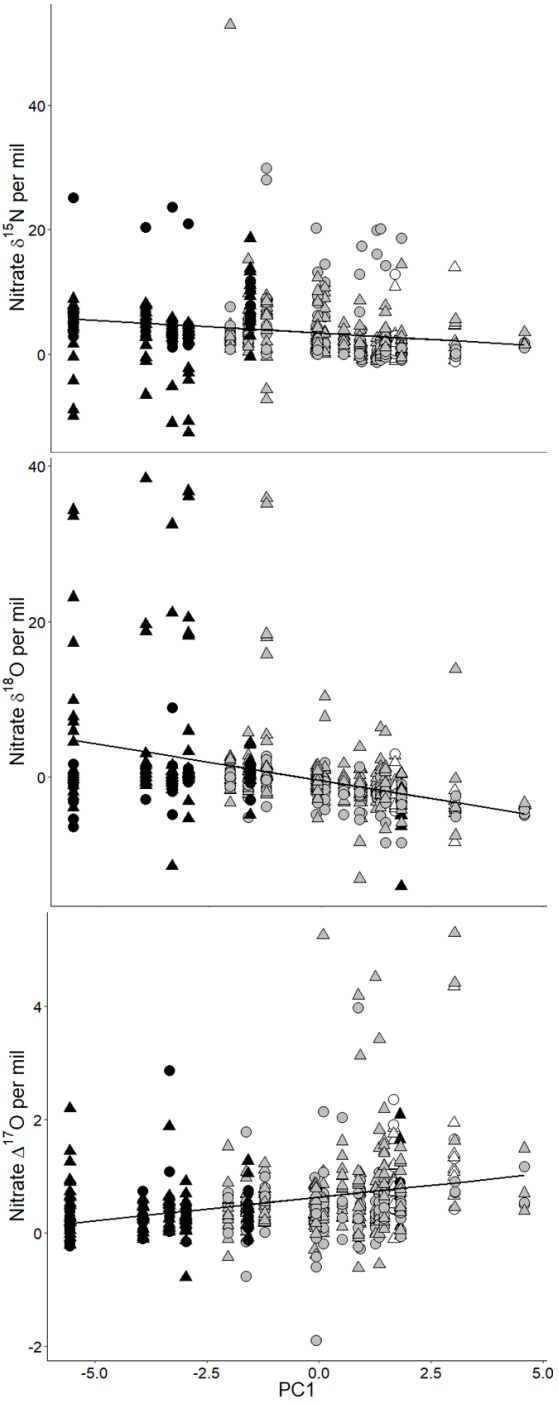

the principal components, with elevation closely behind. The normal hydrologic year had a negative relative effect on $\delta^{15}N$ signatures, and we can visualize the difference between years in Figure 2, where we see lower $\delta^{15}N$ signatures during the 2016 water year and higher signatures during the 2015 drought.

Principal component regression analysis highlighted the additional effect of human-modified land use on the signatures of $\delta^{18}O$ in rivers. The top model identified via AIC was the original global model (2) described above, with an AIC of 3017, a delta AIC of 0, and a model weight of 0.8. Here, the relative effect of season was found to be largest in the spring and the fall. Differences between years were again found to be significant, with the normal hydrologic year having a positive effect on $\delta^{18}O$ ($p = 0.0005$), and drought exhibiting a negative effect ($p = 0.001$). PC1 had a statistically significant, negative relative effect on the signatures of $\delta^{18}O$, and PC2 showed a significant, positive relative effect ($p = 0.0$, $p = 0.025$, respectively). In the middle panel of Figure 2 we can see how $\delta^{18}O$, like signatures of $\delta^{15}N$, vary along the PC1 axis. The relative effect of drought on $\delta^{18}O$ signatures is mostly seen in rain and rain-snow driven systems that are characterized by human-modified land-use and lower elevations. The relative contribution of each explanatory variable is visualized in Figure 3. Land-use characteristics explained the largest variance in the principal components, with elevation again falling closely behind. As stated above, the normal hydrologic year had a positive effect on $\delta^{15}N$ signatures and we can visualize the difference between years in Figure 2, where $\delta^{18}O$ signatures are clearly more enriched during the 2016 water year and more depleted during the 2015 drought.

We see similarly interesting trends in the $\Delta^{17}O$ values of NO_3 in the final principal component regression model. This analysis successfully depicts the variation in $\Delta^{17}O$ value along *both* an elevational and land-use gradient. The top model identified via AIC was again the original global model (3) described above, with an AIC of 968, a delta AIC of 0, and a model weight of 0.8. The largest relative effect of season was found in the summer, but all seasons

Table 2. *Results from the principal component regression analysis for each nitrate triple isotope ($\delta^{15}N$, $\delta^{18}O$, and $\Delta^{17}O$). Note that the semi-partial r^2 are squared correlations between each principal component and the dependent variable.*

	Variable	Semi-partial r^2	β	t	P
$\delta^{15}N$	Intercept	--	2.4	3.9	0.0001***
	PC1	0.03	-0.4	-3.7	0.0002***
	PC2	0.0009	0.1	0.7	0.5037
	Year (Wet)	--	-1.7	-3.5	0.0005***
	Season (Spring)	--	4.2	5.1	0.0000***
	Season (Summer)	--	3.6	5.0	0.0000***
	Season (Winter)	--	0.7	1.0	0.3355
$\delta^{18}O$	Intercept	--	-2.2	-3.3	0.0011**
	PC1	0.1	-0.9	-8.6	0.0000***
	PC2	0.01	0.4	2.2	0.0255*
	Year (Wet)	--	2.7	5.0	0.0000***
	Season (Spring)	--	1.9	2.0	0.0419*
	Season (Summer)	--	-0.8	-1.1	0.2931
	Season (Winter)	--	0.01	0.02	0.9859
$\Delta^{17}O$	Intercept	--	0.3	3.5	0.0005***
	PC1	0.09	0.1	7.1	0.0000***
	PC2	0.03	-0.1	-3.9	0.0001***
	Year (Wet)	--	0.1	2.3	0.0244*
	Season (Spring)	--	0.2	2.2	0.0260*
	Season (Summer)	--	0.5	5.4	0.0000***
	Season (Winter)	--	0.2	2.5	0.0114*

showed a statistically significant relative effect (spring p = 0.03, summer p = 0.0, winter p = 0.01, fall p = 0.0005). Differences between years were again found to be significant, and these differences can be seen to vary among flow classes in Figure 2. PC1 has a statistically significant (p = 0.0), positive relative effect on the signatures of $\Delta^{17}O$, and PC2 showed a significant (p = 0.0001), negative relative effect. In the bottom panel of Figure 2 we can see how $\Delta^{17}O$, like signatures of $\delta^{15}N$ and $\delta^{18}O$, varies along the PC1 axis, yet trended in a different direction. The relative effect of drought on $\Delta^{17}O$ signatures is seen in largely rain-snow and snow driven systems that are characterized by steep gradients, high elevations and greater influence of ice and snow. $\Delta^{17}O$ signatures are clearly higher during the 2016 water year and lower during the 2015 drought, particularly in systems influenced by cooler precipitation. Figure 3 shows that while again land-use characteristics explained the largest variance in the principal components, elevational characteristics slightly rise in their % contribution to the variance of the final model.

Discussion

We found the isotopic composition of NO_3 to vary with increasing human-derived impacts on the landscape, and the response of riverine N sources to differ with physical watershed characteristics and river hydrologic type. $\delta^{15}N$ and $\delta^{18}O$ signatures were positively related to higher human population density impervious surfaces, and agricultural areas, while $\Delta^{17}O$ signatures reflected the influence of cool precipitation in higher elevation systems. These results suggest that differences in land-use, physical, and geomorphic watershed features of the individual rivers in the Puget Sound watersheds are associated with variation in sources of N from both the land and the atmosphere. This variation highlights the different watershed characteristics that drive human-derived N sources and consequent riverine water quality. The association between watershed features of N sources provide a powerful basis to understand how water quality and N source differ with hydrologic regimes. Patterns in N isotopic variation during normal hydrologic conditions and a year of drought reveals additional insight into how water quality in each of these hydrologic regimes may be affected individually by future hydroclimatic shifts.

Figure 3. *Percent variation in nitrate triple isotopes ($\delta^{15}N$, $\delta^{18}O$, and $\Delta^{17}O$) explained by each of the original landscape predictors, based on the collection contribution to the first two principal components used in the PCR model.*

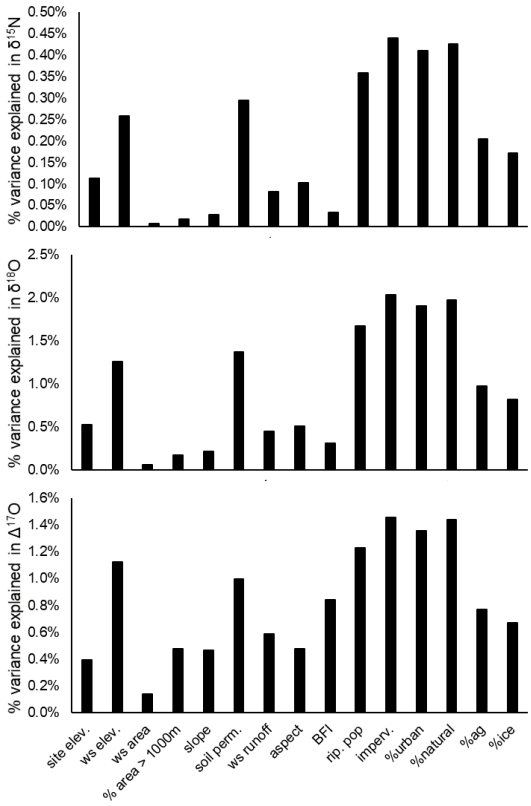

Given the development patterns of the Puget Sound watersheds, it is not surprising that the proportion of agricultural and urban land was reflected in the $\delta^{15}N$ and $\delta^{18}O$ signatures of riverine NO_3. Rivers with relatively enriched $\delta^{15}N$, and $\delta^{18}O$ of NO_3 were overall associated with human-modified land use at the urban fringe. The land-use explanatory variables in PC1 explained almost half of the variation (40.1%) in the dependent variables (i.e. isotopic signatures). These results are consistent with previous work done in the Puget Sound watersheds by Vlah and Holtgrieve (submitted) where temperature was related to similar watershed characteristics. While the explanatory power of PC2 was indeed quite a bit less than PC1 (17.5%), the imprint of variables associated with gradient and elevation was found to be significant in atmospheric sources of NO_3 ($\Delta^{17}O$). There was, however, a great deal of variability observed due to hydrologic and climatic differences associated with different flow class, season, and hydrologic water year.

The response of NO_3 triple isotopes to changes in watershed physical features and land-use patterns varied depending on the flow classification (rain vs. rain-snow vs. snow-driven hydrologies) of the river. Rain-dominated systems displayed enriched signatures of $\delta^{15}N$, and $\delta^{18}O$ of NO_3, representing a higher proportion of human-derived N sources in these systems. Conversely, relatively depleted signatures were associated with snow-dominated systems, showing a decrease in the imprint of wastewater and fertilizer shifts as we move to higher elevation systems with less human-impact. Enriched $\Delta^{17}O$ signatures were found in river systems with higher watershed elevation, snow-driven hydrologies, and presence of glaciers, indicating a link between watershed ice and snow cover and supply of atmospheric Nr to rivers. This analysis provides evidence that atmospheric delivery of N is greater in rivers with higher watershed elevation and snow-driven hydrologies, while rivers with lower watershed elevation, driven by runoff from rain, are most likely to be impacted by human-derived activities.

What seems to be most interesting about this exercise, is the differences seen in NO_3 isotopic signatures between a normal hydrologic year and a year of drought. We can depict these differences visually in Figure 2, but the relative effect of drought is also captured in each of our models, and this varies across the season. Under normal conditions of flow, $\delta^{15}N$, and $\delta^{18}O$ signatures are comparatively more depleted, than the 2015 drought year. This is indicative of more precipitation falling as rain rather than snow, delivering more direct runoff from the watershed. Principal regression of the global model was best fit to the $\Delta^{17}O$ data, highlighting the influence of season and drought on atmospheric sources of NO_3. Summer reflected the largest relative contribution to enriched signatures of $\Delta^{17}O$, with this effect predicted as being most pronounced during a normal hydrologic year and being absent during years of drought. This suggests that the delivery of atmospheric N is highly dependent on the timing and magnitude of discharge driven by summertime snowpack melt and this seasonal variation may change with predictions of altered hydrologic regimes.
The identification of the key drivers of N sources elucidates potential emerging threats to river and downstream water quality in different hydrologic regimes. For example, in rain-snow and snow driven watersheds, the magnitude and timing of N delivery is likely to be altered by drought conditions. Decreases in snowpack and increases in precipitation as rain may shift the late season pulse of nutrients to a greater year-round delivery of N from terrestrial runoff, including agricultural and urban land-uses. This analysis highlights such expected changes in N sources and should be used to help point

managers towards areas of most concern for the Puget Sound watersheds.

Acknowledgements

We thank Julian Olden for providing the methodology of quantifying variable contributions in principal component regression, Sydney Clark and Erin Williamson for laboratory isotopic analysis and advice, and Julia Hart for additional laboratory support. We acknowledge the Washington Department of Ecology for providing the samples at hand and thank University of Washington's School of Aquatic and Fishery Sciences and the Northwest Climate Science Adaptation Center for supporting this research.

References

Banas, N. S., L. Conway-Cranos, D. A. Sutherland, P. MacCready, P. Kiffney, and M. Plummer. 2015. Patterns of river influence and connectivity among subbasins of Puget Sound, with application to bacterial and nutrient loading. Estuaries and Coasts 38:735-753. 10.1007/s12237-014-9853-y

Barnes, R. T., P. A. Raymond, and K. L. Casciotti. 2008. Dual isotope analyses indicate efficient processing of atmospheric nitrate by forested watersheds in the northeastern US. Biogeochemistry 90:15-27. 10.1007/s10533-008-9227-2

Beechie, T., E. Buhle, M. Ruckelshaus, A. Fullerton, and L. Holsinger. 2006. Hydrologic regime and the conservation of salmon life history diversity. Biological Conservation 130:560572. 10.1016/j.biocon.2006.01.019

Burnham, K. P., & Anderson, D. R. (2003). Model selection and multimodel inference: a practical information-theoretic approach. Springer Science & Business Media.Brooks and Williams 1999

Clough, T. J., L. E. Buckthought, F. M. Kelliher, and R. R. Sherlock. 2007. Diurnal fluctuations of dissolved nitrous oxide (N2O) concentrations and estimates of N2O emissions from a spring-fed river: implications for IPCC methodology. Global Change Biology 13:10161027. 10.1111/j.1365-2486.2007.01337.x

Divers, M. T., E. M. Elliott, and D. J. Bain. 2014. Quantification of nitrate sources to an urban stream using dual nitrate isotopes. Environmental Science & Technology 48:1058010587. 10.1021/es404880j

Elser, J. J., T. Andersen, J. S. Baron, A. K. Bergstrom, M. Jansson, M. Kyle, K. R. Nydick, L. Steger, and D. O. Hessen. 2009. Shifts in lake N:P stoichiometry and nutrient limitation driven by atmospheric nitrogen deposition. Science 326:835-837. 10.1126/science.1176199

Galloway, J. N., J. D. Aber, J. W. Erisman, S. P. Seitzinger, R. W. Howarth, E. B. Cowling, and B. J. Cosby. 2003. The nitrogen cascade. BioScience 53:341-356.

Galloway, J. N., A. R. Townsend, J. W. Erisman, M. Bekunda, Z. C. Cai, J. R. Freney, L. A. Martinelli, S. P. Seitzinger, and M. a. Sutton. 2008. Transformation of the nitrogen cycle: Recent trends, questions, and potential solutions. Science 320:889-892. 10.1126/science.1136674

Holtgrieve, G. W., D. E. Schindler, W. O. Hobbs, P. R. Leavitt, E. J. Ward, L. Bunting, G. Chen, B. P. Finney, I. Gregory-Eaves, S. Holmgren, M. J. Lisac, P. J. Lisi, K. Nydick, L. A. Rogers, J. E. Saros, D. T. Selbie, M. D. Shapley, P. B. Walsh, and A. P. Wolfe. 2011. A coherent signature of anthropogenic nitrogen deposition to remote watersheds of the northern hemisphere. Science 334:1545-1548. 10.1126/science.121226

Howarth, 1988. Nutrient Limitation of Net Primary Production in Marine Ecosystems. Annual Review of Ecology and Systematics 19:1, 89-110.

Kendall, C., E. M. Elliott, and S. D. Wankel. 2007. Tracing anthropogenic inputs of nitrogen to ecosystems.in R. Michener and K. Lajtha, editors. Stable Isotopes in Ecology and Environmental Science. Blackwell Publishing, Malden, MA.

Liang, X., D. P. Lettenmaier, E. F. Wood, and S. J. Burges. 1994. A simple hydrologically-based model of land-surface water and energy fluxes for general-circulation models. Journal of Geophysical Research-Atmospheres 99:14415-14428. 10.1029/94jd00483

Mauger, G. S., J. H. Casola, H. A. Morgan, R. L. Strauch, B. Jones, B. Curry, T. M. BuschIsaksen, L. Whitely-Binder, M. B. Krosby, and A. K. Snover. 2015. State of Knowledge: Climate Change in Puget Sound. Report prepared for the Puget Sound Partnership and the National Oceanic and Atmospheric Administration. Climate Impacts Group, University of Washington, Seattle.

Mohamedali, T., M. Roberts, B. Sackmann, and A. Kolosseus. 2011. Puget Sound Dissolved Oxygen Model: Nutrient Load Summary for 1999-2008. Page 144. Washington State Department of Ecology, Olympia, WA.

Olden, J., and P.R. Peres-Neto, 2003. An approach for quantifying variable contributions in principal component regression and its utility for ecological research.

Paerl, H.W., R. L. Dennis, and D. R. Whitall. 2002. Atmospheric deposition of nitrogen: Implications for nutrient over-enrichment of coastal waters. Estuaries 25:677-693.

R Core Team. (2017). R: A Language and Environment for Statistical Computing. Vienna, Austria. Retrieved from https://www.r-project.org/

Rabalais, N. N., R. E. Turner, and W. J. Wiseman. 2002. Gulf of Mexico hypoxia, aka "The dead zone". Annual Review of Ecology and Systematics 33:235-263. 10.1146/annurev.ecolsys.33.010802.150513

Reidy Liermann, C. A., Olden, J. D., Beechie, T. J., Kennard, M. J., Skidmore, P. B., Konrad, C. P., & Imaki, H. (2012). Hydrogeomorphic classification of Washington State River to support emerging environmental flow management strategies. River Research and Applications, 28(9), 1340–1358. http://doi.org/10.1002/rra.1541

Sigman, D. M., K. L. Casciotti, M. Andreani, C. Barford, M. Galanter, and J. K. Bohlke. 2001. A bacterial method for nitrogen isotopic analysis of nitrate in seawater and freshwater. Analytical Chemistry 73:4145-4153.

USDA. (2017). National Resources Conservation Service.

USGS. (2017). National Water Information System.

Valiela, I., 2006. Global Coastal Change. Blackwell Publ. Oxford, U. K. 359 pp.

Valiela, I., C. Owens, E. Elmstrom, and J. Lloret. 2016. Eutrophication of Cape Cod estuaries: Effect of decadal changes in global-driven atmospheric and local-scale wastewater nutrient loads. Marine Pollution Bulletin DOI:10.1016/j.marpolbul.2016.06.047.

Vlah, M. and G. Holtgrieve. (Submitted). Multi-scale controls on river temperature: a multivariate, autoregressive time series approach.

Wong, C., & M. Rylko, 2014. Health of the Salish Sea as measured using transboundary ecosystem indicators. Aquatic Ecosystem Health & Management 17, 46

Electronic Journal of Applied Multivariate Statistics
Volume 9, 2018

Article

The influence of interference competition and foraging conditions on partial prey consumption

Alex Lincoln
School of Aquatic and Fishery Sciences, University of Washington
E-mail: alinc2@uw.edu

Received March 2019; accepted in revised form April 2019; published June 2019

Abstract

Partial prey consumption is frequently observed in both invertebrate and vertebrate predators. This selectivity is often attributed to predator limitations (gut limitation or satiation) or as part of an energy-maximizing foraging strategy (optimal foraging), however the potential effects of social interactions between predators has not yet been considered as an explanatory mechanism. Our objective was to uncover whether interference competition between brown bears (*Ursus arctos*) is influential in driving patterns of partial consumption of sockeye salmon (*Oncorhynchus nerka*) in southwestern Alaska. We used an ordination approach to show that increases in bear abundance, a measure likely indicative of increased interference, resulted in less selective consumption of salmon, particularly at high prey abundances. Activity levels of subordinate and dominant bears did not significantly explain partial consumption. Much more variation was explained in consumption of female compared to male fish, likely due to the increased frequency of selective consumption (i.e., belly tissue consumption) observed in female fish. Foraging conditions (prey availability, date) explained more variation in partial consumption than bear-related variables, suggesting that interference competition may only have a weak effect, although results show that considering both categories of predictors may improve our capacity to predict changes in foraging under environmental perturbations.

Introduction

Partial prey consumption is pervasive throughout the animal kingdom. Phylogenetically diverse groups ranging from insects to terrestrial and aquatic mammals have been documented to partially consume prey items and discard remains (Lucas 1985, Hauser et al. 2008, Vucetich et al. 2012). Although this behavior is common, knowledge about the causes of partial prey consumption and the variation therein is limited. It has been hypothesized that partial consumption may arise as part of an optimal foraging strategy to maximize energy intake, whereby a prey carcass is analogous to a patch, and predators evaluate the benefits and costs of continuing to eat a carcass which offers diminishing energetic returns versus abandoning a partially eaten carcass to kill another prey item (Cook and Cockrell 1978, Sih 1980, Vucetich et al. 2012). For example, following this proposed mechanism, when prey availability (and thus encounter rates) are high and the costs of capturing prey are low, less biomass is consumed per prey (Hohberg and Traunspurger 2009). While this proposed mechanism may explain consumption patterns well in controlled laboratory settings, the costs of foraging extend beyond energetics when predators forage in the field.

Predators in natural settings must compete with other predators of the same or different species for food resources. These resources may be limited in quantity, but also in access, particularly in predators that interfere with one another behaviorally. Animals that display aggression when competing for food may experience increased foraging costs through energy expended while fighting or defending food, lost foraging opportunities while fighting

or avoiding conspecifics, and the potential risk of bodily harm. Thus, in systems where interference competition is strong, we would expect that the costs of foraging would include not only energetic costs of prey capture, but also risk and time costs associated with interference. If variation in partial prey consumption is at least partly a product of balancing costs and benefits as suggested by optimal foraging theory, then we might expect that the decision of how much of each prey item to consume would also be influenced by the extent of interference competition present in a system. The effect of interference competition may be particularly relevant in solitary predators that may aggregate around an ephemeral prey resource, resulting in increased opportunities for inter-predator interactions.

Brown bears (*Ursus arctos*) are one example of a solitary predator that exhibits partial prey consumption and may interact directly with one another while foraging. Bears in coastal regions aggregate during the summer and fall to prey upon Pacific salmon (*Oncorhynchus spp.*), which are only available to bears over a limited time period when salmon return to freshwater streams to spawn. Consumption of salmon is commonly partial and selective, with bears consuming lipid-rich portions of the fish (i.e., brain in males, gonads in females) and discarding less energetic portions (Gende et al. 2001, Reimchen 2000). However, there is a large amount of variability in selective consumption of specific fish body parts, as bears may consume close to the entire biomass of a fish in some circumstances but may consume almost nothing in others. This behavior may be attributed, in part, to multiple factors that work in concert, including salmon abundance (Gende et al. 2001), habitat characteristics (Andersson and Reynolds 2018) timing within the season (Gende et al. 2001), and prey characteristics like fish sex, size, and energetic condition (Reimchen 2000, Gende et al. 2001, Lincoln and Quinn 2018). However, a substantial amount of variation in consumption remains unexplained by this suite of variables, and it is currently unknown if and to what degree interference competition may contribute to partial prey consumption. Given that bears are not social foragers, interference between individuals has the potential to be influential.

Interference competition may be expected to impact the extent to which a salmon carcass is consumed in situations when negative interactions between bears would be predicted to occur; that is, when there is a higher density of bears and therefore more interactions. While bears may not always physically fight with each other, presence of two bears along the same stream reach may drive the subordinate bear off of the foraging grounds. As a result, during high bear densities, subordinate bears especially may change the amount of time spent eating versus fishing during the limited time in which they will be undisturbed along the stream. This may appear as decreased selectivity in prey consumption of individual fish (i.e., increased consumption per fish), if more time is spent eating captured salmon than fishing for new ones. Bears encountering one another may also interrupt consumption events in progress and may force subordinate bears to prematurely abandon kills. This may appear as increased prey selectivity to the observer (i.e., reduced consumption per fish). Therefore, we may find that consumption patterns may vary with predator density, though the directional relationship between amount consumed per prey and predator density is unclear. Interestingly, there is a relationship between intraspecific aggression between bears and salmon availability (Egbert and Stokes 1976), with decreased aggression at high salmon availability. Presumably, the presence of other bears is not as threatening to a given bear's salmon supply if salmon are very abundant. Thus, salmon availability may mediate the effects of interference competition on partial consumption. As such, we expect that bear density may be important in predicting partial consumption patterns at low but not high salmon abundances.

In addition to the effects of bear abundance and the potential interaction with prey availability, if interference competition plays a role in driving patterns of partial prey consumption we would expect that bears of varying social status will consume prey differently. Larger male bears are often avoided by other bears, and female bears with cubs are often the most intolerant of other bears (Egbert and Stokes 1976), likely because some large dominant males can be infanticidal (Ben-David et al. 2004). Thus, the risks of foraging for salmon are much greater for sow-cub groups than for individual adult bears, which likely reduces the time sow-cub groups spend foraging for salmon. Individual subordinate bears also spend less time foraging along salmon streams than dominant bears (Gende and Quinn 2004b). Given this time limitation, we would expect that sow-cub groups and subordinate bears may choose to more completely consume fish than would more dominant bears that are frequently present along these streams and may spend more time fishing. Therefore, we would expect that relative activity levels of subordinate and

dominant bears would also explain patterns of partial salmon consumption.

The goal of this study was to explore whether brown bear consumption of sockeye salmon (*O. nerka*) was influenced by the number and social status of bears foraging along a salmon stream. We anticipated that patterns of partial consumption of male and female fish would differ, as has been previously documented (Ruggerone et al. 2000, Gende et al. 2001), and we hypothesized that as bear abundance and activity levels of subordinate bears such as sows and cubs increased, we would observe more complete consumption. We also expected that these influences of interference competition, as measured by the influence of bear abundance and social status of bears, would primarily arise in low prey availability conditions due to the inverse relationship between inter-bear aggression and prey availability. By considering these factors alongside other variables known to be influential in partial consumption decisions, namely foraging conditions such as timing and prey availability, we intended to contribute to a more complete understanding of the relative importance of interference competition in consumption decisions.

Methods

Study site description and carcass surveys

Long-term research in the Wood River system of Bristol Bay, Alaska provides an excellent opportunity to explore the relationship between the predators and partial consumption of their prey. Hansen Creek is a spring-fed tributary of Lake Aleknagik and is a shallow (averaging 10 cm deep) and narrow (averaging 4 m wide) creek. Bear predation rates on sockeye are relatively high in this creek (Quinn et al. 2016), and sockeye overwhelmingly dominate the system (Pess et al. 2014), limiting any confounding effects of bear consumption of other salmon species. During daily surveys from mid-July to mid-August 2013-2017, the consumption choices of brown bears were recorded over a range of annual and daily salmon abundances. Sockeye carcasses encountered in the stream and within 3 meters of the bank were identified to sex and assessed for cause of death (bear kill or other); bear kills were distinguished by severe wounds. For all bear-killed fish, presence or absence of consumption of five body part categories was recorded (brain, body, belly, hump, and/or skin). “Body” consumption encompassed consumption of several other categories (i.e., belly, hump, skin, but not brain), however we chose to consider it to be a different category to indicate that consumption of that carcass was more complete, while belly, hump, or skin consumption indicated more selective and less complete consumption.

Prey availability and timing describe foraging conditions that have previously been shown to influence partial consumption of salmon by bears (Gende et al. 2001, Andersson and Reynolds 2018). Thus, in addition to carcass data, daily fish abundance in Hansen Creek was determined from counts of live fish during stream surveys. The habitat in Hansen Creek is shallow and simple, with few undercut banks, which enabled visual counts of virtually every fish in the stream on a given day. Annual fish abundance was determined from the sum of all dead fish observed over the season and the number of live fish counted on the last survey day of the year. The annual abundance of fish in 2014 was four times higher than any other year, and an unusual and large-scale pre-spawning mortality event occurred in this year (Tillotson and Quinn 2017). This resulted in a very large quantity of high quality (i.e., ripe) carcasses available to bears for scavenging. Given that this likely influenced bear predation and consumption, we chose to exclude this year from our analyses of partial consumption decisions.

Bear abundance and social status

From 2013-2017, a separate study focused on bear abundance and movement between streams provided additional information about the bear population using Hansen Creek (Wirsing et al. 2018). Two unbaited hair snares were positioned at two stations along the creek, each paired with a camera trap. Every 1-2 days (occasionally every 3-4 days), hair snares were checked and hair samples deposited on the wire by passing bears were collected. Analysis of DNA from collected hair follicles allowed for a non-invasive capture-mark-recapture estimate of the number of bears occupying Hansen Creek over the sockeye salmon run (see Wirsing et al. 2018 for additional details). From this data, we can relate the number of unique bears foraging along the creek in each year to the patterns of partial salmon consumption observed. Camera trap images supplemented annual bear abundances with information about the social status of bears. Although images did not allow for identification of individuals or precise social status, the data did allow for differentiation between solo adult bears and sows with cubs.

An activity index for individual adults (i.e., likely dominant bears) and sow-cub groups (i.e., sows with 1-3 cubs, likely subordinate bears) was determined based on the number of encounters observed during each 2-day period. We considered encounters separated by >5 minutes to be separate encounters. Since these activity levels were determined from images at just two locations along Hansen Creek, this data represents an index of activity, rather than a comprehensive evaluation of bear activity along the entire creek. However, it is reasonable to use this index to describe which social groups were primarily foraging along the entire creek during a given time period, since Hansen Creek is relatively small in length (about 2 km long) and so bears may easily forage along the entire creek during a single day or night.

Statistical Analysis

Since reliable measures of bear activity were available across 2-day windows of time, we aggregated fish consumption data to match the resolution of available bear data. Thus, each 2-day period represented a unit of replication, and our response matrix consisted of 'period x body parts', with the number of each body part consumed in each time period. Thus, each fish may have been represented more than once in this matrix if multiple body parts were consumed from a single carcass. To first explore whether any variation in partial consumption patterns could be explained by interference competition (as measured by annual bear abundance and indices of activity by social group), we constructed an explanatory matrix which consisted of 'period x bear variables', with the number of unique bears present in the year of each period and the number of camera trap encounters by individual adult bears or sow-cub groups (i.e., activity levels by each social group) in each period. Secondly, we sought to determine how foraging conditions influence partial consumption, and so we constructed a second explanatory matrix which consisted of 'period x foraging conditions', with the average daily fish abundance, annual fish abundance, and mid-point Julian date in each period. Both the response matrix and the explanatory matrices were log-transformed to reduce skewness, and the response matrix was row standardized such that the data represented relative abundances of each consumption pattern in each time period. Data was screened for outliers, missing data, and insufficient variables; as a result, 'skin' consumption was removed from the response matrix due to low occurrence of this consumption pattern.

Previous work has found differences in partial consumption between sexes (Ruggerone et al. 2000, Reimchen 2000, Andersson and Reynolds 2018), and so we first tested whether consumption patterns were different between male and female fish using a permutational analysis of variance (perMANOVA; Anderson 2001). We augmented this analysis with a permutation test for homogeneity of dispersion (Anderson 2006), to evaluate whether any significant difference between consumption patterns of male and female fish was due to differences in variance. Data from this analysis was visualized using a principal coordinate analysis (PCoA) using a Bray Curtis dissimilarity coefficient to compare the abundances of each consumption pattern between each fish sex. We determined whether separating subsequent analyses of consumption patterns by sex was appropriate based on these perMANOVA results, and by overlaying eigenvectors in the PCoA plot, we were able to determine which consumption patterns were more or less common for fish of each sex.

Next, we used a redundancy analysis (RDA) to investigate the relationship between (a) bear-related variables and partial consumption patterns, and (b) foraging conditions and partial consumption patterns. Although response data was a count of consumption patterns, RDA was an appropriate approach given that a detrended correspondence analysis determined that a linear response model was appropriate for our data (gradient length <2; Legendre and Legendre 1998). Furthermore, after transforming data into relative frequencies, a Euclidean-based method like RDA was suitable for ordination of count data (Legendre and Gallagher 2001), and allowed for inclusion of double-zeros in our measure of similarity between time periods. This was desired for our data, as double-zeros were informative (i.e., mutual absence of a consumption pattern between two time periods was meaningful, as this absence was known and directly observed). Significance of each ordination, axis, and variable were tested via a Monte Carlo randomization procedure. We also separated data into high and low fish abundance conditions (≥150 fish and <150 fish respectively) and conducted an RDA on each set of data to evaluate whether prey abundance affected the relationship between bear-related variables and consumption patterns. The threshold for low or high prey abundance conditions was based on our knowledge of the system (<150 fish represents a density of <0.02 fish/m^2), and to split the data into relatively even groups (n=23 in high availability

conditions and n=18 in low availability conditions). Finally, we conducted a partial RDA (pRDA) to identify the overlap in variation explained by bear-related variables and foraging conditions. All analyses were performed using R version 3.4.0.

Results

Partial consumption patterns were significantly different between female and male fish, as shown by perMANOVA results (p=0.01). More belly tissue was consumed in female fish, while more brain, body, and hump tissue was consumed in male fish (Figure 1, Table 1). In addition to different consumption of body parts, the variance of partial consumption patterns in male and female fish was also significantly different (p=0.001), with more variation in female fish consumption than male fish consumption. Because of these differences between male and female fish, subsequent analyses were separated by sex.

Figure 1. *Principal coordinate analysis (PCoA) ordination of partial consumption patterns with confidence ellipses for female (red) and male (blue) fish.*

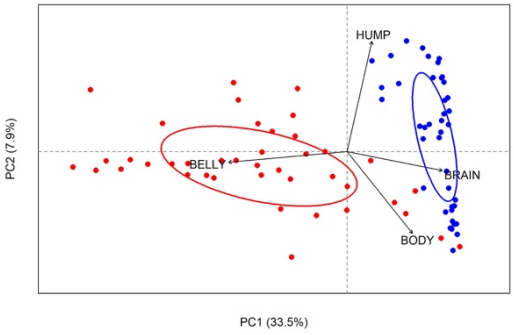

Redundancy analyses (RDA) revealed that bear-related variables (annual number of unique bears, individual adult activity, sow-cub activity) explained significant proportions of variability in the data; 27.5% of variation was explained in partial consumption patterns of female fish (p=0.001), and 14.3% of variation was explained in partial consumption patterns of male fish (p=0.06). In females, the annual number of bears was correlated (loading = -0.65) with the first ordination axis (RDA1; Table 2), however none of the variables were strongly correlated with RDA2. Examination of triplot results revealed that consumption of body tissue (i.e., less selective, more complete consumption) tended to occur in years of high bear abundance, while more selective consumption of belly tissue tended to occur in years of lower bear abundance (Figure 2a). In male fish, both the annual number of bears and activity by individual adult bears were negatively and moderately loaded onto RDA1 (loadings = -0.43 and -0.48 respectively), but again variables were not strongly correlated with RDA2 and this second ordination axis did not explain much variation (2.1%). As observed in female fish, less selective consumption of male fish (body tissue) tended to occur in years of high bear abundance and in periods with high activity of individual adult bears, and more selective brain consumption tended to occur when fewer bears were present in that year (Figure 2b). Additionally, consumption of belly

Table 1. *Percentage of female and male fish observed with each partial consumption pattern, calculated as the number of each body part summed over all study years divided by the sum of all body parts consumed. Each fish observed may have had multiple body parts consumed, and so percentages do not correspond to the percentages of fish with each consumption pattern.*

	Body	Brain	Hump	Belly
Female	30.7%	28.7%	7.2%	33.5%
Male	38.0%	43.9%	14.5%	3.6%

Table 2. *Structure correlation coefficients (loadings) between the first two ordination axes (RDA1 and RDA2) and either bear variables or foraging conditions for each fish sex. Larger magnitude indicates a stronger relationship of each variable with the axis. Axes are presented with % of variance explained. Bolded values indicate variables that were significant in each RDA model ($p < 0.05$).*

	Female		Male	
Bear Variable	Axis 1 (24.5%)	Axis 2 (2.4%)	Axis 1 (12.2%)	Axis 2 (2.1%)
# of Unique Bears	**-0.65**	-0.00	**-0.43**	0.14
# Adult Activity	-0.15	-0.26	-0.48	-0.17

Sow-cub Activity	-0.24	-0.11	-0.14	-0.15
Foraging Conditions	Axis 1 (41.5%)	Axis 2 (6.5%)	Axis 1 (20.6%)	Axis 2 (2.9%)
Daily Fish Abund	**0.84**	-0.07	**0.50**	0.17
Annual Fish Abund	0.30	-0.33	0.10	0.22
Date	-0.05	**-0.44**	**-0.46**	0.18

Table 3. *Structure correlation coefficients (loadings) between the first two ordination axes (RDA1 and RDA2) and bear-related variables for fish of each sex at high and low average daily fish abundances. High daily abundance includes time periods with an average fish abundance ≥ 150 fish (n=23), while low daily abundance includes periods with < 150 fish (n=18). Larger magnitude of the loadings indicates a stronger relationship of each variable with the axis. Each axis is presented with % variance explained. Bolded values indicate variables that were significant in each RDA model (p < 0.05).*

	Female		Male	
High Daily Abundance	Axis 1 (28.7%)	Axis 2 (1.8%)	Axis 1 (15.7%)	Axis 2 (2.1%)
# of Unique Bears	**-0.66**	0.04	-0.50	0.15
# Adult Activity	-0.22	0.21	-0.49	-0.27
Sow-cub Activity	-0.50	-0.09	-0.18	-0.24
Low Daily Abundance	Axis 1 (11.1%)	Axis 2 (4.8%)	Axis 1 (13.6%)	Axis 2 (6.7%)
# of Unique Bears	-0.33	0.27	0.14	-0.37
Ind. Adult Activity	-0.40	0.07	-0.29	-0.28
Sow-cub Activity	-0.02	0.23	0.08	-0.11

Figure 2. *Redundancy analysis (RDA) ordination of partial consumption patterns in each two-day period explained by corresponding predator attributes (A and B) and foraging conditions (C and D). Consumption patterns of female fish (A and C) are separated from those of male fish (B and D). RDA1 and RDA2 scores are plotted as points, consumption descriptors are capitalized and labeled in black, and predictor variables are represented as vectors.*

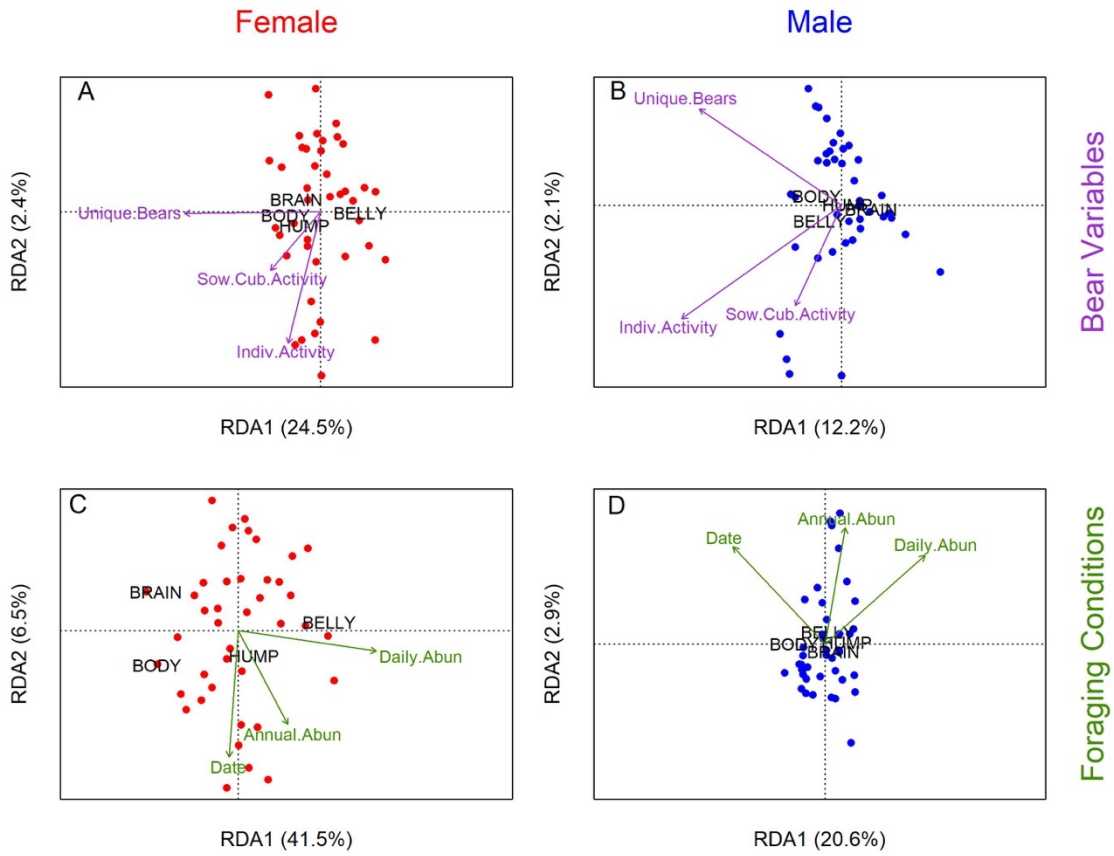

Figure 3. *Variation explained by each set of explanatory variables, resulting from a partial redundancy analysis (pRDA). Values at the intersection of each Venn Diagram represent the percentage of variation jointly explained by the two explanatory matrices, while values in the regions that do not overlap represent the percentage of variation uniquely explained.*

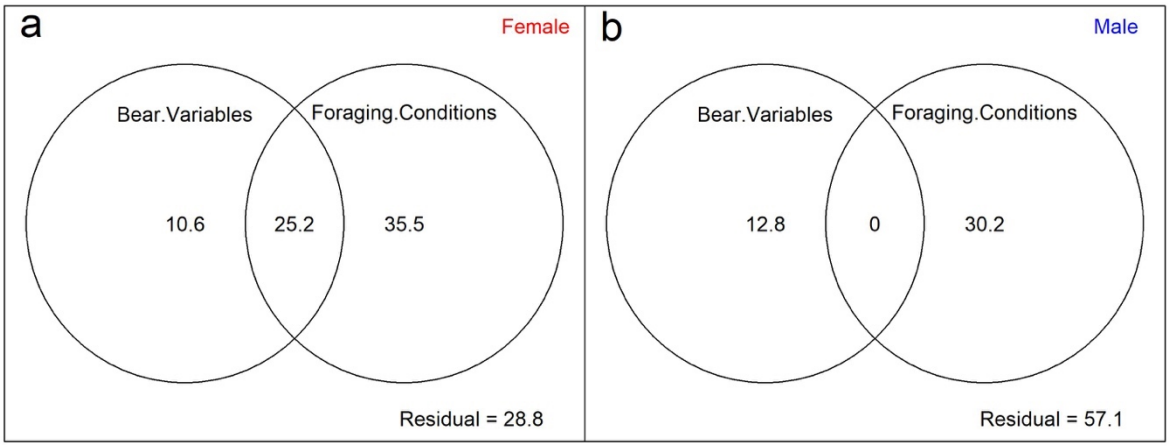

Table 4. *Summary of constrained ordination (RDA) results. Bold values are statistically significant.*

Model = consumption ~ bear variables	Female				Male			
	df	Variance	*F*	*p*	df	Variance	*F*	*p*
Axes								
RDA1	1	0.98	12.48	**0.001**	1	0.49	5.25	**0.04**
RDA2	1	0.10	1.22	0.56	1	0.09	0.92	0.72

Constraining Variables								
Number of Unique Bears	1	0.98	12.44	**0.001**	1	0.27	2.94	**0.04**
Individual Adult Activity	1	0.08	1.05	0.35	1	0.26	2.76	0.05
Sow-cub Activity	1	0.04	0.54	0.61	1	0.04	0.46	0.65
Residual	37	2.90			37			

Model = consumption ~ foraging conditions

Axes								
RDA1	1	1.66	30.30	**0.001**	1	0.82	10.10	**0.002**
RDA2	1	0.26	4.72	**0.04**	1	0.11	1.41	0.51
Constraining Variables								
Daily Fish Abundance	1	1.63	29.73	**0.001**	1	0.47	5.75	**0.004**
Annual Fish Abundance	1	0.10	1.80	0.17	1	0.06	0.73	0.51
Date	1	0.25	4.47	**0.01**	1	0.46	5.62	**0.001**
Residual	37				37			

Model = consumption ~ bear variables (at high prey availability)

Axes								
RDA1	1	1.14	7.91	**0.01**	1	0.63	3.68	0.16
RDA2	1	0.07	0.48	0.93	1	0.12	0.72	0.85
Constraining Variables								
Number of Unique Bears	1	1.06	7.26	**0.003**	1	0.41	2.41	0.09
Individual Adult Activity	1	0.06	0.40	0.70	1	0.26	1.53	0.20
Sow-cub Activity	1	0.12	0.85	0.46	1	0.08	0.47	0.72
Residual	19				19			

Model = consumption ~ bear variables (at low prey availability)

Axes								
RDA1	1	0.44	1.86	0.59	1	0.55	2.41	0.39
RDA2	1	0.19	0.81	0.82	1	0.27	1.18	0.62
Constraining Variables								
Number of Unique Bears	1	0.26	1.11	0.35	1	0.26	1.13	0.33
Individual Adult Activity	1	0.32	1.33	0.29	1	0.04	0.18	0.93
Sow-cub Activity	1	0.07	0.29	0.83	1	0.52	2.30	0.10
Residual	14				14			

tissue in male fish may have been more frequent in periods of higher activity by individual adult bears.

Daily fish abundance did have an effect on the relationship between consumption patterns and bear-related variables in female but not male fish. Substantially more variation was explained by bear-related variables in female fish consumption during periods with a high daily fish abundance compared to periods with low fish abundance. The first two ordination axes explained 30.5% of variation in female consumption when ≥150 fish were present in the stream, while only 15.9% of variation was explained by the first two axes when <150 fish were present (Table 3). Only the number of unique bears was moderately correlated with the first ordination axis in the RDA of female consumption during high daily fish abundance (loading = -0.66), however this correlation was substantially weaker in low fish abundances (loading = -0.33). In male fish, the percentage of variation explained by the first two RDA axes remained roughly similar across prey availability categories (17.8% and 20.3%), and none of the variables loaded heavily onto either

of the first ordination axes in either RDA (Table 3).

Foraging conditions also explained a significant proportion of partial consumption patterns for both female (p=0.001) and male fish (p=0.001). In female fish, the first two ordination axes explained 48.0% of variation, which was substantially more than the proportion of variation explained by bear-related variables (Table 2). Daily fish abundance loaded most heavily onto the first ordination axis (loading=0.84), and date was weakly correlated with the second ordination axis (loading=-0.44). In male fish, foraging conditions also explained more variation in consumption patterns than did bear-related variables (Table 2), with both daily fish abundance and date loading most heavily onto the first ordination axis (loadings = 0.50 and -0.46 respectively). Neither measure of fish abundance nor date was strongly correlated to the second ordination axis. Relationships between foraging conditions and partial consumption patterns were consistent for both males and females. Under higher daily fish abundances, more selective consumption was observed (female belly tissue and male belly and/or hump tissue), while more complete consumption (body) was more often observed under lower daily fish abundance (Figure 2c-d). Earlier in the season, more consumption of female brain and belly tissue and male brain tissue was observed (more selective consumption), while later in the season more body consumption was observed (less selective consumption). A summary of all ordination results is presented in Table 4.

Combined together, predator attributes and foraging conditions explained 71.2% and 42.7% of variation in partial consumption of female and male fish, respectively (Figure 3). Bear-related variables uniquely explained 10.6% of variation in partial consumption of female fish, while foraging conditions explained 35.5% of variation, and 22.9% of variation was jointly explained by bear variables and foraging conditions (Figure 3). In male fish, bear variables and foraging conditions explained distinct variability (12.8% and 30.2% respectively), as revealed by a lack of any jointly explained variance.

Discussion

Following results previously documented (Ruggerone et al. 2000), partial consumption patterns were different between male and female fish, with more belly tissue consumption in female fish and more brain, body, and hump tissue consumption in male fish. Selective consumption of bellies in females but not males followed expectations from an energy-maximizing foraging strategy, as gonad tissue in females (i.e., eggs) is much higher in energy compared to male gonad tissue (Hendry and Berg 1999). Greater variation in female consumption patterns was observed compared to male consumption patterns, possibly due to differences in belly consumption between the sexes. Belly tissue was much more frequently consumed from females than males (Table 1), presumably due to presence of energy-rich eggs in females. Since male fish lack high-energy eggs, belly tissue is almost never consumed and so consumption patterns in male fish were much more consistent.

It is likely that more variation is observed in female fish consumption due to variability in female spawning status. The probability of belly consumption is much higher in ripe compared to spawned-out females (Lincoln and Quinn 2018), and we may predict that bears would attempt to target ripe females because of their high-energy eggs. However, while bears may be able to visually distinguish between newly-arrived fish and those very close to senescence due to difference in coloration and presence of fungus, it may be much more difficult to determine the spawning status of a fish prior to capture. Females tend to spawn within four days of entering a stream (McPhee and Quinn 1998), and often may not develop features that visually signal spawned-out status (fungus, coloration) until days after spawning. Therefore, even if bears seek to target ripe fish while fishing, it may become apparent that a fish is spawned out only after capture. In such circumstances, bears may choose to consume tissues other than belly tissue, whereas when a ripe fish is captured, bears will likely consume belly tissue. As such, consumption patterns may vary with the encounter and capture rates of ripe versus spawned-out females, which varies with date since the abundance of ripe fish in the creek is higher early in the season compared to later. In time periods when capture rates of ripe females are high we may observe very consistent selective consumption of belly tissue, but when capture rates are lower we may see more varied consumption responses, and this difference likely contributes to the greater variability in observed female consumption patterns.

A significant amount of variation in both male and female consumption was explained by bear-related variables. Less selective consumption was observed in years of higher

bear abundance, following expectations that increased bear densities may increase perceived foraging risk and thus influence partial consumption. Bears are time-limited while foraging for salmon due to the temporary availability of spawning salmon (Schindler et al. 2013), and high bear densities may further decrease time spent foraging on a stream for some bears because of perceived increases in the cost of fishing (i.e., through an increased risk of aggressive encounters). In this situation, bears may place a high value on any fish that is captured since additional fishing opportunities are limited, and therefore bears may be encouraged to consume fish to a near-full extent (i.e., brain and body consumption). By contrast, when bear densities are low, and the risk of negative interactions with other bears is lower, bears may spend more time fishing and so can afford to be choosier in consumption of salmon body parts. Interestingly, neither the activity of individual adult bears nor the activity of sow-cub groups was significantly related to consumption patterns. This suggests that partial consumption decisions are made independently of whether a bear is dominant or subordinate. Alternatively, it is also possible that our assumption that these groupings corresponded to differences in social status was flawed, and so these metrics may not have been as informative as we had hoped. Indeed, the social status of any one bear is difficult to ascertain, particularly without direct and prolonged observation, as social status is likely a combined product of sex, size, aggression, relatedness, mating history, and reproductive status (Egbert and Stokes 1976, Ben-David et al. 2004).

Contrary to our prediction that interference competition and thus bear numbers and social status would be most important during low prey availability, results from our analysis separating low- and high-prey availability conditions showed the opposite; less variation was explained in female consumption by bear-related variables during low prey availability than in high prey availability. This finding may be a product of the relationship between bear activity and prey abundance. Bears foraging on salmon move across the landscape to track the phenology of salmon runs (Schindler et al. 2013, Deacy et al. 2016), and so may be expected to primarily be active on salmon streams during the peak of the salmon run. Indeed, we see low bear activity at the beginning and end of the season but more activity during the middle of the run (data not presented here). As such, in periods of low fish abundance, there may have been so few bears present that essentially no interactions occurred between bears, and the threat of aggressive encounters was essentially zero. Therefore, bear numbers and activity may not have had much importance if interference never occurs. However, in periods of higher fish abundance, when more bears may be present along the stream, there may be a greater potential for interactions between bears, and so bear-related variables may have become important. We recognize that our metric of bear abundance is measured on an annual scale, and so does not include information about the temporal distribution of these bears throughout the season, and that activity indices also do not necessarily indicate bear density in a given time period since a high activity index could describe high activity by a single individual. Given that our bear abundance estimates do not directly correspond to each 2-day period, we cannot determine for certain if results may be explained by this reasoning.

While bear-related variables did explain a portion of variation, particularly in female fish, foraging conditions explained a much larger portion of variation in both males and females. Relationships between foraging conditions and consumption patterns confirmed findings from other studies. As seen elsewhere (Gende et al. 2001, Lincoln and Quinn 2018), bears showed increased selectivity under high daily fish availability, following predictions from optimal foraging theory which suggest that the cost of prey capture is influential in determining the extent of prey consumption. Consumption patterns also varied with date, which may be explained by one or multiple mechanisms. First, increased selectivity at the beginning of the season may suggest that bears may anticipate additional prey options later on in the season. Bears may have learned the timing of salmon runs, which are remarkably consistent between years (Quinn 2018), and so early in the run they may choose to only eat choice tissues. Carcasses eaten later in the season may have more complete consumption if bears know that the end of the salmon run is approaching, and so any additional nutritional needs must be met before the resource disappears. This is interesting, if true, as it indicates that bears are not in such dire need of salmon nutrition at the beginning of the season that they eat everything captured. Secondly, patterns of decreasing selectivity with date may be a product of decreasing prey quality over time. Later in the season, salmon tissues are generally of lower energetic content (Hendry and Berg 1999), since many have spawned and are near death. As such, bears may need to eat more of each

salmon to fulfill the same energetic requirement as was met earlier in the season with selective consumption of belly or brain tissue. This pattern of decreasing selectivity as the season progressed as also observed by Andersson and Reynolds (2018). These foraging conditions explained more variation than bear-related variables, suggesting that the effects of interference competition may be weak in comparison to these effects of prey availability and timing.

Combined, bear variables and foraging conditions explained more variation in female fish consumption than in male fish, despite greater variation in female fish consumption. This may be explained by increased selectivity observed in female fish. Belly consumption clearly represented selective consumption, while body consumption was clearly indicative of a lack of selectivity and more complete consumption. Since belly consumption was much more prevalent in female fish than male fish, this allowed for clear differentiation between periods with high and low selectivity in female but not male fish, through the number of bellies eaten. This clear gradient of selectivity was not present in male fish, due to bears foraging almost exclusively on non-belly tissues.

While hump consumption was also predicted to represent selectivity, hump consumption was not common in fish of either sex (Table 1), and so did not contribute much in differentiating between periods with high and low selectivity in foraging behavior. Interestingly, the descriptor scores for hump tissue consistently fell near the origin of each ordination, suggesting that none of the variables explored in the current study explained this consumption pattern. As mentioned in another study (Lincoln and Quinn 2018), instead of an adaptive consumption pattern, hump consumption may instead arise mainly as a product of how bears capture male fish; the pronounced hump morphology of males may make it easy to bite males on the hump, and so consumption may begin from this point. Similarly, brain consumption was also expected to reveal selective consumption, however brain tissue was often but not always consumed alongside body tissue, and so brain consumption could have represented either very selective consumption, with less than 5% of all tissue consumed, or non-selective consumption, with up to 99% of tissue consumed if eaten alongside body tissue (Gende et al. 2001). As such, it was much more difficult to differentiate between periods of high or low selectivity in partial consumption of male fish, and so explanatory variables were not able to explain these patterns as well as in female fish. This finding appears to be preserved across systems, as others have also found a higher probability of selective consumption in female fish compared to male fish in British Columbia (Andersson and Reynolds 2018).

This difference in the degree of selectivity in consuming male and female fish may also explain why variation was partitioned differently for male and female fish; there was substantial overlap in the amount of variation explained by both foraging conditions and bear-related variables in female but not male fish. The shared variation may be attributed to covariation between foraging conditions and bear-related variables. Specifically, we observed a negative correlation between daily fish abundance and the annual number of bears present ($r = -0.64$), which matches relationships revealed between these two variables and female belly consumption in ordination triplots (Figure 2). More female belly consumption was observed when fewer bears were present in that year, and under higher daily salmon abundance. These relationships were not observed in male fish, and so this covariation between bear-related variables and foraging conditions did not contribute to explaining patterns of male fish consumption; bear variables and foraging conditions did significantly explain consumption of other body parts in male fish, but did not do so jointly. Thus, the difference in the extent of shared variation between fish sexes is also explained by differences in belly consumption between fish sexes.

In summary, interference competition does appear to partly explain some patterns of partial prey consumption. The data analyzed here suggested that foraging conditions may be more influential, compared to predator-related variables, in driving different patterns of partial consumption. We recognize that a substantial proportion of variation was left unexplained by all variables explored, particularly in consumption of male fish (57.1%). This analysis did not include data on fish characteristics such as fish size or condition, which are almost certainly important explanatory factors since they play a role in prey discarding by brown bears in the same system (Lincoln and Quinn 2018). Beyond fish traits, remaining variation may also be attributable to differences in foraging between bears of different age- or size-classes, individuality in foraging behavior, and/or because of differences in availability of alternative food sources (e.g., berries, ungulates) both between years and within years.

In light of these other potential sources of variation, it is notable that bear abundance and activity levels of subordinate and dominant bears did significantly explain patterns, especially given that the resolution of the data was coarse and prevented matching specific predators or predator densities to individual fish consumed. Had we been able to do this, we expect that a greater proportion of variation in consumption patterns would have been explained by these variables related to interference competition. As it is, results presented here suggest that partial prey consumption may arise from more than just an optimal foraging strategy; in addition, social interactions and the resulting interference competition between predators may partly explain variation that cannot be attributed to energy maximization.

Acknowledgements

Support for this project was provided by many contributors, including but not limited to the Pacific Seafood Processors Association, the Bristol Bay Regional Seafood Development Association, independent companies in the Pacific salmon seafood industry, the National Science Foundation, the Gordon and Betty Moore Foundation, Alaska Department of Fish and Game, National Oceanic and Atmospheric Administration, Bristol Bay Economic Development Corporation – Bristol Bay Science Research Institute, the University of Washington's Royalty Research Fund, and the H. Mason Keeler Endowment to the University of Washington. Many students and staff members in the University of Washington Alaska Salmon Program contributed to fieldwork, but we especially thank Jackie Carter and Chris Boatright

References

Anderson, M.J. 2001. Permutation tests for univariate or multivariate analysis of variance and regression. Can. J. Fish. Aquat. Sci. 58(3):626-639.

Anderson, M.J. 2006. Distance-based tests for homogeneity of multivariate dispersions. Biometrics 62:245-253.

Andersson L.C., and J.D. Reynolds. 2018. Habitat features mediate selective consumption of salmon by bears. Can. J. Fish. Aquat. Sci. 75:955-963.

Ben-David M., K. Titus, and L.V.R. Beier. 2004. Consumption of salmon by Alaskan brown bears: A trade-off between nutritional requirements and the risk of infanticide? Oecologia 138:465–474.

Cook RM, and B.J. Cockrell. 1978. Predator ingestion rate and its bearing on feeding time and the theory of optimal diets. J. Anim. Ecol. 47:529–547.

Deacy, W., W. Leacock, J.B. Armstrong, and J.A. Stanford. 2016. Kodiak brown bears surf the salmon red wave: direct evidence from GPS collared individuals. Ecology 97(5):1091-1098.

Egbert, A.L., and A.W. Stokes. 1976. The social behavior of brown bears on an Alaskan salmon stream. Int. C. Bear 3:41-56.

Gende, S.M., and T.P. Quinn. 2004. The relative importance of prey density and social dominance in determining energy intake by bears feeding on Pacific salmon. Can. J. Zool. 82(1):75-85.

Gende, S.M., T.P. Quinn, and M.F. Willson. 2001. Consumption choice by bears feeding on salmon. Oecologia 127:372–382.

Hauser, D.D.W., C.S. Allen, H.B. Rich, Jr., and T.P. Quinn. 2008. Resident harbor seals (*Phoca vitulina*) in Iliamna Lake, Alaska: summer diet and partial consumption of adult sockeye salmon (*Oncorhynchus nerka*). Aquat. Mamm. 34(3):303-309.

Hendry, A.P., and O.K. Berg. 1999. Secondary sexual characters, energy use, senescence, and the cost of reproduction in sockeye salmon. Can. J. Zool. 77:1663–1675.

Hohberg, K., and W. Traunspurger. 2009. Foraging theory and partial consumption in a tardigrade-nematode system. Behav. Ecol. 20:884–890.

Legendre, P., and E.D. Gallagher. 2001. Ecologically meaningful transformations for ordination of species data. Oecologia 129:271-280.

Legendre, P., and L. Legendre. 1998. Numerical Ecology. Elsevier.

Lincoln, A.E., and T.P. Quinn. 2018. Optimal foraging or surplus killing: selective consumption and discarding of salmon by brown bears. Behavioral Ecology doi: 10.1093/beheco/ary139.

Lucas, J.R. 1985. Partial prey consumption by antlion larvae. Anim. Behav. 33(3):945-958.

McPhee, M.V., and T.P. Quinn. 1998. Factors affecting the duration of nest defense and reproductive lifespan of female sockeye salmon, *Oncorhynchus nerka*. Environ. Biol. Fishes 51:369–375.

Pess, G.R., T.P. Quinn, D.E. Schindler, and M.C. Liermann. 2014. Freshwater habitat associations between pink (*Oncorhynchus gorbuscha*), chum (*O. keta*) and Chinook

salmon (*O. tshawytscha*) in a watershed dominated by sockeye salmon (*O. nerka*) abundance. Ecol. Freshw. Fish 23:360–372.

Quinn, T.P. 2018. The behavior and ecology of Pacific salmon and trout, Second Edition. University of Washington Press.

Quinn, T.P., C.J. Cunningham, and A.J. Wirsing. 2016. Diverse foraging opportunities drive the functional response of local and landscape-scale bear predation on Pacific salmon. Oecologia 183(2):415-429.

Reimchen, T.E. 2000. Some ecological and evolutionary aspects of bear-salmon interactions in coastal British Columbia. Can. J. Zool. 78:448–457.

Ruggerone, G.T., R. Hanson, and D.E. Rogers. 2000. Selective predation by brown bears (*Ursus arctos*) foraging on spawning sockeye salmon (*Oncorhynchus nerka*). Can. J. Zool. 78:974–981.

Schindler, D.E., J.B. Armstrong, K.T. Bentley, K. Jankowski, P.J. Lisi, and L.X. Payne. 2013. Riding the crimson tide: mobile terrestrial consumers track phenological variation in spawning of an anadromous fish. Biol. Letters 9:20130048.

Sih, A. 1980. Optimal foraging: partial consumption of prey. Am. Nat. 116:281–290.

Tillotson, M.D., and T.P. Quinn. 2017. Climate and conspecific density trigger pre-spawning mortality in sockeye salmon (*Oncorhynchus nerka*). Fish. Res. 188:138–148.

Vucetich, J.A., L.M. Vucetich, and R.O. Peterson. 2012. The causes and consequences of partial prey consumption by wolves preying on moose. Behav. Ecol. Sociobiol. 66(2):295-303.

Wirsing, A.J., T.P. Quinn, C.J. Cunningham, J.R. Adams, A.D. Craig, and L.P. Waits. 2018. Alaskan brown bears (*Ursus arctos*) aggregate and display fidelity to foraging neighborhoods while preying on Pacific salmon along small streams. Ecol. Evol. 00:1-14.

Electronic Journal of Applied Multivariate Statistics
Volume 9, 2018

Article

Effects of parental low pH exposure on gonadal and larval gene expression in the Olympia oyster (Ostrea lurida)

Laura H. Spencer
School of Aquatic and Fishery Sciences, University of Washington
E-mail: lhs32@uw.edu

Received March 2019; accepted in revised form April 2019; published June 2019

Abstract

Ocean acidification threatens calcifying marine organisms, particularly those with vulnerable larval stages. Positive carryover of environmental exposure is a hypothesized mechanism for one generation to impart acclimatory "memories" to the next. Parental carryover effects were investigated in the Olympia oyster, with adults exposed to two winter temperatures for 60 days (ambient: 6.1±0.2°C; elevated: 10.2±0.5°C) followed by two pH treatments for 52 day (ambient: 7.82±0.02; low: 7.31±0.02). Elevated winter temperature resulted in significantly more developed gonad tissue, indicating that gametogenesis occurred or resorption did not. Reproductive tissue was less developed in oysters held in low pH, but only if they entered with undeveloped gonad, suggesting that resorption of gametes did not occur. Fecundity over 50 days was unaffected by pH, but timing varied by winter temperature. Counter to predictions, typical stress-related proteins were not heavily upregulated in gonad tissue. Principal Component Analysis revealed that larval gene expression was influenced by parental pH exposure. Nine larval genes differed significantly by parental pH, which were related to cytoskeleton microtubules (Tuba3a), translation (rpl8), DNA repair (USP47), aerobic respiration (COI), mitochondrial electron transport (mt:ND5), protein transport (TBC1D2), and transcription (hnrnpd). Together, these results that offspring physiology is affected by parental exposures.

Introduction

One of the primary environmental repercussions of global carbon emissions is ocean acidification. Ocean acidification is caused by diffusion of carbon dioxide from the atmosphere into the ocean where it reacts with water to form carbonic acid, which both reduces the ocean pH and removes carbonate ions from solution. Carbonate ions are critical components of calcite and aragonite, the two primary forms of calcium carbonate that marine organisms use to build shells. Calcareous marine organisms are vulnerable to these chemical shifts, particular those with sensitive larval stages that build natal shells. Of the calcifiers, oyster taxa are increasingly studied due to their economic importance and ecosystem services (Grabowski et al. 2012).

Evidence that farmed oysters are already exhibiting negative effects from ocean acidification (OA) has led to researchers focusing on potential mechanisms to improve the outlook for oyster aquaculture and restoration programs (Barton et al. 2012). Oyster breeding programs are leveraging species' high genetic diversity to select for lines that are more resilient to ocean-acidification (for example, E. L. Thompson et al. 2015). In wild populations, genetic diversity, small effective population size, and r-selected reproductive strategies may allow for genetic drift to amplify OA-resilient genotypes (see the sweepstakes reproduction hypothesis, Hedgecock and Pudovkin 2011). The rapid rate at which ocean chemistry is changing, however, is outpacing the rate at which adaptation occurs through mutation and natural selection, thus without another mechanism wild oyster populations are predicted to severely decline.

There may, however, be cause for optimism with insights from the emerging field of

epigenetics. Epigenetics suggests the environment can trigger changes in genomic markers, which can be passed to offspring and influence gene expression, thus transferring acclimatization between generations. A series of studies on the Sydney rock oyster (*Saccostrea glomerata*) provide evidence for positive transgenerational carryover effects in oysters. Adult low pH exposure during reproductive conditioning results in larvae that are larger and grow faster under a similarly low pH environment (Parker et al. 2015), and expression of key stress-response genes differ depending on parental exposure (Goncalves et al. 2016). In the reef building coral, *Pocillopora damicornis*, adults held in low pH during larval brooding produce offspring with lower basal metabolism but elevated metabolism under direct low pH (Putnam and Gates 2015). Negative carryover effects are also documented. For example, female Pacific oysters (*Crassostrea gigas*) exposed to low pH prior to reproductive conditioning produce fewer surviving larvae (Venkataraman et al., 2019). The complex interactions between an organism's genotype, complete environmental life history, timing and magnitude of low pH exposure, and how and when reproduction occurs may determine if carryover effects are beneficial, or detrimental.

Here, we investigate whether adult-only exposure to low pH affects reproduction, gonad physiology and offspring physiology in *Ostrea lurida,* the Olympia oyster. *O. lurida* is a the only oyster species native to the Pacific coast of North America, inhabiting estuaries where shifts in ocean carbonate chemistry are occurring more rapidly than in other regions of the world (Feely et al. 2012). Overharvest and pollution devastated populations in the early 1900's, and current estimates indicate that total *O. lurida* acreage is 2% of the historic level (Polson and Zacherl 2009). The Olympia oyster is being actively restored, but there are concerns that ocean acidification will impede successful restoration. Indeed, larval *O. lurida* exposed to low pH display slower growth into the juvenile stage (Hettinger et al. 2012). However, there is also evidence that *O. lurida* is more resilient to ocean acidification compared to the non-native Pacific oyster, potentially due to slower growth and calcification rates (Waldbusser et al. 2016). Unknown are how ocean acidification affects adult physiology, reproduction, and whether adult exposure influences offspring physiology. If adult exposure can prepare the next generation for more acidic conditions, it may mitigate ocean acidification's negative effects on the vulnerable larval stages of *O. lurida*.

Using QuantSeq and Principal Component analysis, we assess global gene expression in gonad tissues from adults directly exposed to low pH (7.31), and whole body tissues of newly released larvae never directly exposed. We hypothesize that adult low pH exposure alters both gonad and larval expression of stress-related genes even under ambient conditions. Universal stress-response proteins such as the inducible heat shock complex (e.g. HSP70) are commonly upregulated under direct exposure to low pH. Proteins involved in the oxidative stress response such as cytochrome P450 and peroxiredoxin, and other molecular functions such as cytoskeleton stability and mitochondrial metabolism, are hypothesized as important factors for organisms responding to ocean acidification (Anderson et al. 2015). Unlike previous studies using qPCR to target these key genes, this study leverages transcriptomic analysis which allows for non-biased, global analysis of molecular, physiological differences. Additionally, because ocean acidification is co-occurring with ocean warming, an elevated temperature treatment prior to pH exposure is included to mimic elevated winter temperatures experienced during the 2014-2016 marine heat wave, and predicted under future climate scenarios. The temperature pre-treatments elucidate the effects of extremely low pH (7.3) due to summer upwelling events on reproduction, given current and future winter temperature regimes.

Methods

Adult oyster source and history

Adult *Ostrea lurida* from four genetic groups were used in this study (Figure 1) to include genetically diverse organisms, which are known to have varying reproductive characteristics. Three groups were first-generation hatchery-produced oysters (32.1 ± 5.0mm), all hatched in central Puget Sound (Port Gamble Bay) in 2013 as described in Heare et al. 2018. The broodstock used to produce these F1 oysters were wild, harvested from Fidalgo Bay in North Puget Sound (F), Dabob Bay in Hood Canal (D), and Oyster Bay in South Puget Sound (O-1), which are considered genetically distinct subpopulations. The fourth group was second-generation, hatchery-produced oysters (O-2, 21.9 ± 3.3mm) from the aforementioned Oyster Bay group in 2015, as described in Silliman et al. 2018 (preprint), from a single pulse of larval release and thus likely one family. All groups

were maintained in pearl nets in Clam Bay ©, adjacent to the Kenneth K Chew research center.

Figure 1: *Sites in Puget Sound, WA where Ostrea lurida populations' progenitors were collected (F, D, O) and where oysters were housed prior to experiment (C): Fidalgo Bay (F), Dabob Bay (D), Clam Bay (C), Oyster Bay (O).*

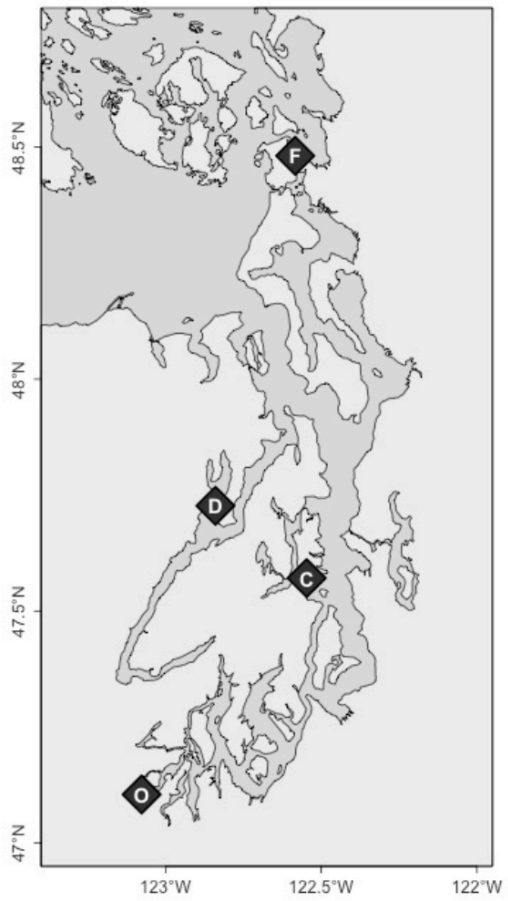

Temperature pre-treatment to manipulate gonad stage

Prior to pH treatments, the adult oysters were maintained at two temperature regimes (6.1±0.2°C and 10.2±0.5°C) for 60 days beginning December 6, 2016. The two temperatures correspond to historic local winter temperature (6°C), and anomalously warm winter temperature (10°C) as experienced during the 2014-2016 marine heat wave (Gentemann, Fewings, and García-Reyes 2017). Oysters from each genetic group (100 for O-1 and F groups, 60 for D group, and 300 for O-2) were divided into 4 bags, 2 bags per temperature, and held in two 50L flow-through experimental tanks (1.2L/min). Temperature in the 6°C group was maintained using Teco Aquarium Chiller (TK-500), and recorded continuously with Onset HOBO Water Temperature Data Loggers (U22-001). Tanks were drained, cleaned, and rotated between treatments on a weekly basis, and oysters were checked for mortality.

pH treatment and water chemistry

Following a 10-day recovery period from the temperature treatments, oyster populations were divided and held at ambient pH (7.82±0.02) and low pH (7.31±0.02) for 52 days (February 15 to April 8, 2016) (Table 1). Animals were housed in six 50L flow-through tanks (1.2L/min), 3 replicates tanks per pH treatment, and fed from a shared algae header tank daily with 300-500 mL of Shellfish Diet 1800® (Reed Mariculture) diluted in 200L of ambient pH seawater (Helm and Bourne 2004), dosed continuously with Iwaki Metering Pump. Low pH treatment water was prepared using CO_2 injection as described in Venkataraman et al. (2019). Briefly, filtered seawater (1um) first recirculated through a 1,610 liter reservoir with off-gas chimney to equilibrate with the atmosphere, then flowed into 757 liter treatment reservoirs recirculating through venturi injectors. Durafet pH probes (Honeywell Model 51453503-505) and a Dual Input Analytical Analyzer (Honeywell Model 50003691-501) monitored pH in treatment reservoirs with readings every 180 seconds, and using solenoid valves injected CO_2 gas through lines at 15 psi in 0.4 second pulses if pH exceeded the 7.22 set point. Water chemistry was continuously monitored in experimental tanks using Durafet pH sensors and temperature (10.4±0.4°C) was measured using HOBO Pendant Temperature Data Loggers (UA-002-64). Twice weekly, 1L water samples were collected from experimental tanks and temperature (°C), salinity (PSU), and pH (mV, converted to pH_T) were measured immediately using Traceable Digital Thermometer (Model 15-077, Fisher), Bench/Portable Conductivity Meter (Model 23226-505, VWR), and a Combination pH Electrode (Model 11278-220, Mettler Toledo), respectively. Simultaneously, discrete water samples (120 mL) were collected in duplicate from experimental tanks and preserved with 50uL mercuric chloride (HgCl) for total alkalinity. Standard pH curves were generated on each sampling day prior to pH measurements using TRIS buffer prepared in-house at 5 temperatures. Experimental and algae tanks were drained and cleaned twice weekly and oysters monitored for mortality. Once a week, experimental tanks, reservoir tanks and associated plumbing lines were rotated.

Gonad tissue sampling for stage, sex, and gene expression

A subset of oysters from each treatment were sampled for gonad stage and sex immediately before and after pH treatments. Prior to pH treatment 15 oysters were sampled from O-1, O-2, and F groups, and 9 from D group. Post pH exposure, 9, 6, and 15 oysters were sampled from each treatment for O-1/F, D, and O-2 groups, respectively (distributed equally among replicates tanks). Whole visceral mass was excised and preserved in histology cassettes using PAXgene Tissue FIX System, and processed for gonad analysis by Diagnostic Pathology Medical Group, Inc. (Sacramento, CA).

Adult gonad samples were assigned sex and stage using designations as per (da Silva, Fuentes, and Villalba 2009). To aid in the staging, presence/absence were assigned for spermatogonia/oogonia (undifferentiated), spermatocytes, spermatozoa, oocytes, and ova, and atresia. Fisher's Exact Test of Independence tested differences in sex and gamete stages between 3 comparisons: 1) between temperature treatment groups (chilled, not chilled) to assess the effect of elevated winter temperature, and to estimate gonad status that entered the pH treatment; 2) gonad between low and ambient pH after 52 days in pH treatments (within chilled and not chilled groups) to determine whether pH affected gonad sex ratios and development; and 3) gonad status before and after pH treatments to estimate whether gametes developed, were resorbed, or sex ratios changed during pH treatment (for chilled/not chilled groups separately).

Larval tissue collection, reproductive onset and fecundity

On April 11th reproductive conditioning began by raising temperatures gradually to 14.9±1.1°C until May 1st, then spawning was induced at 18.1±0.1°C and broodstock allowed to spawn volitionally for 70 days. Oysters were held in separate 19L flow-through spawning tanks (8L/hr) by population and treatment, and fed live algae cocktail at 66,000 ± 12,000 cells/mL. Six spawning groups were used for each treatment: two each with F and O-1 populations (14-17 oysters), and one each with D and O-2 populations (9-16 and 111-126 oysters, respectively). The large number of O-2 oysters were used due to their small size and relatedness. *O. lurida* are viviparous spermcasters, brooding larvae to the veliger stage. To capture larvae upon release, outflow was collected in 7.5L buckets using 100 um screens made from 15.25 cm polyvinyl chloride rings and 100 um nylon mesh. Larvae, first observed on May 11th, were collected and counted with triplicate drop counts every one or two days for 60 days.

Larval production was compared between treatments for differences in spawn timing and fecundity. Triplicate drop counts from each daily collection were averaged. Summary statistics for each spawning bucket were compared between treatments (6 spawn tanks per treatment, 12 total), and included: average daily larvae released, cumulative larvae released, maximum larvae released in one day, date of first release, date of maximum release, and number of substantial release days (greater than 10,000 larvae). Cumulative and daily release values were also normalized by the number of broodstock * average broodstock length (cm) and compared between treatments. Distributions were assessed using `qqp` in the `car` package for {R} (Fox and Weisberg 2011), and log-transformed if necessary to meet normal distribution assumptions. Differences in aforementioned summary statistics between pH treatments were assessed using Two-Way ANOVA (aov) and Tukey Honest Significant Differences with `TukeyHSD`.

Gonad & larval gene expression

RNA was isolated from fixed gonad and frozen larval samples. To control for the population-specific effects on gene expression, and due to sequencing capacity limitations, gene expression was only assessed in gonad and larvae from South Sound F1 population (O-1).

Gonad expression was assessed for all four adult treatments. Larval expression was assessed for two treatment groups, pH_{amb}/T_{amb} ("unstressed") and $pH_{low}/T_{.high}$ ("stressed", n=4 per group), released at minimum 3 days apart from separate spawning buckets (to ensure genetic diversity of larval samples). For gonad, tissue was isolated from paraffin blocks using a razor blade and corresponding slide to identify and target only gonad tissue, and isolated using PAXgene fixed tissue RNA kit following manufacturer's instructions with the following adjustments: To homogenize, glass beads were added to each sample and vortexed for ~45 minutes at speed 9. Max centrifuge speeds of 13rpm and 15rpm were used for steps 4, 7 & 12, and 22-24 respectively. Final elution volume was 50ul (two rinses of 20ul and 30ul). To isolate larval RNA, frozen larvae were homogenized in liquid nitrogen with stone mortar and pestle, then isolated following the

RNAzol® RT protocol for Total RNA Isolation. RNA pellet was resuspended in DEPC-treated water and quantified using the Qubit RNA assay with Qubit 3.0 Fluorometer, 2.0ul of each sample for quantification. RNA was sequenced using the QuantSeq method (also known as TagSeq), which sequences only the 3' end of strands, allowing for accurate gene expression data at a reduced cost (Meyer, Aglyamova, and Matz 2011). Library preparation, Illumina sequencing, and demultiplexing were performed at the University of Chicago Genomics Facility.

Demultiplexed Illumina sequence files were inspected for quality using FastQC, adaptor-trimmed and quality filtered (90% bases for >20 quality score) using the FASTX Toolkit. Pseudo-counts of trimmed sequences were determined using Kallisto, aligned against a denovo transcriptome assembled in house using Trinity. The Trinity assembled transcriptome was generated from *O. lurida* gonad RNASeq reads, then collapsed to remove isoforms using `cd-hit-est` in the cd-hit package, and annotated using Blast against the Uniprot/SwissProt database. Read counts were assessed for differential gene expression between pH groups, with gonad and larval RNA assessed separately. Gonad samples were also tested for differential expression between female-only and hermaphroditic oysters. Normalized counts were rounded up to the nearest integer, and contigs with zero counts across all samples were removed, resulting in 12,894 gonad contigs, and 4,410 larval contigs retained for analysis. Sample qualities were assessed using a combination of total counts, heatmap of the count matrix, and by reviewing an initial PCA biplot of all samples together. Gonad samples 3 and 13 had very low gene counts (less than 600), and were removed from the dataset (Figure 2). Using the DESeq package (Love, Huber, and Anders 2014), the Kallisto-normalized counts were tested for significant differences between pH groups. Briefly, the DESeq analysis uses log2 fold change and tests for group differences using the Wald test.

Principal component analysis (PCA) was applied to visualize relationships between samples using all gene counts, and to identify the genes that most influence samples in principal component space. Gene counts were regularized logarithm transformed (`rlog`, DESeq), which reduces heteroskedasticity (very common in gene count data) and incorporates the experiment-wide trend of variance over mean, producing data on the log2 scale and normalized with respect to library size. PCA was then performed on variance-covariance matrix of the normalized counts using `prcomp`. Prinicipal component (PC) axes were tested for significance using Monte carlo permutation test with `ordi.monti` in the Biostats package with 1000 permutations, and PC scores were assessed for multivariate normality using Shapiro-Wilk Normality Test (`shapiro.test`). Due to the large number of variables used in PCA, only the top 10 contributors to each PC and differentially expressed contigs were included as eigenvectors in PCA biplots. One-way perMANOVA tested for significant differences in gonad and larvae global expression between overwintering temperature (gonad), sex (gonad) and pH (gonad, larvae) on Euclidean distance matrices (1000 permutations, `adonis`). Differences in group dispersions were assessed using `betadisper` in the Vegan package.

All data analysis was performed in R version 3.3.1 using RStudio interface.

Figure 2: *Heatmaps of raw gene counts for gonad and larval tissues, separation. Heatmaps were used to confirm sample quality. Gonad samples 13 and 3 were not included in analyses*

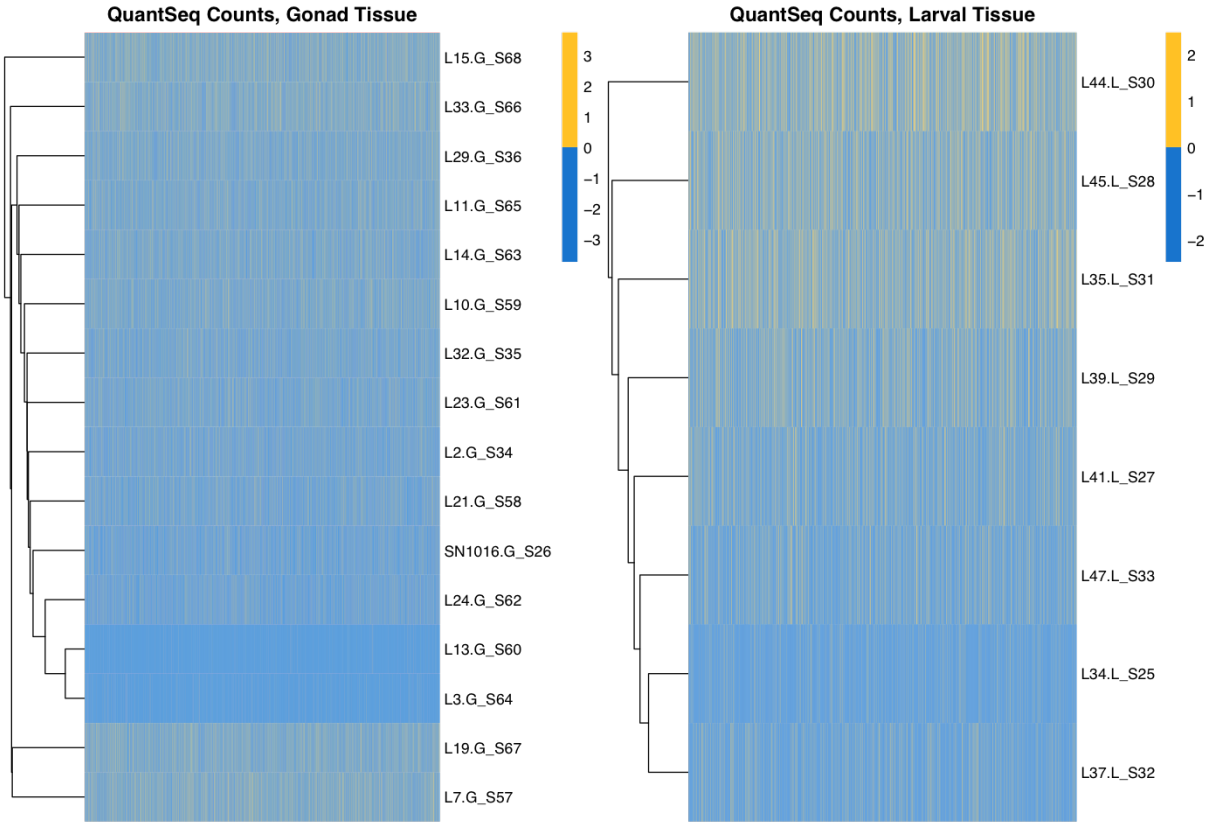

Results

Gonad sex and stage

Gonad stage but not sex was different between the chilled (6°C) and not chilled (10°C) groups prior to pH treatment (p=7.41e-05, Fisher's Exact Test of Independence), with a higher percentage of oysters containing advanced and late-stage gametes in the unchilled group, and the chilled group with significantly more spawned and regressed gonad tissue (Figure 3). As a result, the chilled group entered pH treatment with significantly less advanced gonad tissue. There were significant changes in the chilled groups' gonad stages after pH treatment (p=1.12e-06 & p=0.018 for ambient and low pH, respectively), and between pH treatments (p=0.00829). This indicates that gamete development occurred during the 7 week pH treatment in the chilled group, but that oysters in low pH had less developed gonad tissue compared to ambient pH. No significant differences in gonad sex or stage were observed in the unchilled group after pH treatment. Considerable hermaphroditism was observed within individuals across all groups, with 77.7% of all oysters containing both male and female gametes, and 8.7% and 13.6% of oysters containing only male and female gametes, respectively (N=264).

Fecundity and reproductive timing

Over 60 days, 18.5 million larvae were collected from 767 oysters (122 daily collections of >10,000 larvae). Between treatment groups, no differences were observed in the distribution of daily larvae released, average daily release, maximum release, or cumulative larvae collected (2-way ANOVA). Differences in the timing of release were observed between chilled/unchilled groups, where the date of maximum release was on average 8.3 days later in the chilled group ($F(1,22) = 5.73$, $p=0.0256$). No pH effect was observed on larval release timing or magnitude.

***Figure 3**: Gonad stage and sex before pH treatment (n=54) and after 52 days in ambient pH (7.82±0.02, n=39) and low pH (7.31±0.02, n=39). Gonad developed during the 52 days in both treatments, but oysters in low pH had significantly less developed gonad compared to ambient pH (Fisher's Exact Test, p=0.00829). Sex ratios did not differ significantly between treatments.*

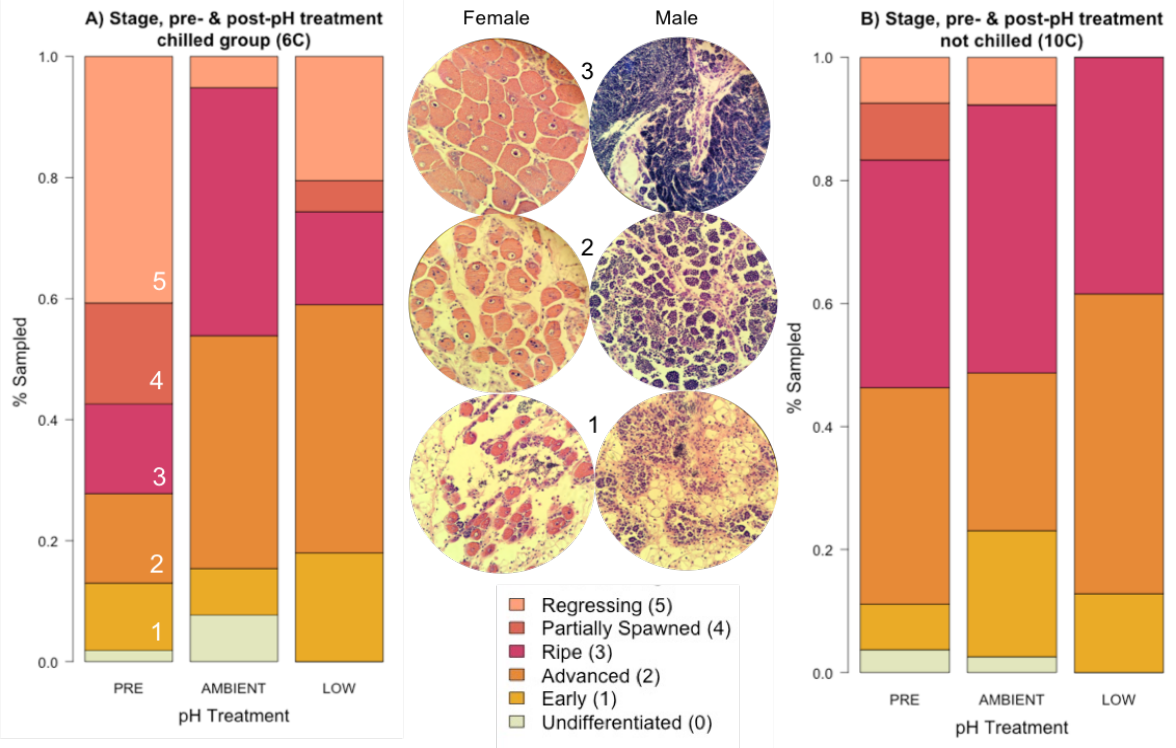

Gonad gene expression

In gonad tissues, 27 genes differed significantly by pH treatment, and 87 differed by gonad sex (female vs. non-female, which included hermaphroditic oysters), but these differences were not preserved after correcting for multiple comparisons (n=12,894). The first four principal components were significant and explained 50% of the total variance. Several genes differentially expressed between gonad sex contributed highly to PC axes (+ in Table 2). One unknown gene (#2) was both identified as differentially expressed between parental pH treatment and a top contributor to and positively correlated with PC4 (* in Table 2). Biplots support the influence of gonad sex on gene counts, and slight clustering by pH within sex (Figure 4). The permANOVA tests indicate no global gene expression differences between temperature ($F(1,14)=0.74$, $p=1$), pH ($F(1,14)=2.2$, $p=0.16$) or sex ($F(1,14)=1.1$, $p=0.26$). No dispersion differences were detected for any group comparisons ($F(1,14)=0.074$, 1.4, 0.03, and $p=0.79$, 0.26, and 0.88 for temperature, pH, and sex, respectively).

Larval gene expression

Nine larval genes were significantly different between parental pH group (DESeq analysis Wald test, $p<0.05$, Figure 5), 6 of which matched with known genes from the Uniprot database (Table 3). USP47, COI, mt:ND5 and TBC1D2, and one unknown gene (#4) were less abundant in larvae from low pH parents, while Tuba3a, rpl8, and two unknown genes (#18, #21) were more abundant. These differences were not preserved after correcting for multiple comparisons (n=4,410). PCA biplot of all larval gene counts revealed clustering by parental pH exposure (Figure 5). The first two principal

***Figure 4**: Biplots of gonad gene expression principal component scores along significant axes, P1-P4. Samples are shown by ambient and low pH exposure (52 days in 7.82±0.02 and 7.31±0.02, respectively), and by gonad sex (female [F]) and hermaphroditic [H]). Eigenvectors shown are the top 10 contributors for each PCxPC comparison). No clustering by overwintering temperature treatment was observed, so temperature was not included. Gonad sex was the dominant factor influence sample clustering. Within sex, where was slight clustering by pH treatment along PC1 and PC3. Global expression did not differ significantly by temperature (F(1,14)=0.72, p=1.0), pH (F(1,4)=1.2, p=0.18) or sex (F(1,14)=0.98, p=0.40) (1-way perMANOVA).*

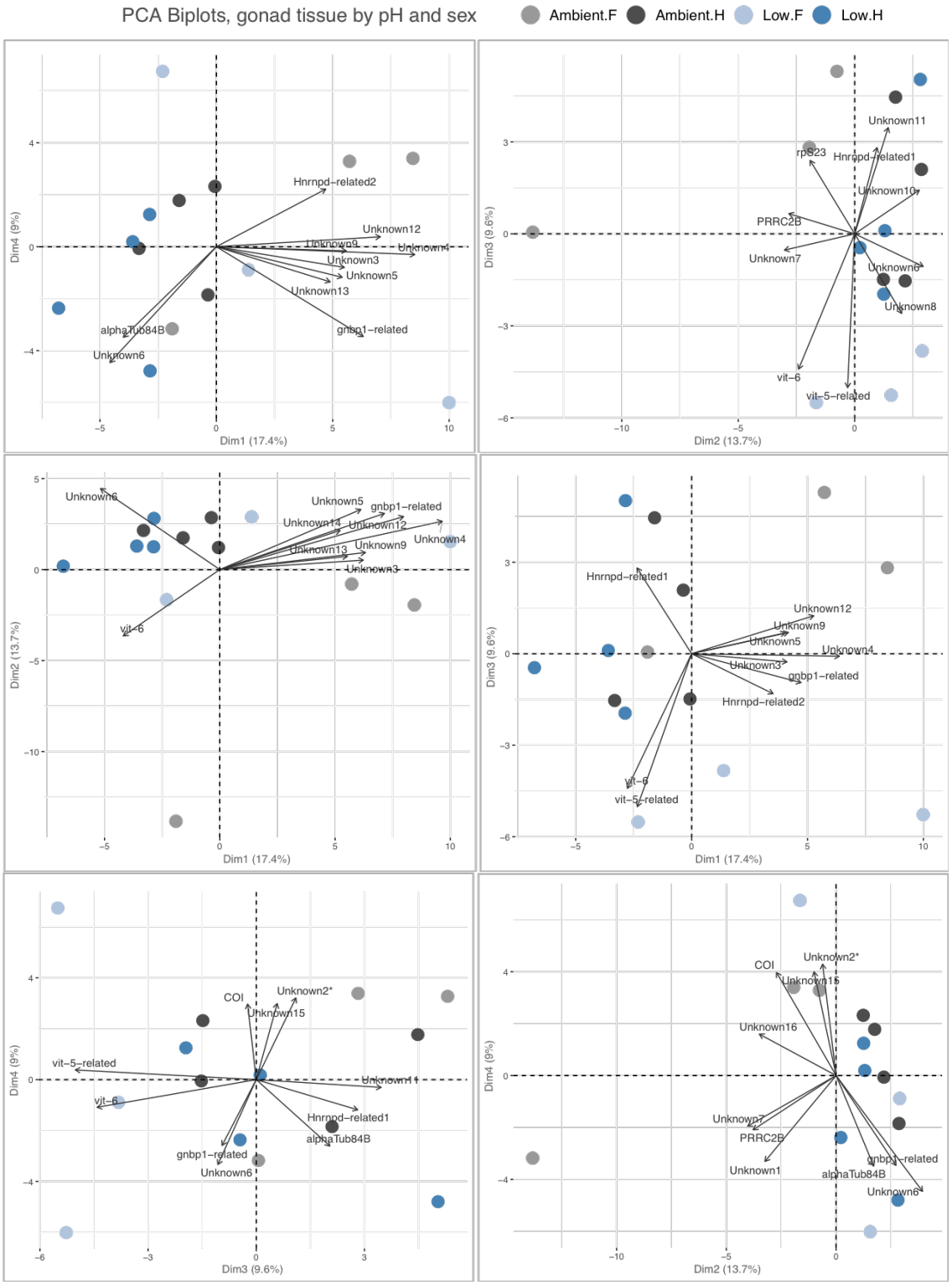

Table 1: Carbonate chemistry parameters for three time points during the pH treatments, which are averages (± SE) from three replicate tanks per treatment. All parameters except for total alkalinity differed significantly between control/ambient (Ctrl.) and experimental/low (Exp.) tanks (One-way ANOVA). More details are available in *Venkataraman et al., 2019*. Definitions: pCO_2=partial pressure of CO_2; DIC=dissolved inorganic carbon; $\Omega_{calcite}$=calcite saturation state; $\Omega_{aragonite}$=aragonite saturation state.

Day	pH*** F(1,16) = 5838, p = 6.12e-22		Total Alkalinity (µmol/kg) F(1,16) = 1.38, p = 0.257		pCO_2 (µatm)*** F(1,16) = 235, p = 5.44e-11		DIC (µmol/kg)* F(1,16) = 7.12, p = 0.0168		$\Omega_{calcite}$*** F(1,16) = 529, p = 1.10e-13		$\Omega_{aragonite}$*** F(1,16) =527, p = 1.14e-13	
	Ctrl.	Exp.	Ctrl.	Exp.	Ctrl.	Exp.	Ctrl.	Exp.	Ctrl.	Exp.	Ctrl.	Exp.
5	7.82 ± 0.004	7.33 ± 0.002	2307.41 ± 25.45	2332.36 ± 31.05	747.51 ± 13.94	2481.23 ± 29.83	2233.41 ± 25.29	2408.51 ± 31.76	1.86 ± 0.02	0.62 ± 0.01	1.16 ± 0.012	0.58 ± 0.007
33	7.81 ± 0.005	7.31 ± 0.004	2747.00 ± 21.13	2917.60 ± 18.36	912.22 ± 12.69	3309.52 ± 7.22	2664.57 ± 19.99	3020.99 ± 17.99	2.23 ± 0.03	0.77 ± 0.02	1.40 ± 0.020	0.48 ± 0.014
48	7.82 ± 0.015	7.29 ± 0.004	2611.40 ± 31.01	2808.39 ± 12.24	863.47 ± 42.42	3343.89 ± 49.49	2533.28 ± 35.45	2920.52 ± 15.11	2.13 ± 0.06	0.68 ± 0.01	1.32 ± 0.035	0.42 ± 0.004

***Figure 5**: Biplot of larval gene expression principal component scores along significant axes (left), P1 and P2, and genes differentially expressed by parental pH (right). Larvae were produced under common environmental conditions. Eigenvectors shown includes top 13 contributors to principal components. Eigenvectors for three additional differentially expressed genes, mt:ND5, Unknown21, and TBC1D2, were also included. Clustering by parental pH is evident, but global expression did not differ significantly by treatment (F(1,6)=1.13, p=0.26, One-way perMANOVA). Nine genes were differentially abundant, 7 if which were identified from the Uniprot/SwissProt database and code for proteins involved in DNA repair (USP47), cytoskeleton microtubules (Tuba3a), aerobic respiration (COI), mitochondrial electron transport (mt:ND5), translation (rpl8), and transcription (Hnrnpd-related2).*

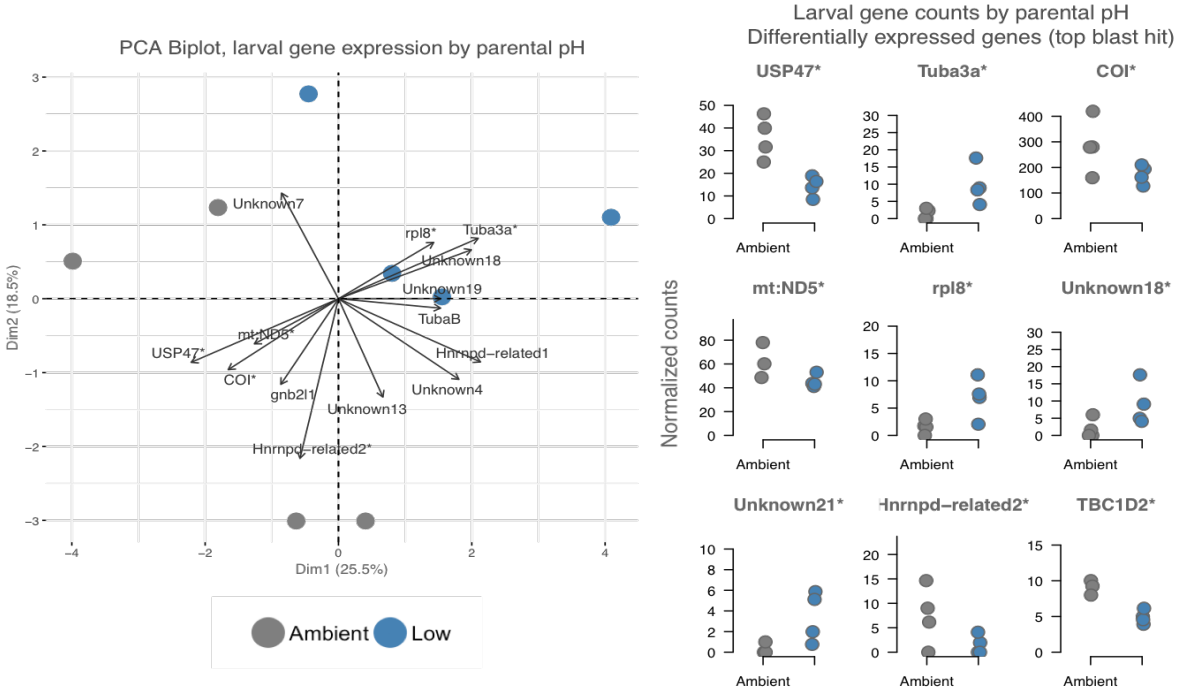

Table 2: Gonad PCA results*. Eigenvalues and variance explained for significant principal components, PC1-4 (50% combined variance explained), with structure coefficients for the top 10 contributors (genes) to each PCxPC comparison. Protein and biological functions are provided, if known. (*) and (+) indicates genes that were also differentially expressed between pH treatment and gonad sex, respectively, and* ***bold*** *are genes that were also top contributors in larval PCA.*

Principal Component	**PC1**	**PC2**	**PC3**	**PC4**	
Eigenvalue (p-value)	23.35 (p=0)	18.3 (p=0)	12.85 (p=0)	12.08 (p=0)	
% var. explained	17.4%	13.7%	9.6%	9.0%	
Gene	**Structure Coefficients**				**Protein &** ***function***
Unknown9 +	0.921	0.137	0.153	-0.027	
Unknown3 +	0.91	0.076	-0.059	-0.132	
Unknown4 +	**0.91**	**0.25**	**-0.012**	**-0.032**	
Unknown13	**0.871**	**0.114**	**0.055**	**-0.241**	
Unknown12 +	0.849	0.31	0.201	0.046	
Unknown14	0.811	0.334	-0.07	-0.334	
Unknown5 +	0.799	0.432	0.135	-0.174	
gnbp1-related +	0.781	0.338	-0.157	-0.428	Beta-1,3-glucan-binding protein: *carbohydrate metabolic process, innate immune*
Hnrnpd-related2	**0.741**	**-0.028**	**-0.277**	**0.350**	**Heterogeneous nuclear ribonucleoprotein D0:** ***Biological rhythms, Transcription***
Unknown7 +	**0.396**	**-0.642**	**-0.113**	**-0.311**	
PRRC2B +	0.353	-0.761	0.177	-0.42	Protein PRRC2B*: RNA binding*
COI	0.223	-0.481	-0.057	0.702	Cytochrome c oxidase subunit 1: *Aerobic respiration*
Unknown2*	0.04	-0.085	0.203	0.592	
rpS23	0.019	-0.398	0.497	0.104	40S ribosomal protein S23: *cytoplasmic translation, protein synthesis*
Unknown11	0.003	0.319	0.767	-0.068	
Unknown15	-0.08	-0.116	0.09	0.461	
Unknown8	-0.102	0.431	-0.554	-0.154	
Unknown10	-0.275	0.526	0.27	-0.057	
Unknown1	-0.347	-0.456	0.208	-0.465	
vit-5-related	-0.364	-0.047	-0.78	0.059	Vitellogenin-5 related: *reproduction*
Unknown16	-0.389	-0.491	-0.086	0.224	
vit-6	-0.401	-0.349	-0.64	-0.158	Vitellogenin-6: *reproduction*
Unknown6	-0.479	0.412	-0.149	-0.468	
alphaTub84B +	-0.518	0.222	0.354	-0.453	Tubulin alpha-1 chain: *Microtubules in cytoskeleton*
Hnrnpd-related1	**-0.563**	**0.23**	**0.673**	**-0.284**	**Heterogeneous nuclear ribonucleoprotein D0:** ***Transcription***

Table 3: Larval PCA results. *Eigenvalues and variance explained for significant principal components, to PC1 and PC2 (44% combined variance explained), with structure coefficients for the top 16 contributors (genes). Protein and biological functions are provided, if known. (*) indicates genes that were also differentially expressed between parental pH treatment, and* ***bold*** *are genes also identified in gonad PCA.*

Principal Component	**PC1**	**PC2**	
Eigenvalue (p-value)	5.67 (p=0)	4.12 (p=0)	
% var. explained	25.5%	18.5%	
Gene	**Structure Coefficients**		**Protein** / **Biological Function**
Tuba3a*	0.873	0.341	Tubulin alpha-3 chain: *Microtubules in cytoskeleton*
Unknown20	0.841	0.032	
Unknown18	0.839	0.279	
TubaB	0.819	-0.068	Tubulin beta chain: *Microtubules in cytoskeleton*
Unknown4	**0.818**	**-0.494**	
rpl8*	0.798	0.426	60S ribosomal protein L8: *Cytoplasmic translation*
Unknown19	0.777	0	
CPVL	0.745	-0.081	Putative serine carboxypeptidase CPVL: *Proteolysis, immune response*
Hnrnpd-related1	**0.520**	**-0.209**	**Heterogeneous nuclear ribonucleoprotein D0: *Biological rhythms, Transcription***
Unknown13	**0.415**	**-0.828**	
Hnrnpd-related2	**-0.228**	**-0.854**	
Unknown7	**-0.422**	**0.706**	**Heterogeneous nuclear ribonucleoprotein D0: *Biological rhythms, Transcription***
gnb2l1	-0.444	-0.594	Guanine nucleotide-binding protein subunit beta-2-like 1: *Apoptosis, Biological rhythms, Cell cycle, Gastrulation, Growth regulation, Translation regulation*
mt:ND5*	-0.728	-0.352	NADH-ubiquinone oxidoreductase chain 5:
COI*	-0.736	-0.427	Cytochrome c oxidase subunit 1: *Aerobic respiration*
USP47*	-0.876	-0.341	Ubiquitin carboxyl-terminal hydrolase 47: *DNA repair*

components were significant, explaining 27.5% and 18.5% of the total variance in the variance-covariance matrix (44% combined). Larval samples with low pH history were positively correlated with PC1, whereas larvae whose parents were not exposed to low pH were negatively correlated with PC1. Within the top 16 gene contributors to PC1 and PC2, known

genes that were also differentially expressed include (in descending order of % contributions with (+) and (-) indicating positive and negative correlations, and (2) and (1) indicating PC axis, respectively): Hnrnpd-related2 (2-), USP47 (1-), Tuba3a (1+), COI (1-), and rpl8 (1+). Combined, the overlaps between differential expression and principal component analyses suggest that larvae with low pH parental history upregulated genes related to cytoskeleton microtubules (Tuba3a) and ribosomal protein production (rpl8), and downregulated genes related to transcription (Hnrnpd-related2), DNA repair (USP47), aerobic respiration (COI). No pH effects were detected on global gene counts ($F(1,6)=1.12$, $p=0.25$, permANOVA), and dispersion did not differ between pH ($F(1,6)=0.30$, $p=0.61$).

Transgenerational gene expression comparison

Five genes were identified as top principal component contributors in both gonad and larval PCA (Tables 2 and 3), two Hnrnpd-related genes that are putative transcription regulators, and three unknown genes. Other top contributing genes that were common between gonad and larval principal components and were closely related but not identical, coded for proteins such as tubulin, cytochrome c-oxidase 1, and ribosomal proteins involved in protein production and translation. A key commonality between the gonad and larval PCA and differential analyses include the upregulation of tubulin-related genes and downregulation in aerobic respiration related genes, both observed in gonad directly exposed to low pH and in larvae with no direct exposures, but with low pH parental history

Discussion

Reproduction

Gamete development was slowed in severe low pH for oysters that entered pH undeveloped. Low pH likely alters *O. lurida* physiology by shifting resources to somatic maintenance and stress response processes, and away from reproduction, resulting in slower rate of gamete growth (Sokolova et al. 2012). These results align with previous studies on other oyster species held in low pH during reproductive conditioning. Gametogenesis was slowed in the both the Eastern oyster (*Crassostrea virginica*) (Boulais et al. 2017) and Sydney rock oyster (*Saccostrea glomerata*) (Parker et al. 2018). In both of these studies, hypercapnia also altered sex ratios but in opposing directions, as the Eastern oyster skewed male, while the Sydney rock oyster skewed female. While sex ratios in this study did not differ significantly between treatment, the less developed low pH group tended to have a lower percentage of females.

Although it was slowed, gametogenesis was not inhibited by severe low pH. There was a 26% increase in late-stage gonad tissue after 52 days of exposure. Future research should assess reproductive activity in a range of pH below 7.3 to determine when gametogenesis is fully inhibited. While not a target of this study, it is significant that gonads progressed at all despite oysters being held two degrees below the reported 12.5°C threshold for gametogenesis in Puget Sound (Hopkins 1936). This is consistent with reports of low-temperature reproduction in a northern Puget Sound *O. lurida* population (Barber et al. 2016), indicating that other assemblages can also be reproductively active at lower temperatures (in this case, 10.4±0.4°C).

Timing and magnitude of larval release were not affected by parental pH exposure, despite the delayed gonad development after the pH treatment. Molecular triggers that induce spawning behavior are thus not likely impacted by a recent and severe parental pH exposure. Gamete viability and fertilization success were not directly measured due to the Olympia oyster's brooding behavior, but no difference in daily or cumulative larval release indicate that, overall, there is no effect of a previous, sustained low pH exposure on fecundity. This is significant, because it establishes that ocean acidification during gametogenesis only, not during spawning, may not affect *O. lurida* reproductive success, given that other requirements are met when needed (for example, ample phytoplankton).

Gene Expression

Low pH exposure during early life stages can have lasting effects on calcifying marine invertebrates, including the Olympia oyster (Hettinger et al. 2012). Here, we show that when only the parent is exposed to low pH, offspring physiology can also be altered. Larvae with parental low pH history differential expressed six known genes, which are involved in the cytoskeleton (Tuba3a), mitochondrial electron transport (mt:ND5), cytoplasmic translation (rpl8), protein transport (TBC1D2), aerobic respiration (COI), and DNA repair (USP47). These results suggest that a physiological memory of pH exposure was transferred from parent to offspring. Four of these functional categories (cytoskeleton,

mitochondrial electron transport, aerobic respiration, protein transport) are observed responses to direct exposure to environmental stressors such as low pH, thermal shock, hypoxia, infection, and toxins (Anderson et al. 2015). In this study, changes to these molecular processes were measured in larvae under ambient, unstressed conditions, indicating that pH effects are not isolated to an individual, but can persist to the next generation.

The cytoskeleton is emerging as one of the most important cellular functions that is disrupted by ocean acidification (Emma L. Thompson et al. 2012; Wei et al. 2015; Dineshram et al. 2012). Oxidative stress caused by free radicals, which are more prevalent as pH decreases, is believed to damage the cytoskeleton (Tomanek 2011). Separate proteomic analyses of two *Crassostrea* oyster species and tissues support the hypothesis that cytoskeleton is a primary target of hypercapnia-induced oxidative stress, as exposure resulted in increased abundances of cytoskeleton proteins (*C. gigas* ctenidia: talin-1, dynein heavy chain 3, and coactosin; *C. virginica* mantle: multiple actin isoforms) (Timmins-Schiffman et al. 2014). In this study Tuba3a and Tubaβ, genes which code for tubulin components which are major constituents of cytoskeletal microtubules, were more abundant in larvae with low pH parental history, despite no direct exposure. A prior transgenerational oyster study (Goncalves et al. 2016) also found that cytoskeleton-related genes (coding for actin) were upregulated in larvae from pH-exposed progenitors when exposed to low pH themselves. While not differentially expressed, a tubulin-coding gene was also a top contributor to the adult gonad principal components along which low pH samples positively correlated, further evidence that the cytoskeleton-related genes are upregulated under hypercapnia.

Previous studies have identified metabolic depression in oyster larvae grown under direct low pH exposure (Dineshram et al. 2012). The present study provides evidence that the metabolism is also depressed in offspring from exposed progenitors. Two metabolic genes were less abundant in low pH larvae: a gene called mt:ND5, which is involved in the mitochondrial electron transport, and COI which codes for cytochrome c-oxidase and supports aerobic respiration. A slower metabolism is one trait by which researchers hypothesize that *O. lurida* may be more resilient to ocean acidification (Waldbusser et al. 2016), but as a carryover effect its benefits are not clear.

It is possible that parental pH exposure primes gametes to up- or down-regulate genes, either through changes in maternal provisioning such as maternal RNA deposited in ova, or via changes to the epigenome. Transgenerational epigenetic modifications are increasingly being considered as possible carryover mechanism. DNA methylation in oysters is predominantly intragenic (within genes), and negatively associated with gene expression which is hypothesized to mediate splice variants (Gavery and Roberts 2013). Stress-induced DNA hypo-methylation in oysters may be a mechanisms for increased phenotypic heterogeneity and resilience to stressors in offspring, however this connection has not yet been documented (Roberts and Gavery 2012). In this study, it is possible that parental effects on larval gene expression were not truly transgenerational, but rather inter-stage, as gonad histology suggests that gametogenesis occurred during pH treatment, thus gametes or germ cells were exposed to low pH in-utero. To truly decipher whether transgenerational carryover effects of low pH are caused by changes to the parental epigenome, researchers must follow phenotype through, at minimum, three generations, since the germ cells that ultimately produce the 3rd generation are present within gametes.

Conclusion

This is the first transcriptomic documentation of ocean acidification-induced changes in a non-stressed second generation. Depressed metabolism, downregulation of protein transport, and upregulation of cytoskeleton indicates that oyster larvae were equipped with a memory of parental exposure. Future studies must explore whether these carryover effects are epigenetic in nature or changes to gametes via maternal effects or direct exposure, and most importantly whether the changes will prepare the larvae for the challenge of ocean acidification.

Acknowledgements

Our gratitude to the following people who assisted with this project's many daily tasks: Grace Crandall, Kaitlyn Mitchell, Olivia Smith, Megan Hintz, Rhonda Elliott, Lindsay Alma, Sam White, Hollie Putnam, Brent Vadopalas, Bayer and Jackson Roberts, the husband Ian and my mom Anne. This project would not be possible without the support and encouragement of the Puget Sound Restoration Fund, which housed the experiment and whose staff contributed expert knowledge of Olympia oyster reproduction and husbandry: Ryan Crim, Stuart Ryan, Alice Helker, Brian Allen, Betsy Peabody, Josh Bouma, and Joth Davis. Thank

you to my committee members Rick Goetz, Jacqueline Padillo-Gamiño, and Steven Roberts.This work was supported by the National Science Foundation Graduate Research Internship Program, the University of Washington College of the Environment Hall Conservation Research Award, and the National Shellfisheries Association Melbourne Carriker Award.

References

Anderson, Kelli, Daisy A. Taylor, Emma L. Thompson, Aroon R. Melwani, Sham V. Nair, and David A. Raftos. 2015. "Meta-Analysis of Studies Using Suppression Subtractive Hybridization and Microarrays to Investigate the Effects of Environmental Stress on Gene Transcription in Oysters." PloS One 10 (3): e0118839.

Barber, Julie S., Jackie E. Dexter, Sarah K. Grossman, Courtney M. Greiner, and James T. Mcardle. 2016. "Low Temperature Brooding of Olympia Oysters (Ostrea Lurida) in Northern Puget Sound." Journal of Shellfish Research 35 (2): 351–57.

Barton, Alan, Burke Hales, George G. Waldbusser, Chris Langdon, and Richard A. Feely. 2012. "The Pacific Oyster, Crassostrea Gigas, Shows Negative Correlation to Naturally Elevated Carbon Dioxide Levels: Implications for near-Term Ocean Acidification Effects." Limnology and Oceanography 57 (3): 698–710.

Boulais, Myrina, Kyle John Chenevert, Ashley Taylor Demey, Elizabeth S. Darrow, Madison Raine Robison, John Park Roberts, and Aswani Volety. 2017. "Oyster Reproduction Is Compromised by Acidification Experienced Seasonally in Coastal Regions." Scientific Reports 7 (1): 13276.

Dineshram, R., Kelvin K. W. Wong, Shu Xiao, Ziniu Yu, Pei Yuan Qian, and Vengatesen Thiyagarajan. 2012. "Analysis of Pacific Oyster Larval Proteome and Its Response to High-CO2." Marine Pollution Bulletin 64 (10): 2160–67.

Feely, Richard A., Terrie Klinger, Jan A. Newton, and Meg Chadsey. 2012. Scientific Summary of Ocean Acidification in Washington State Marine Waters. US Department of Commerce, National Oceanic and Atmospheric Administration, Office of Oceanic and Atmospheric Research.

Fox, John, and Sanford Weisberg. 2011. An R Companion to Applied Regression. Vol. Second Edition. Thousand Oaks CA: Sage.

Gavery, Mackenzie R., and Steven B. Roberts. 2013. "Predominant Intragenic Methylation Is Associated with Gene Expression Characteristics in a Bivalve Mollusc." PeerJ 1 (November): e215.

Gentemann, Chelle L., Melanie R. Fewings, and Marisol García-Reyes. 2017. "Satellite Sea Surface Temperatures along the West Coast of the United States during the 2014-2016 Northeast Pacific Marine Heat Wave: Coastal SSTs During 'the Blob.'" Geophysical Research Letters, NOAA Tech. Rep. NMFS SSRF-671, 44 (1): 312–19.

Goncalves, Priscila, Kelli Anderson, Emma L. Thompson, Aroon Melwani, Laura M. Parker, Pauline M. Ross, and David A. Raftos. 2016. "Rapid Transcriptional Acclimation Following Transgenerational Exposure of Oysters to Ocean Acidification." Molecular Ecology 25 (19): 4836–49.

Grabowski, Jonathan H., Robert D. Brumbaugh, Robert F. Conrad, Andrew G. Keeler, James J. Opaluch, Charles H. Peterson, Michael F. Piehler, Sean P. Powers, and Ashley R. Smyth. 2012. "Economic Valuation of Ecosystem Services Provided by Oyster Reefs." Bioscience 62 (10): 900–909.

Heare, J. Emerson, Samuel J. White, Brent Vadopalas, and Steven B. Roberts. 2018. "Differential Response to Stress in Ostrea Lurida as Measured by Gene Expression." PeerJ 6 (January): e4261.

Hedgecock, Dennis, and Alexander I. Pudovkin. 2011. "Sweepstakes Reproductive Success in Highly Fecund Marine Fish and Shellfish: A Review and Commentary." Bulletin of Marine Science 87 (4): 971–1002.

Hettinger, Annaliese, Eric Sanford, Tessa M. Hill, Ann D. Russell, Kirk N. S. Sato, Jennifer Hoey, Margaux Forsch, Heather N. Page, and Brian Gaylord. 2012. "Persistent Carry-over Effects of Planktonic Exposure to Ocean Acidification in the Olympia Oyster." Ecology 93 (12): 2758–68.

Hopkins, A. E. 1936. "Ecological Observations on Spawning and Early Larval Development in the Olympia Oyster (Ostrea Lurida)." Ecology 17 (4): 551–66.

Love, Michael I., Wolfgang Huber, and Simon Anders. 2014. "Moderated Estimation of Fold Change and Dispersion for RNA-Seq Data with DESeq2." Genome Biology 15 (12): 550.

Meyer, E., G. V. Aglyamova, and M. V. Matz. 2011. "Profiling Gene Expression Responses of Coral Larvae (Acropora Millepora) to Elevated Temperature and Settlement Inducers Using a Novel RNA-Seq

Procedure." Molecular Ecology 20 (17): 3599–3616.

Parker, Laura M., Wayne A. O'Connor, Maria Byrne, Michael Dove, Ross A. Coleman, Hans-O Pörtner, Elliot Scanes, Patti Virtue, Mitchell Gibbs, and Pauline M. Ross. 2018. "Ocean Acidification but Not Warming Alters Sex Determination in the Sydney Rock Oyster, Saccostrea Glomerata." Proc. R. Soc. B 285 (1872): 20172869.

Parker, Laura M., Wayne A. O'Connor, David A. Raftos, Hans-Otto Pörtner, and Pauline M. Ross. 2015. "Persistence of Positive Carryover Effects in the Oyster, Saccostrea Glomerata, Following Transgenerational Exposure to Ocean Acidification." PloS One 10 (7): e0132276.

Polson, Maria P., and Danielle C. Zacherl. 2009. "Geographic Distribution and Intertidal Population Status for the Olympia Oyster, Ostrea Lurida Carpenter 1864, from Alaska to Baja." Journal of Shellfish Research 28 (1): 69–77.

Putnam, Hollie M., and Ruth D. Gates. 2015. "Preconditioning in the Reef-Building Coral Pocillopora Damicornis and the Potential for Trans-Generational Acclimatization in Coral Larvae under Future Climate Change Conditions." The Journal of Experimental Biology 218 (15): 2365–72.

Roberts, Steven B., and Mackenzie R. Gavery. 2012. "Is There a Relationship between DNA Methylation and Phenotypic Plasticity in Invertebrates?" Frontiers in Physiology 2 (January): 116.

Silva, Patricia Mirella da, José Fuentes, and Antonio Villalba. 2009. "Differences in Gametogenic Cycle among Strains of the European Flat Oyster Ostrea Edulis and Relationship between Gametogenesis and Bonamiosis." Aquaculture 287 (3–4): 253–65.

Sokolova, Inna M., Markus Frederich, Rita Bagwe, Gisela Lannig, and Alexey A. Sukhotin. 2012. "Energy Homeostasis as an Integrative Tool for Assessing Limits of Environmental Stress Tolerance in Aquatic Invertebrates." Marine Environmental Research 79 (August): 1–15.

Thompson, E. L., W. O'Connor, L. Parker, P. Ross, and D. A. Raftos. 2015. "Differential Proteomic Responses of Selectively Bred and Wild-Type Sydney Rock Oyster Populations Exposed to Elevated CO2." Molecular Ecology 24 (6): 1248–62.

Thompson, Emma L., Daisy A. Taylor, Sham V. Nair, Gavin Birch, Paul A. Haynes, and David A. Raftos. 2012. "Proteomic Discovery of Biomarkers of Metal Contamination in Sydney Rock Oysters (Saccostrea Glomerata)." Aquatic Toxicology 109 (March): 202–12.

Timmins-Schiffman, Emma, William D. Coffey, Wilber Hua, Brook L. Nunn, Gary H. Dickinson, and Steven B. Roberts. 2014. "Shotgun Proteomics Reveals Physiological Response to Ocean Acidification in Crassostrea Gigas." BMC Genomics 15 (November): 951.

Tomanek, Lars. 2011. "Environmental Proteomics: Changes in the Proteome of Marine Organisms in Response to Environmental Stress, Pollutants, Infection, Symbiosis, and Development." Annual Review of Marine Science 3: 373–99.

Waldbusser, George G., Matthew W. Gray, Burke Hales, Chris J. Langdon, Brian A. Haley, Iria Gimenez, Stephanie R. Smith, Elizabeth L. Brunner, and Greg Hutchinson. 2016. "Slow Shell Building, a Possible Trait for Resistance to the Effects of Acute Ocean Acidification." Limnology and Oceanography 61 (6): 1969–83.

Wei, Lei, Qing Wang, Xuanxuan Ning, Changkao Mu, Chunlin Wang, Ruiwen Cao, Huifeng Wu, et al. 2015. "Combined Metabolome and Proteome Analysis of the Mantle Tissue from Pacific Oyster Crassostrea Gigas Exposed to Elevated pCO2." Comparative Biochemistry and Physiology. Part D, Genomics & Proteomics 13 (March): 16–23.

Electronic Journal of Applied Multivariate Statistics
Volume 9, 2018

Article

Characterization of Pacific oyster *Crassostrea gigas* proteomic response to natural environmental differences

Yaamini R. Venkataraman
School of Aquatic and Fishery Sciences, University of Washington
E-mail: yaaminiv@uw.edu

Received March 2019; accepted in revised form April 2019; published June 2019

Abstract

Global climate change is rapidly altering coastal marine ecosystems that are important for food production. A comprehensive understanding of how organisms will respond to these complex environmental changes can come only from observing and studying species within their natural environment. To this end, the effects of environmental drivers—pH, dissolved oxygen content, salinity, and temperature—on Pacific oyster *Crassostrea gigas* physiology were evaluated in an outplant experiment. Sibling juvenile oysters were outplanted to eelgrass and unvegetated habitat at 5 different estuarine sites within the Acidification Nearshore Monitoring Network in Washington State, USA, to evaluate how regional environmental drivers influence molecular physiology. Within each site, we also determined if eelgrass presence, which buffered pH conditions, changed the oysters' expressed proteome. A novel, 2-step, gel-free proteomic approach was used to identify differences in protein abundance in *C. gigas* ctenidia tissue after a 29 d outplant by (1) identifying proteins in a data-independent acquisition survey step and (2) comparing relative quantities of targeted environmental response proteins using selected reaction monitoring. While there was no difference in protein abundance detected between habitats or among sites within Puget Sound, *C. gigas* outplanted at Willapa Bay had significantly higher abundances of antioxidant enzymes and molecular chaperones. Environmental factors at Willapa Bay, such as higher average temperature, may have driven this protein abundance pattern. These findings generate a suite of new hypotheses for lab and field experiments to compare the effects of regional conditions on physiological responses of marine invertebrates.

Introduction

Global climate change will influence estuarine dynamics and impact the organisms that inhabit these environments. Estuaries are already variable across spatial and temporal scales in terms of phytoplankton production (Pennock & Sharp 1986), nutrient availability (Paerl et al. 2014), heavy metal contamination (Liu et al. 2015), salinity (Banas et al. 2004), and carbonate chemistry (Feely et al. 2010, Pelletier et al. 2018). Since climate change will affect these parameters, it is important to consider how estuarine organisms will respond.

Proteomics, the study of protein abundance and expression, can be used to shed light on physiological changes at a molecular level. Proteins direct all major cellular functions; thus, examining protein abundance provides direct evidence of an organism's physiological response to the estuarine environment (Tomanek 2014). The proteome is dynamic, as it must rapidly respond to perturbation, providing mechanistic information that standard gene expression and mRNA quantification studies cannot (Veldhoen et al. 2012, Flores-Nunes et al. 2015a). As a result of the proteome's dynamic nature, proteins analyzed at the time of collection represent an organism's response to the environment in near real-time. Long-term exposure to environmental

conditions, as well as natural organismal aging, are also reflected in the proteome (Hercus et al. 2003). Discovery-based proteomic methods can elucidate responses to environmental drivers (Flores-Nunes et al. 2015a). Several studies have connected protein abundances with changes in laboratory-simulated environmental conditions, identifying key proteins and mechanisms involved in specific environmental responses (Timmins-Schiffman et al. 2014, Dineshram et al. 2016, Meng et al. 2017). While these studies provide insight into organismal adaptation and physiology, laboratory studies alone cannot fully encapsulate the effects of multiple environmental drivers within an ecosystem context (Riebesell & Gattuso 2015).

Although challenging, *in situ* field studies provide a necessary biological realism when considering variable environments (Slattery et al. 2012, Cornwall & Hurd 2016). Such experiments can be leveraged to study the effects of multiple environmental drivers on organismal physiology and to incorporate realistic variability, as opposed to examining the effect of a single stressor on an organism (Riebesell & Gattuso 2015). Through transcriptomics, Chapman et al. (2011) demonstrated the power of an *in situ* experimental design for examining the impacts of regional environmental conditions on eastern oyster *Crassostrea virginica* physiology. Transcript signatures from *C. virginica* sampled from various locations in the southeastern United States revealed that temperature, pH, salinity, dissolved oxygen, and pollutant load at each location impacted gene expression. Furthermore, they were able to disentangle the interactions of these environmental factors on gene expression. RNA and protein abundances can be influenced by several environmental factors, and *in situ* studies can determine which drivers will be more important to consider for organismal physiology.

Marine invertebrates have proven to be informative bioindicators in proteomic studies to examine the effects of *in situ* conditions on organismal physiological responses to environmental change. When marine invertebrates have been exposed to varying environmental conditions, proteomics have demonstrated changes in cellular defense, immune responses, and genome function (Veldhoen et al. 2012). Changes in protein abundance in bivalves like the Pacific oyster *Crassostrea gigas* and blue mussels *Mytilus edulis* spp. have been used to develop biomarkers for environmental contaminants (Slattery et al. 2012, Beyer et al. 2017). Proteomic responses to natural environmental drivers have also been evaluated in bivalves. For example, shotgun proteomic analysis of *M. edulis* ctenidia from Baltic Sea microcosms revealed that low salinity conditions led to decreased abundance of cytoskeleton proteins, as well as calcium-binding messenger calmodulin, which plays an important role in signaling and intracellular membrane trafficing pathways (Campos et al. 2016). Using a growing wealth of genomic information to understand how these species fare under differential environmental conditions is critical for monitoring natural populations and commercial aquaculture.

Pacific oyster *C. gigas* rearing in estuarine environments in Washington State (WA), USA, provides an ideal system to examine the effect of *in situ* environmental conditions on the expressed proteome. *C. gigas* are extensively farmed in 2 different estuarine systems that show substantial regional variation: Puget Sound and Willapa Bay. Puget Sound is a complex estuarine system with interconnected sub-basins, each with different freshwater inputs, residence times, and stratification levels (Feely et al. 2010, Bianucci et al. 2018, Pelletier et al. 2018). Willapa Bay is a large, shallow estuary on the Pacific coast that exchanges approximately half its water volume with the Pacific Ocean at each tide (Banas et al. 2004, 2007). Seasonality and location within Puget Sound dictates temperature, dissolved oxygen, salinity, and pH conditions, while Willapa Bay conditions are influenced by diurnal fluctuations and proximity to either the ocean or rivers draining into the bay (Banas et al. 2007, Feely et al. 2010, Ruesink et al. 2015).

Both Puget Sound and Willapa Bay also host eelgrass *Zostera* spp. beds that affect environmental conditions, such as oxygen concentrations, on diurnal time scales. The 2012 Washington State Blue Ribbon Panel on Ocean Acidification outlines key early actions, which include the examination of 'vegetation-based systems of remediation' (Action 6.1.1) to improve local pH through photosynthetic drawdown of carbon dioxide. This experiment set out to test whether protein abundance patterns reflect reduced stress within vegetation. For example, eelgrass beds may reduce emersion stress relative to unvegetated areas through shading, the retention of water, and increased evaporative cooling at low tide. They can also ameliorate effects of ocean acidification through photosynthetic activity. Reduced pathogen prevalence has also been

documented in seagrass beds, but not specifically in eelgrass (Lamb et al. 2017). In contrast, eelgrass beds may drive more extreme carbonate chemistry conditions (Pacella et al. 2018). Lowe et al. (2018) also found that *C. gigas* shell strength and survival was significantly lower in eelgrass habitats in WA. Understanding how different aquaculture grow-out locations and habitats will affect the oyster's ability to persist through environmental change is crucial for the industry and the ecosystem.

The purpose of this study was to use proteomic techniques to uncover the impacts of environmental drivers on Pacific oyster physiological outcomes in estuarine environments in WA. Naturally existing environmental variation was harnessed by outplanting *C. gigas* in different locations within Puget Sound and Willapa Bay, and habitat effects were taken into consideration by placing oysters in eelgrass and unvegetated habitats. Gel-free proteomic methods were used to examine the effects of outplant conditions on relative quantities of all expressed proteins in a series of *in situ* experiments in order to identify differentially abundant proteins. We predicted that differences in environmental drivers at each outplant location and within outplant habitats would yield unique protein abundance patterns. Oysters at outplant locations with warmer water temperatures, more variable water temperatures, lower dissolved oxygen content, lower salinity, or lower pH may have higher abundances of proteins related to environmental response. Eelgrass beds were expected to ameliorate stressful conditions, resulting in lower abundances of environmental stress response proteins than oysters in unvegetated habitats...

Methods

Shellfish deployment

Sibling juvenile *Crassostrea gigas* (average shell length: 27.2 mm; age: 2 mo) were outplanted for 29 d starting 19 June 2016 at 5 locations: Case Inlet (CI), Fidalgo Bay (FB), Port Gamble Bay (PG), Skokomish River Delta (SK), and Willapa Bay (WB) in Washington State, USA (Table 1, Fig 1). These sites were selected for differences in environmental parameters, as well as for the presence of unvegetated areas and eelgrass beds within each site. All sites were part of the Acidification Nearshore Monitoring Network (ANeMoNe; Washington Department of Natural Resources), which is a network of sensors placed in various WA locations to monitor marine chemistry. Prior to the outplant, oysters were reared in a controlled hatchery setting. At each site and habitat combination, custom-built Durafet-based sensors (Honeywell) were used to monitor pH. Commercially available MiniDOT loggers (Precision Measurement Engineering) were used to measure dissolved oxygen, and Odyssey loggers were used to measure conductivity. All sensors recorded temperature measurements, and all sensors logged at 10 min intervals across the outplant period, with the exception of SK, where sensors were installed 2 d into the outplant period. At each site, juvenile oysters were placed in bags of 5 oysters each directly onto the substrate at a tidal height of –1.5 ft mean lower low water (MLLW), both inside and outside of eelgrass beds (n = 15 per habitat type), for a total of 30 outplanted oysters site^{-1}. The animals were uniformly placed less than a lateral distance of 0.5 m from the sensors at the same tidal height as the instruments. Oysters were housed in exclusion cages to prevent predation. Juvenile oysters remained at each site for a 29 d exposure period. Because the ctenidia is the primary site where oysters interact with the environment, ctenidia samples were dissected at the end of the outplant and held on dry ice until storage at –80°C (Beyer et al. 2017, Meng et al. 2017).

Environmental data were treated as follows. Conductivity observations were removed when less than zero, which occurs when the instrument is dry at low tide. Remaining observations were converted to salinity measurements using the 'swSCTp' function in the 'oce' package in R 3.5.0 (Kelley & Richards 2018, R Core Team 2018), with temperature at 25°C and pressure at 10 dbar (100 kPa). For dissolved oxygen, pH, and salinity data sets, data were removed when collected by probes (1) during low tide or (2) when tidal depth was <1 foot (<30.5 cm) to remove readings where the probes may have been exposed. Values collected during low tide or a depths <30.5 cm were retained for temperature data sets. Outliers were screened using the Tukey method for temperature, dissolved oxygen, pH, and salinity data sets (Hoaglin et al. 1986). Uniform outplant tidal heights were checked using 'prop.test' in R (R Core Team 2018).

A non-metric multidimensional scaling analysis (NMDS) was used to evaluate differences in environmental parameters. First, mean and variance were calculated for each day of the outplant. Values were log transformed, and a separate Gower's distance matrix was

calculated for daily mean and daily variances, accounting for missing data. The NMDS was conducted with the Gower's distance matrix to visually compare means or variances between sites and habitats. Significant differences between site and habitat were identified using a 1-way analysis of similarities (ANOSIM) for each environmental parameter. Pairwise ANOSIM tests for significant 1-way ANOSIM results and 2-way ANOSIM tests by site and habitat were not conducted due to lack of replicates within each site–habitat combination. R scripts are available in the supplementary Github repository (Venkataraman et al. 2018).

Protein discovery

To identify select protein targets for characterization across locations and environmental conditions, a subset of tissue samples was analyzed with data-independent acquisition (DIA) mass spectrometry analysis. Two tissue samples were used from each site to make a peptide library and maximize the amount of protein abundance data collected from each sample.

Protein quantification

Tissue samples were homogenized in a solution of 50 mM NH_4HCO_3 with 6 M urea (500 per l). Tissues were then sonicated 3 times (Sonic Dismembrator Model 100; Fisher Scientific) for 10 s each and cooled between sonications in a bath of ethanol and dry ice. Protein quantities were measured with the Pierce BCA Protein Assay Kit microplate assay with a limited quantity of sonicated sample (11 µl). The protein concentration was measured via spectroscopy at 540 nm in a Labsystems Multiskan MCC/340 and accompanying Ascent v.2.6 software. Protein concentrations were calculated based on a standard curve with BSA (Pierce) per manufacturer's instructions.

Protein digestion

Protein digestion followed the protocol outlined in Timmins-Schiffman et al. (2017). To each sample of 30 µg protein,1.5 M Tris pH 8.8 buffer (6.6 µl) and 200 mM tris(2-carboxyethyl)phosphine (TCEP) (2.5 µl) were added. After solvent additions, each sample's pH was verified to be basic (pH ≥ 8), and placed on a 37°C heating block for 1 h. Iodoacetamide (200 mM, 20 µl) was then added to each sample to maximize digestion enzyme access to protein cleavage sites. Samples were covered with aluminum foil to incubate in the dark for 1 h at room temperature. Afterwards, diothiolthreitol (200 mM, 20 µl) was added and samples were incubated at room temperature for 1 h. Lysyl endopeptidase (Wako Chemicals) was then added to each sample in a 1 µg enzyme:30 µg oyster protein ratio, followed by 1 h of incubation at room temperature. Urea was diluted with NH_4HCO_3 (25 mM, 800 µl) and HPLC-grade methanol (200 µl). Trypsin (Promega) was added to each sample in a 1 µg trypsin:30 µg oyster protein ratio for overnight digestion at room temperature.

Peptide isolation

After overnight incubation, samples were evaporated to near dryness at 4°C with a speed vacuum (CentriVap® Refrigerated Centrifugal Concentrator Model 7310021). Samples were then reconstituted in 100 µl of a 5% acetonitrile and 0.1% trifluoroacetic acid (Solvent A) to isolate peptides. If samples were not at pH ≤ 2, then 10–20 µl aliquots of 10% formic acid were added until this pH was achieved.

Before desalting peptide samples, Macrospin C18 columns (The Nest Group) were prepared by adding 200 µl of a 60% acetonitrile with 0.1% trifluoroacetic acid (Solvent B). The columns were spun for 3 min at 2000 rpm (448 rcf), and flow-through liquid from the column was discarded. The spinning and discarding process was completed a total of 4 times. To wash columns, 200 µl of Solvent A was added to each column. The columns were once again spun for 3 min at 2000 rpm (448 rcf) and liquid was discarded afterwards; the solvent addition, spinning, and discarding process was completed a total of 3 times.

To bind peptides to the columns, digested peptides were added to prepared columns, then the columns were spun at 3000 rpm (1008 rcf) for 3 min. The filtrate was pipetted back onto the column and spun again at 3000 rpm (1008 rcf) for 3 min. Solvent A (200 µl) was added to each column 3 separate times, then the column was spun for 3 min at 3000 rpm (1008 rcf) to wash salts off the column.

Peptides were eluted with 2 additions of 100 µl of Solvent B to each column. Columns were spun at 3000 rpm (1008 rcf) for 3 min and the peptide fraction (filtrate) was reserved. Samples were placed in a speed vacuum at 4°C until they were nearly dry (approximately 2 h), to dry the peptides. Peptides were reconstituted with 60 µl of 3% acetonitrile + 0.1% formic acid, and stored at –80°C.

Internal standard addition

The Peptide Retention Time Calibration Mixture (PRTC; Pierce) is used as an internal standard to ensure consistency of peptides

detected and measured throughout a mass spectrometry run. The stock solution of PRTC was diluted to 0.2 pmol μl^{-1} using 3% acetonitrile with 0.1% formic acid. In a clean centrifuge tube, 6 µg of oyster protein and 0.376 pmol of PRTC were mixed together as per the PRTC user's guide. Sample volume was brought up to 15 µl using a 3% acetonitrile and 0.1% formic acid solution. A quality control solution was also prepared (1 µl PRTC + BSA:3 µl 3% acetonitrile and 0.1% formic acid solution).

DIA mass spectrometry

Peptides were analyzed on an Orbitrap Fusion Lumos mass spectrometer (Thermo Scientific) using DIA mass spectrometry. DIA analyses were completed as a comprehensive, non-random analytical method for detecting peptide ions present within a sample to create a peptide library. The peptide library was then leveraged to develop a targeted proteomics assay for quantification (see Section 2.5). A 30 cm analytical column and 3 cm pre-column were packed in-house with 3 µm C18 beads (Dr. Maisch). Samples were run in a randomized order. A blank injection followed each sample, with procedural blanks run at the very end. Every injection was 3 µl, which included 1 µg of oyster protein and 0.0752 pmol of PRTC. Peptides were analyzed in MS1 over the *m*/*z* range of 450–950 with 12 *m*/*z* wide windows with 5 *m*/*z* overlaps (Egertson et al. 2013). MS1 resolution was 60 000 and the automatic gain control (AGC) target was 400 000 with a 3 s cycle time. The MS2 loop count was set to 20 and MS2 data were collected with a resolution of 15 000 on charge state of 2 with an AGC target of 50 000. No dynamic exclusion was used.

Peptide-centric proteomic analyses

Unknown peptide spectra from mass spectrometry samples were matched with known peptides using peptide-centric analysis in the PECAN software (Ting et al. 2015). Raw mass spectrometry files were converted to mzML files, then demultiplexed using MSConvert (Chambers et al. 2012). The *C. gigas* proteome was digested with *in silico* tryptic digest using the Protein Digestion Simulator (Riviere et al. 2015). All known peptides from the mzML files were identified in comparison to the digested *C. gigas* proteome (Riviere et al. 2015).

The PECAN-generated spectral library (.blib) file was used to detect peptides of interest in raw DIA files in Skyline (MacLean et al. 2010). Skyline identified peptides using chromatogram peak picking, where ions that elute at the same time and mass are detected as a peptide (file available at https://panoramaweb.org/aqqYoa.url). All PRTC peptides and approximately 100 different oyster proteins and their peptide transitions were manually checked for retention time and peak area ratio consistency to determine a Skyline auto peak picker error rate (24.3 ± 25%, range: 0–100%).

Proteins had to satisfy 4 criteria to be considered appropriate targets for the study. (1) After an extensive literature search, functions related to oxidative stress, hypoxia, heat shock, immune resistance, shell formation, growth, and cellular maintenance were determined useful for evaluating environmental response. Proteins with annotations matching these functions were considered potential targets. (2) Protein data were then evaluated in Skyline to ensure there were no missing data for any peptide or sample. (3) Peaks with significant interference from other peptides were not considered. (4) Proteins needed at least 2 peptides with 3 transitions $peptide^{-1}$ to quality as a potential target for downstream assays. The 15 proteins (41 peptides and 123 transitions) that matched all of these criteria were selected as targets (Table 2).

Selected reaction monitoring assay

Following the protein discovery phase (i.e. DIA), proteins were isolated as described above from an additional 5 randomly selected samples per site and habitat combination (for a total of 5 oysters $group^{-1}$) and analyzed with selected reaction monitoring (SRM). Samples were prepared as described for DIA, except tissue samples were homogenized in 100 □l, and peptide samples were evaporated at 25°C after peptide isolation.

Proteins of interest identified from the DIA analysis were used as targets in a SRM assay following the workflow and informatic pipeline of Timmins-Schiffman et al. (2017). Target peptide transitions were monitored using SRM on a Thermo TSQ Vantage. SRM data were collected during a gradient of 2–60% acetonitrile over 40 min. All samples were run in technical duplicates in a randomized order with a 1 □g oyster peptide and 0.0752 pmol PRTC injection. A quality control injection and blank injection were run after every 5 sample injections, and PRTC peptides were monitored throughout the experiment.

Target peptide specificity

To ensure SRM assay specificity to oyster peptides of interest, oyster peptides were diluted in a background matrix of similar complexity (Pacific geoduck *Panopea generosa* peptides), then analyzed using the oyster SRM assay. An oyster-specific SRM target would decrease in abundance with a decreasing abundance of oyster peptides in a mixture. Non-specific peptides—more likely to be found in background matrix of similar complexity—or peptides susceptible to interference would not correlate with oyster peptide abundance, and therefore would be uninformative. A total of 5 *C. gigas* samples used for SRM were randomly selected and pooled in equal quantities. A 10 sample oyster:geoduck dilution series was prepared and run using the same methods as other SRM samples.

Target analysis

Raw SRM files, a background *C. gigas* proteome, and the PECAN spectral library file from DIA were used to create a Skyline document (file available at https://panoramaweb.org/aqqYoa.url). Correct transition peaks were selected based on predicted retention times from DIA results by comparing the relative retention times between identical PRTC peptides in the DIA and SRM datasets (R^2 = 0.99431). Based on peptide specificity analyses, heat shock protein 70 B2 and one constituent peptide of glucose-6-phosphate 1-dehydrogenase were removed from analyses.

Further filters were applied to the data to maintain only high quality peptides and transitions in the analysis. Coefficients of variation (CVs) were calculated between technical replicates for each peptide transition. Peptides were removed from the data set if CV > 20%. To maintain high sample quality, any sample missing data for more than 50% of peptide transitions was deemed poor quality for downstream analyses, and was excluded. Abundance data were normalized using total ion current (TIC) values from the mass spectrometer.

Averaged technical replicate data were used to determine if peptides were differentially abundant between outplant sites and habitats. Before proceeding with the analysis, peptide abundances were subjected to a Hellinger transformation, to give low weights to any peptides with low counts. A NMDS was used to visually compare relative peptide abundance. One-way ANOSIM tests by site, region (Puget Sound vs. Willapa Bay), and habitat, as well as a 2-way ANOSIM test by site and habitat were used to determine significant differences. Pairwise ANOSIM tests and post hoc similarity percentage (SIMPER) analyses were conducted for each 1- or 2-way ANOSIM result significant at the $p < 0.05$ level. The first 10 SIMPER entries were deemed influential peptides for each significant comparison.

The importance of environmental variables for explaining peptide abundance was evaluated with a redundancy analysis (RDA). For each site and habitat combination, mean and variance were calculated for pH, dissolved oxygen, salinity, and temperature over the course of the entire outplant. Environmental variables were then used as predictors to constrain peptide abundance. Predictors with missing values were not included. A triplot was used to visually assess differences in peptide abundance by site and habitat and the influence of individual peptides and environmental parameters. ANOVA was used to calculate significance of the RDA and environmental variables, with predictors deemed significant at $p < 0.05$. Since estuarine sites are highly variable, a second RDA was conducted constraining peptide abundance by environmental conditions on the day of collection to evaluate the robustness of the proteomic methods. R scripts are available in the supplementary Github repository (Venkataraman et al. 2018).

Results

Conditions at outplant locations

Outplanted oysters experienced environmental variables representative of standard summer conditions in Puget Sound (PS) and WB. Wild or cultured oysters were present at the same tidal elevation as sensors, so outplant conditions represent the experiences of non-experimental organisms. NMDS plots revealed mean environmental conditions were more similar among sites than variances. Both NMDS had stress values less than 0.20 and were considered appropriate multivariate representations of environmental data (mean NMDS: stress = 0.0170, p = 0.0100; variance NMDS: stress = 0.0340, p = 0.0100). Mean dissolved oxygen and temperature were significantly different between sites (Table 3; ANOSIM; dissolved oxygen: R = 0.4063, p = 0.0530; temperature: R = 1.0000, p = 0.0020), but not between habitats. Variances of all environmental parameters were significantly different between sites (Table 4; ANOSIM; pH: R = 0.5313, p = 0.0180; dissolved oxygen: R = 0.6800, p = 0.0030; salinity: R = 0.8400, p =

0.0130; temperature: R = 0.9400, p = 0.0010). WB had the warmest but least variable temperature of 18.0 ± 1.3°C compared to averages ranging from 14.8 ± 1.8°C to 16.1 ± 1.7°C in PS (Table 5, Fig. 2). All variance values, mean pH, and mean salinity were not significantly different between habitats (Tables 3 & 4).

Although oyster position was standardized by tidal height, outplanted oysters experienced different amounts of exposure at low tide at each site due to differences in tidal amplitude (χ_4^2 = 25.29, p < 0.0001). Oysters at FB spent the highest percent of time emersed at tides <30.5 cm MLLW (13.99%; 188 h), followed by PG (10.93%; 146 h), SK (10.29%; 138 h), CI (9.35%; 125 h), and WB (8.48%; 113 h). CI and FB outplants (p = 0.0021), FB and SK outplants (p = 0.0324), and FB and WB outplants (p < 0.0001) spent significantly different amounts of time emersed during low tide conditions.

DIA mass spectrometry

Out of 39 816 predicted proteins in the *Crassostrea gigas* FASTA proteome, 9047 proteins were detected in *C. gigas* across 5 sites and 2 habitats using DIA (Skyline auto peak picker error rate 24.3 ± 25%, range: 0–100%). Proteins detected included, but were not limited to, those annotated from processes such as responses to hypoxia and oxidative stress, removal of superoxide radicals, protein folding, muscle organ development, and negative regulation of apoptosis (raw data: PeptideAtlas accession no. PASS01305).

SRM assay

Differential abundance of protein targets was evaluated at the peptide level after combining technical replicates. Proteins were considered differentially abundant if at least one monitored peptide was differentially abundant. There was no significant difference in SRM peptide abundance between unvegetated and eelgrass habitats across sites (1-way ANOSIM; R = 0.0440, p = 0.1220). Abundance data from both habitats were pooled for downstream analyses comparing protein abundances among sites (raw data: PeptideAtlas accession no. PASS01304).

Rank distances between peptide abundances in multivariate space revealed differences in peptide abundance between WB versus the other 4 sites (NMDS: stress = 0.0750, p = 0.0099). The 1-way ANOSIM by site demonstrated no significant differences in peptide abundance (R = 0.0640, p = 0.065), but a 1-way ANOSIM by region (PS vs. WB) revealed a trend towards peptide abundance differences (R = 0.2260, p = 0.0530). Peptide abundance was significantly different between FB and WB (Table 6; pairwise ANOSIM; R = 0.2568, p = 0.0350). Environmental variables explained 29% of variance in peptide abundance, but the proportion of variation explained was not significant (ANOVA for RDA; $F_{6,19}$ = 1.3064; p = 0.1950). Temperature mean and variance were the 2 most influential environmental predictors of peptide abundance, but were not significant at the 0.05 level (ANOVA on RDA; Table 7; temperature mean: $F_{1,19}$ = 2.2375, p = 0.0650; temperature variance: $F_{1,19}$ = 2.1627, p = 0.0670). Peptides differentially abundant between FB and WB were primarily positively loaded onto temperature mean, with 2 negatively loaded on temperature variance. Robustness of analysis was evaluated by performing a second RDA to predict peptide abundance based on mean and variance of temperature and pH at the time of collection. Due to missing values, dissolved oxygen and salinity could not be included in the analysis. Temperature variance was the most influential predictor of peptide abundance at the time of collection, but was not significant at the 0.05 level (ANOVA on RDA; $F_{1,13}$ = 2.2312, p = 0.0800).

Peroxiredoxin-5 (PRX), catalase (EC 1.11.1.6) (CAT), NAD(P) transhydrogenase (NADPt), glucose-6-phosphate 1-dehydrogenase (G6PD), carbonic anhydrase (CA), and protein disulfide-isomerase 1 and 2 (PDI) had peptides that were identified as differentially abundant between WB and FB by SIMPER analysis (Fig. 3). FB peptide composition was differentiated by CA abundance, while all other significantly abundant proteins differentiated WB. These proteins are involved in general cellular stress responses like reactive oxygen species neutralization or protein folding (Table 8). All differentially abundant proteins were detected at higher levels in the WB oysters than in oysters from the other 4 PS locations (CI, FB, PG, and SK), regardless of protein function (Fig. 4). No differences in protein abundance were detected among the PS sites (Table 6).

Discussion

Among sibling Pacific oysters placed at 5 sites in Washington State, we found higher abundances of 7 proteins—antioxidant enzymes and molecular chaperones —in oysters outplanted at WB. Significant differences in

protein abundances were detected between WB and either FB or SK; no differences were observed among PS sites. Increased antioxidant and molecular chaperone protein abundance are conserved stress responses consistently documented as responses to extreme temperatures, hyposalinity, low pH, and air exposure (Tomanek 2014, Zhang et al. 2015). Warmer and less variable temperature conditions at WB may have driven differential protein abundances (Fig. 3). Validation of RDA results by correlating peptide abundance to environmental conditions at the time of collection demonstrates that proteomic methods are suitable for evaluating the influence of month-long environmental variation on organismal physiology.

To our knowledge, this is the first time combined use of DIA and SRM analytical methods have been applied in an ecological context. Previously, both gel-based (Parker et al. 2011b, Zhang et al. 2015, Campos et al. 2016) and gel-free (Dineshram et al. 2016, Timmins-Schiffman et al. 2017, Müller et al. 2018) proteomic methods have been used in lab settings to evaluate the effects of environmental conditions on organismal physiology, with gel-based methods having a limited dynamic range. Similar gel-free methods have also been used to examine physiology of other non-model marine species (Plumel et al. 2013, Kültz et al. 2015). Our methods allowed for increased acquisition of proteomic data for a non-model organism. We detected over 9000 proteins with DIA—far more than previous studies have detected. The application of a novel, 2 step, gel-free proteomic approach broadened the scope of proteins detected in the DIA phase, thus revealing more possibilities for SRM target design and also completing the first step for future proteomic studies in this species. The SRM assay allowed investigation of specific biomarkers with a high-throughput analysis.

Antioxidant enzymes and acid–base regulation

Higher antioxidant enzyme abundances can be a direct response to an increase in reactive oxygen species (ROS) (Limón-Pacheco & Gonsebatt 2009, Zhang et al. 2015). During electron transport, oysters can produce ROS that induce oxidative stress if not neutralized (Abele et al. 2007, Limón-Pacheco & Gonsebatt 2009). PRX and CAT scavenge these ROS and degrade them before they cause cellular harm, while NADPt maintains the cellular redox state (Limón-Pacheco & Gonsebatt 2009, Sussarellu et al. 2012, Flores-Nunes et al. 2015b). Higher abundances of antioxidant enzymes in WB oysters suggests the need for ROS scavenging to acclimatize to local conditions.

Elevated antioxidant enzyme abundance at WB may be a response to higher levels of ROS brought on by heat stress. Mollusc species, like *Crassostrea gigas*, have been known to increase ROS production at higher temperatures (Abele et al. 2007, Tomanek 2014). Warmer and more variable temperature conditions at WB could be driving ROS production and in turn, higher abundances of PRX, CAT, and NADPt to ameliorate ROS-associated stress (Zhang et al. 2015). The shallow bathymetry of WB may have also contributed to elevated ROS presence and the need for antioxidant enzymes. At low tide, shallow waters would warm faster, leading to the higher temperatures observed at WB (Table 1). Warmer waters at low tide may prompt oysters to spend more time with their shells closed, inducing hypoxia and hypercapnia. Low oxygen concentrations within the shell could then augment ROS levels (Guzy & Schumaker 2006). Oysters could respond through increased abundance of antioxidant enzymes (Sussarellu et al. 2012).

The need for WB outplants to regulate internal acid–base conditions is demonstrated by higher abundance of CA in these oysters. *C. gigas* can regulate hemolymph pH by increasing HCO_3^- concentration via the conversion of CO_2 to HCO_3^-, catalyzed by CA (Michaelidis et al. 2005, Wei et al. 2015). If warmer water conditions at WB prompted shell closure, *C. gigas* would need to switch to anaerobic metabolism, inducing a significant reduction in hemolymph pH (Michaelidis et al. 2005). Buffering of hemolymph pH could be accomplished by elevated CA abundance. Although oysters at FB spent more time in low tide conditions that would also prompt shell closure and similar molecular responses, upregulated protein abundance at WB implies conditions at this site required a greater proteomic response in these specific biomarkers for acclimatization.

Higher abundance of G6PD in WB oysters indicates these oysters maintained metabolic activity in warmer temperature conditions. G6PD catalyzes the oxidative portion of the pentose phosphate pathway, and products from this pathway are often the precursors for nucleic and aromatic amino acids (Livingstone 1981). Additionally, G6PD activity generates NADPH and can indirectly regulate the redox environment and ameliorate effects of ROS (Livingstone 1981). For example, exposure to ROS-inducing pollutants led to increased G6PD activity in *C. gigas* ctenidia (Flores-Nunes et al.

2015b). Increased abundance of G6PD in WB not only could have maintained transcription and translation processes, but also levels of cellular and metabolic activity by indirectly dealing with ROS.

ROS are produced in response to many environmental changes; thus, biomarkers of ROS scavenging are difficult to link to a single environmental difference in a variable and complex setting. For example, reduction of ROS was found to be a common response to both increased temperatures and aerial exposure in *C. gigas* (Zhang et al. 2015). Since ROS mediation is a conserved response to several stressors, it is possible that environmental parameters we did not measure (e.g. contaminants, microbiota abundance, trace metals), or a combination of environmental parameters, could explain the observed variation in antioxidant enzyme abundance. Future work at these locations should take these variables into account.

Molecular chaperones involved in protein folding

Much like cellular response to ROS, increased levels of PDI demonstrate a generalist response to conditions at WB. PDI is a general chaperone protein that forms disulfide bonds and assists with protein folding (Vargas-Albores et al. 2009). Higher PDI abundance would reflect a need to refold misshapen proteins. In this regard, PDI would function similarly to molecular chaperones like heat shock proteins. Several invertebrate taxa demonstrate higher PDI abundance when faced with an immune challenge or metal contamination. When faced with an immune challenge, Pacific white shrimp *Litopenaeus vannamei* hemocytes synthesized higher abundances of immune response proteins, followed by elevated abundance of PDI to correct disulfide bonds in these proteins (Vargas-Albores et al. 2009). An immune challenge could also lead to more misfolded proteins that PDI would need to refold to avoid cellular damage (Zhang et al. 2014). In flat oysters *Ostrea edulis*, PDI expression increased in response to disseminated neoplasia (Silvestre et al. 2006, Martín-Gómez et al. 2013). Metal contamination at WB could also elevate PDI abundance; Chinese mitten crabs *Eriocheir sinensis* chronically exposed to cadmium over-expressed PDI (Silvestre et al. 2006, Martín-Gómez et al. 2013). Since neither disease burden or environmental contamination was measured in this study, it is impossible to know if either triggered the PDI response. Examination of these factors in future studies may elucidate the specifics of elevated PDI abundance in WB.

Proteomic responses in PS and between habitats

Due to the observed differences across environmental parameters between WB and PS locations, similar abundances for proteins involved in various environmental responses may be evidence of physiological plasticity. One particular protein that we expected to be differentially abundant was heat shock 70 kDA protein 12A (HSP12A), since WB had higher average temperatures (Table 5). However, this trend was not observed. Higher abundances of heat shock proteins (HSPs) are generally induced when organisms are exposed to thermal stress (Hamdoun et al. 2003, Zhang et al. 2015). In our experiment, the average temperatures *C. gigas* experienced were lower than the 30°C threshold found to induce elevated HSP expression in a controlled setting (Fig. 2, Table 5), which would explain why we did not see elevated HSP12A expression in WB (Hamdoun et al. 2003).

The lack of differential abundance for protein targets—both among PS sites and between unvegetated and eelgrass habitats—was unexpected. These similar proteomic profiles could be due to 4 factors. (1) It is possible that a different suite of environmental response proteins in the SRM assay could have yielded a different view of acclimatization to the various outplant sites; however, the targets we chose have proven to yield insight into a range of environmental responses in previous studies (e.g. Table 8). (2) The outplant duration could have been too short to capture varied physiological response within PS, or oysters could have also acclimatized to conditions in their outplant locations. (3) Post-translational modifications may have influenced how we detected proteins. Abundance between sites or habitats may have been similar, but addition of post-translational modifications may have varied. (4) It is possible that the proteomic response was not different because the environmental conditions that would elicit up- or down-regulation of monitored proteins were similar across these 5 locations. For example, we found no differences in environmental conditions between eelgrass and unvegetated areas, nor any differences in protein responses between these habitats (Tables 3 & 4). Our results suggest that the potential vegetation-based systems of remediation could be limited under current conditions in the field. A recent

comparison of stable isotopes and fatty acid composition in *C. gigas* at eelgrass and unvegetated habitats found no differences in $\delta^{13}C$, $\delta^{15}N$, total fatty acids, or proportional fatty composition in WB outplants, providing another line of evidence that suggests habitat may not affect *C. gigas* physiological performance (Lowe et al. 2018).

Conclusions

Differential abundance of target proteins observed between sibling oysters placed for 29 d in WB or PS indicates that environmental factors at WB tended to increase antioxidant enzyme and molecular chaperone protein abundance in Pacific oysters. This study is one of the first to link regional environmental conditions to physiological responses in PS and WB, as well as compare responses between PS and WB. Understanding the difference between these 2 estuaries is important for the persistence of oyster reefs and aquaculture in the face of climate change. Of the environmental parameters measured, higher mean temperature, as well as less variable temperature conditions at WB may have influenced protein abundance. The lack of protein abundance differences between PS sites may imply that 2016 conditions were well within the tolerances of outplanted *Crassostrea gigas*, so patterns of stress response witnessed under laboratory conditions were not apparent in the field. Together, the results generate a suite of new hypotheses for lab and field experiments comparing the effects of environmental conditions on physiological responses of marine invertebrates.

As global climate change continues to rapidly influence estuarine dynamics, this study illustrates the importance of investigating the effect of multiple modes of change on organismal physiology *in situ*. Our finding that oysters used generalist proteins to ameliorate stressors implies that assays for elucidating responses to multiple drivers *in situ* should include these conserved responses in addition to specific, stressor-related proteins identified in laboratory experiments. Pacific oysters are grown commercially throughout the Pacific Northwest region of the United States, so it is possible the population used for this study has a broad environmental tolerance. Proteomic assays allow for quantification of that tolerance, which is crucial for aquaculture industry and natural resource management. Future *in situ* explorations of environmental drivers on physiology should include a longer outplant duration, additional environmental variables, and multiple sampling points to provide a clearer connection between ecosystem dynamics and physiological performance.

Acknowledgements

This work was funded by the Washington State Department of Natural Resources Interagency Agreement 16-241 and Washington Sea Grant (Award: NA14OAR4170078; Project R/SFA-8). Brittany Taylor (Taylor Shellfish) provided *C. gigas* for the outplant experiment. The University of Washington Proteomic Resource and Priska von Haller assisted with mass spectrometry. Jarrett Egertson (Department of Genome Sciences) helped design the DIA acquisition. Austin Keller (Department of Genome Sciences) adapted MSConvert to correctly demultiplex and convert DIA data files. Sean Bennet (School of Aquatic and Fishery Sciences), and Han-Yin Yang and Brian Searle (Department of Genome Sciences) assisted with running PECAN. We also thank 3 anonymous reviewers for their valuable feedback on the manuscript.

References

Abele E, Philip E, Gonzalez PM, Puntarulo S (2007) Marine invertebrate mitochondria and oxidative stress. Front Biosci 12:933–946</unknown> https://doi.org/10.2741/2115

Banas NS, Hickey BM, MacCready P, Newton JA (2004) Dynamics of Willapa Bay, Washington: a highly unsteady, partially mixed estuary. J Phys Oceanogr 34:2413–2427 doi:10.1175/JPO2637.1

Banas NS, Hickey BM, Newton JA, Ruesink JL (2007) Tidal exchange, bivalve grazing, and patterns of primary production in Willapa Bay, Washington, USA. Mar Ecol Prog Ser 341:123–139 doi:10.3354/meps341123

Beyer J, Green NW, Brooks S, Allan IJ and others (2017) Blue mussels (*Mytilus edulis* spp.) as sentinel organisms in coastal pollution monitoring: a review. Mar Environ Res 130:338–365 PubMed doi:10.1016/j.marenvres.2017.07.024

Bianucci L, Long W, Khangaonkar T, Pelletier G and others (2018) Sensitivity of the regional ocean acidification and carbonate system in Puget Sound to ocean and freshwater inputs. Elem Sci Anth 6:22 doi:10.1525/elementa.151

Campos A, Danielsson G, Farinha AP, Kuruvilla J, Warholm P, Cristobal S (2016) Shotgun proteomics to unravel marine mussel (*Mytilus edulis*) response to long-term exposure to low salinity and propranolol in a Baltic Sea microcosm. J Proteomics 137:97–106 PubMed doi:10.1016/j.jprot.2016.01.010

Chambers MC, Maclean B, Burke R, Amodei D and others (2012) A cross-platform toolkit for mass spectrometry and proteomics. Nat Biotechnol 30:918–920 PubMed doi:10.1038/nbt.2377

Chapman RW, Mancia A, Beal M, Veloso A and others (2011) The transcriptomic responses of the eastern oyster, *Crassostrea virginica*, to environmental conditions. Mol Ecol 20:1431–1449 PubMed doi:10.1111/j.1365-294X.2011.05018.x

Cornwall CE, Hurd CL (2016) Experimental design in ocean acidification research: problems and solutions. ICES J Mar Sci 73:572–581 doi:10.1093/icesjms/fsv118

David E, Tanguy A, Pichavant K, Moraga D (2005) Response of the Pacific oyster *Crassostrea gigas* to hypoxia exposure under experimental conditions. FEBS J 272:5635–5652 PubMed doi:10.1111/j.1742-4658.2005.04960.x

Dineshram R, Chandramouli K, Ko GWK, Zhang H, Qian PY, Ravasi T, Thiyagarajan V (2016) Quantitative analysis of oyster larval proteome provides new insights into the effects of multiple climate change stressors. Glob Change Biol 22:2054–2068 PubMed doi:10.1111/gcb.13249

Egertson JD, Kuehn A, Merrihew GE, Bateman NW and others (2013) Multiplexed MS/MS for improved data-independent acquisition. Nat Methods 10:744–746 PubMed doi:10.1038/nmeth.2528

Feely RA, Alin SR, Newton J, Sabine CL and others (2010) The combined effects of ocean acidification, mixing, and respiration on pH and carbonate saturation in an urbanized estuary. Estuar Coast Shelf Sci 88:442–449 doi:10.1016/j.ecss.2010.05.004

Flores-Nunes F, Gomes T, Company T, Moraes RRM and others (2015a) changes in protein expression of Pacific oyster *Crassostrea gigas* exposed in situ to urban sewage. Environ Sci Pollut Res Int 22:17267–17279 PubMed doi:10.1007/s11356-014-3821-8

Flores-Nunes F, Mattos JJ, Zacchi FL, Serrano MAS and others (2015b) Effect of linear alkylbenzene mixtures and sanitary sewage in biochemical and molecular responses in Pacific oyster *Crassostrea gigas*. Environ Sci Pollut Res Int 22:17386–17396 PubMed doi:10.1007/s11356-015-4486-7

Guzy RD, Schumaker PT (2006) Oxygen sensing by mitochondria at complex III: the paradox of increased reactive oxygen species during hypoxia. Exp Physiol 91:807–819</unknown> https://doi.org/10.1113/expphysiol.2006.033506

Hamdoun AM, Cheney DP, Cherr GN (2003) Phenotypic plasticity of HSP70 and HSP70 gene expression in the Pacific oyster (*Crassostrea gigas*): implications for thermal limits and induction of thermal tolerance. Biol Bull (Woods Hole) 205:160–169 PubMed doi:10.2307/1543236

Hercus MJ, Loeschcke V, Rattan SIS (2003) Lifespan extension of *Drosophila melanogaster* through hormesis by repeated mild heat stress. Biogerontology 4:149–156 PubMed doi:10.1023/A:1024197806855

Hoaglin DC, Iglewicz B, Tukey JW (1986) Performance of some resistant rules for outlier labeling. J Am Stat Assoc 81:991–999 doi:10.1080/01621459.1986.10478363

Kelley D, Richards C (2018) oce: analysis of oceanographic data. R package version 0.9-23. https://CRAN.R-project.org/package=oce</eref>

Kültz D, Li J, Zhang X, Villarreal F, Pham T, Paguio D (2015) Population-specific plasma proteomes of marine and freshwater three-spined sticklebacks (*Gasterosteus aculeatus*). Proteomics 15:3980–3992 PubMed doi:10.1002/pmic.201500132

Lamb JB, van de Water JAJM, Bourne DG, Altier C and others (2017) Seagrass ecosystems reduce exposure to bacterial pathogens of humans, fishes, and invertebrates. Science 355:731–733 PubMed doi:10.1126/science.aal1956

Limón-Pacheco J, Gonsebatt ME (2009) The role of antioxidants and antioxidant-related enzymes in protective responses to environmentally induced oxidative stress. Mutat Res 674:137–147 PubMed doi:10.1016/j.mrgentox.2008.09.015

Liu Z, Pan S, Sun Z, Ma R, Chen L, Wang Y, Wang S (2015) Heavy metal spatial variability and historical changes in the Yangtze River estuary and North Jiangsu tidal flat. Mar Pollut Bull 98:115–129 PubMed doi:10.1016/j.marpolbul.2015.07.006

Livingstone DR (1981) Induction of enzymes as a mechanism for the seasonal control of metabolism in marine invertebrates:

glucose-6-phosphate dehydrogenases from the mantle and hepatopancreas of the common mussel *Mytilus edulis* L. Comp Biochem Physiol B 69:147–156 doi:10.1016/0305-0491(81)90224-8

Lowe AT, Kobelt J, Horwith M, Ruesink J (2018) Ability of eelgrass to alter oyster growth and physiology is spatially limited and offset by increasing predation risk. Estuaries Coasts, doi:10.1007/s12237-018-00488-9

MacLean B, Tomazela DM, Shulman N, Chambers M and others (2010) Skyline: an open source document editor for creating and analyzing targeted proteomics experiments. Bioinformatics 26:966–968 PubMed doi:10.1093/bioinformatics/btq054

Martín-Gómez L, Villalba A, Carballal MJ, Abollo E (2013) Identification of relevant cancer related-genes in the flat oyster *Ostrea edulis* affected by disseminated neoplasia. Mar Biotechnol (NY) 15:159–174 PubMed doi:10.1007/s10126-012-9472-1

Meng J, Wang W, Li L, Yin Q, Zhang G (2017) Cadmium effects on DNA and protein metabolism in oyster (*Crassostrea gigas*) revealed by proteomic analyses. Sci Rep 7:11716 PubMed doi:10.1038/s41598-017-11894-7

Michaelidis B, Haas D, Grieshaber MK (2005) Extracellular and intracellular acid-base status with regard to the energy metabolism in the oyster *Crassostrea gigas* during exposure to air. Physiol Biochem Zool 78:373–383 PubMed doi:10.1086/430223

Müller GAS, Lüchmann KH, Razzera G, Toledo-Silva G, Bebianno MJ, Marques MRF, Bainy ACD (2018) Proteomic response of gill microsomes of *Crassostrea brasiliana* exposed to diesel fuel water-accommodated fraction. Aquat Toxicol 201:109–118 PubMed doi:10.1016/j.aquatox.2018.06.001

Pacella SR, Brown CA, Waldbusser GG, Labiosa RG, Hales B (2018) Seagrass habitat metabolism increases short-term extremes and long-term offset of CO_2 under future ocean acidification. Proc Natl Acad Sci USA 115:3870–3875 doi:10.1073/pnas.1703445115

Paerl HW, Hall NS, Peierls BL, Rossignol KL (2014) Evolving paradigms and challenges in estuarine and coastal eutrophication dynamics in a culturally and climatically stressed world. Estuaries Coasts 37:243–258 doi:10.1007/s12237-014-9773-x

Parker LM, Ross PM, O'Connor WA (2011a) Populations of the Sydney rock oyster, *Saccostrea glomerata*, vary in response to ocean acidification. Mar Biol 158:689–697 doi:10.1007/s00227-010-1592-4

Parker LM, Ross PM, Raftos D, Thompson E, O'Connor WA (2011b) The proteomic response of larvae of the Sydney rock oyster, *Saccostrea glomerata* to elevated pCO_2. Aust Zool 35:1011–1023 doi:10.7882/AZ.2011.056

Pelletier G, Roberts M, Keyzers M, Alin SR (2018) Seasonal variation in aragonite saturation in surface waters of Puget Sound—a pilot study. Elem Sci Anth 6:5 doi:10.1525/elementa.270

Pennock JR, Sharp JH (1986) Phytoplankton production in the Delaware Estuary: temporal and spatial variability. Mar Ecol Prog Ser 34:143–155 doi:10.3354/meps034143

Plumel MI, Wasselin T, Plot V, Strub JM and others (2013) Mass spectrometry-based sequencing and SRM-based quantitation of two novel vitellogenin isoforms in the leatherback sea turtle (*Dermochelys coriacea*). J Proteome Res 12:4122–4135 PubMed doi:10.1021/pr400444m

R Core Team (2018) R: a language and environment for statistical computing. R Foundation for Statistical Computing, Vienna. www.r-project.org

Riebesell U, Gattuso JP (2015) Lessons learned from ocean acidification research. Nat Clim Chang 5:12 doi:10.1038/nclimate2456

Riviere G, Klopp C, Ibouniyamine N, Huvet A, Boudry P, Favrel P (2015) GigaTON: an extensive publicly searchable database providing a new reference transcriptome in the Pacific oyster *Crassostrea gigas*. BMC Bioinformatics 16:401 PubMed doi:10.1186/s12859-015-0833-4

Ruesink JL, Yang S, Trimble AC (2015) Variability in carbon availability and eelgrass (*Zostera marina*) biometrics along an estuarine gradient in Willapa Bay, WA, USA. Estuaries Coasts 38:1908–1917 doi:10.1007/s12237-014-9933-z

Silvestre F, Dierick JF, Dumont V, Dieu M, Raes M, Devos P (2006) Differential protein expression profiles in anterior gills of *Eriocheir sinensis* during acclimation to cadmium. Aquat Toxicol 76:46–58 PubMed doi:10.1016/j.aquatox.2005.09.006

Electronic Journal of Applied Multivariate Statistics
Volume 9, 2018

Article

Regional Steller sea lion (*Eumetopias jubatus*) population structure varies with oceanographic conditions on rookeries and haul-outs in Alaska

Amanda Warlick
School of Aquatic and Fishery Sciences, University of Washington
E-mail: awarlick@uw.edu

Received March 2019; accepted in revised form April 2019; published June 2019

Abstract

Understanding the many factors influencing trends in wildlife abundance is challenging due to the dynamic and interacting forces impacting the variability of population structure and demographic traits over time and space. Despite extensive study, many hypotheses still exist as to the underlying causes of the decline in Steller sea lions (*Eumetopias jubatus*) in Alaska. In this study, aerial survey data from 2008-2017 were examined with the aim of understanding whether age class composition differs between the eastern and western distinct population segments that have exhibited divergent recovery trends, and whether interannual variability is correlated with prevailing oceanographic conditions. Principal component analysis indicated that variability in age class composition is driven by the presence of females, pups, and bulls, particularly at rookery sites. The concentration of reproductively active age classes has not changed significantly over the study period but is correlated with the Pacific Decadal Oscillation in all regions except the western Aleutian Islands where the population continues to decline. Examining population structure using multivariate techniques can reveal patterns that have not otherwise been apparent in studies focused solely on pup versus non-pup age distinctions, thus providing insight into spatio-temporal population dynamics and potential management options for this species.

Introduction

Age-structured models are powerful tools for assessing the status of wildlife populations and are based on vital rates and age class composition, which can in turn be influenced by spatio-temporal variability in endogenous and exogenous factors such as density dependence or oceanographic conditions. Understanding the complex ways in which environmental conditions can affect vital rates such as survival and natality is foundational to studying population dynamics. The underlying mechanisms behind these connections are often complex, numerous, synergistic, or occurring simultaneously, making it challenging to identify factors driving changes in abundance. In these instances, multivariate statistical analyses can elucidate the interactions and relationships between multiple explanatory and response variables in a holistic way that is not always possible with univariate approaches. In this study, Alaska Steller sea lion (Eumetopias jubatus) aerial survey data from 2008-2017 were examined with the aim of ascertaining how observed age class composition might differ between the eastern and western distinct population segments (DPS) that have exhibited divergent population trends, and whether those differences are correlated with prevailing oceanographic conditions.

The North Pacific Ocean basin is governed by multiple long-term oceanographic

oscillations such as the Pacific Decadal Oscillation (PDO) that can influence everything from physical processes such as wind to ecological interactions and animal behaviors such as foraging and reproductive success (Chavez et al. 2003; Hare and Mantua 2000; Lusseau et al. 2004). As sentinels of changes in the marine environment, marine mammal populations can exhibit a number of responses to oceanographic oscillations, including shifts in diet, increased time spent foraging, weaning date, reduced reproductive output, and higher levels of stranding and mortality (Moore 2008; Simmonds and Isaac 2007; York et al. 2008). Over the last three decades, researchers have proposed numerous and competing hypotheses as to the driving forces behind the precipitous decline of Steller sea lions in Alaska throughout the 1970s (Loughlin 1997; Sease and Loughlin 1999; Sease et al 2001), and the subsequent divergent recovery rates observed across the range (Fritz et al. 2013; Fritz et al. 2014; York et al. 1996). While estimated abundance for the eastern DPS and for certain rookeries in the western DPS has increased since the early 2000s (Fritz and Stinchcomb 2005), counts have continued to decline in the western Aleutians, amounting to an approximately 60% decrease in non-pup age classes since 2003 (Fritz et al. 2016).

Though there is disagreement about whether the primary factor driving observed population trends is endogenous (i.e., reduced age-specific survival or fecundity (Holmes et al. 2007; York 1994)) or exogenous (i.e., available quantity and quality of prey (Atkinson et al. 2008; Pascual and Adkison 1994)), most evidence suggests that the factors are multiplicative and change over time and space (Loughlin and York 2000; Holmes et al. 2007). Most research examining nutritional stress, or the 'junk food hypothesis,' have focused on the impacts of oceanographic conditions or predominant prey species on sea lion abundance estimates, though the precise mechanism underlying this connection remains unclear for a long-lived species (Conn et al. 2014). However, there is evidence from many pinniped species that oceanographic conditions can have notable effects on pup body condition, maternal care, or time spent foraging, all of which can ultimately change demographic rates and population dynamics. Rather than examining abundance as the response variable, this study uses age-specific count data to examine the overall shifts and variability in age class composition across rookeries and haul-out sites across seven regions in Alaska. Based on the observed divergence in population recovery rates, I hypothesized that sites might exhibit differing population structure in the western Aleutians compared with other regions and that any temporal changes in population structure might correlate with prevailing oceanographic conditions.

As a species listed under the Endangered Species Act, the decline and subsequent recovery of Steller sea lions has been studied extensively, though few studies have examined age class composition at a finer scale than pups versus non-pups, particularly with respect to oceanographic conditions. Multivariate analyses can reveal patterns that emerge by examining coincident changes in multiple response variables of interest. In this case, information gleaned in this study can be combined with age-specific estimates of survival and natality to generate a more comprehensive understanding of spatio-temporal changes in population dynamics that can inform ongoing conservation and management efforts for this species.

Methods

Study system and species

The western DPS of Steller sea lions breeds on rookeries west of 144°W, an area that encompasses rookery and haul-out sites in the eastern, central, and western Gulf of Alaska and the eastern, central, and western Aleutian Islands (Figure 1). The eastern DPS ranges from the U.S. West Coast up into southeast Alaska, with sites in southeast Alaska included in this analysis as a comparison to data from the western DPS. Each year, adult males (bulls) establish territories beginning in May. Females reach reproductive maturity between the ages of three and six (Pitcher and Calkins 1981) and arrive at rookeries to give birth from late May to early July depending on the region (Pitcher et al. 2001; Kuhn et al. 2017a). At a given rookery, the majority of pups are born within a relatively short time period with females mating again shortly thereafter. Pups nurse throughout the summer and then become more independent and dispersed from females at 2.5 months of age (Raum-Suryan 2002; Kuhn et al. 2017b). Females make short foraging trips throughout the summer breeding season, though their activities can vary depending on environmental conditions and local bathymetric features (Lander et al. 2010; Lander et al. 2011). Females exhibit a high degree of natal rookery site fidelity (Pitcher and Calkins 1981), but recent research suggests a greater degree of

movement between regions within the Gulf of Alaska than was previously believed to occur (Fritz et al. 2016). This region of the North Pacific is highly productive and is influenced by the PDO and the Arctic Oscillation (AO), among other processes.

Data sources and characterization

Aerial and ship-based surveys of Steller sea lions throughout Alaska have been conducted since the 1980s, though with more spatial and temporal consistency beginning in the 2000s (Fritz et al. 2016). Data for this analysis include counts from aerial survey imagery from 2008-2017. This study period was chosen to include years since the transition to medium format images and more consistent regional coverage. Though twin otter aerial surveys are supplemented with ship-based observations and, more recently, unmanned aircraft images (Sweeney 2015), only counts from medium format images are included in this analysis since this method is the most reliable for identifying specific age and sex classes (Snyder et al. 2001). Surveys generally occur from late June to early July after most pups are born and when haul-out rates are likely maximized (Fritz et al. 2016). However, due to the life history characteristics of non-reproductive age classes, detection rates of juveniles and sub-adult males might be lower since these individuals might spend more time in the water throughout the day or arrive at rookeries later in the season. When used for inference about population abundance, these raw counts are used as model inputs in such a way as to obtain estimates in un-surveyed regions, which are then used in further analyses.

A total of 244 survey sites have been identified, 40 within the range of the eastern DPS in southeast Alaska and the remainder in the range of the western DPS (Figure 1). Due to funding availability and the logistics of surveying these remote areas, not all regions have been surveyed annually (Table 1). Sites are classified as being either rookeries (defined as having greater than 50 pups) or haul-outs. Aerial survey images were processed by two analysts who independently assign individuals to five classes: pups, juveniles, sub-adult males, adult females, and bulls. Differences greater than specified thresholds are reconciled between the two observers. Counts from individual images were summed to the site level for a total of 1,008 site-year combinations. Though these are generally high-quality data, it is important to note that site-level data availability and consistency can change from year to year due to weather and other logistical challenges (e.g., clouds or fog might obscure a certain portion of a given site due to chance), which are documented elsewhere (e.g., Fritz et al. 2016).

The PDO index is a measure of oceanographic variability based largely on sea surface temperature (Hare and Mantua 2000). The PDO shifted into a cool phase in the late 2000s and then went into a warm phase beginning in 2012. Monthly index values obtained from the Joint Institute for the Study of the Atmosphere and Ocean[1] were averaged for annual means. Monthly upwelling anomalies in the Gulf of Alaska (60°N 149°W) were obtained from NOAA's Pacific Fisheries Environmental Laboratory and averaged for annual values.

Statistical analyses

To examine differences in Steller sea lion age class composition at identified survey sites, I used principal component analysis (PCA) and principal component regression to identify factors driving the observed variation over time and across regions. Though assumptions of normality required for a PCA can be relaxed for use in an exploratory rather than inferential context, Hellingers transformation (square root of proportion) was applied to raw counts to standardize data (Legendre and Gallagher 2001) skewed by the large number of smaller site counts. Site-year combinations that were either univariate or multivariate outliers were not omitted because this variability is likely related to site size rather than being due to observer bias or sampling error (i.e., for the purpose of this study, imagery is assumed to represent a near census).

PCA is an unconstrained ordination method that reduces the dimensionality of correlated multivariate data to express the maximum amount of variability through the formation of uncorrelated axes (i.e., principal components) that represent weighted linear combinations of the original variables. Through this process, meaningful variability across multiple response variables is condensed into the first few PC axes while noise within the data is deferred to later axes. The significance of PC axes was tested with Monte Carlo randomization ('ordi.monte' in biostats library, McGarigal 2016), where matrix columns are permutated and the distribution of observed eigenvalues is compared with those from the randomization that would represent no correlative structure

under the null hypothesis. Eigenvector coefficients were converted to correlation coefficients and then squared to derive the percentage of variance in each age class accounted for by each principal component. PCA results were visualized with site type (rookery versus haul-out) and region using the 'PCA' family of functions in the FactoMineR R package. To examine changes in age class composition over time, PCAs were conducted on observed counts grouped by year for each separate region due to the uneven sampling design (Table 1).

To examine whether the variability visualized using PCA was significantly different between regions and site type, a permutational multivariate analysis of variance (perMANOVA) was conducted on the Euclidean distance matrix of Hellinger's transformed count data using 'adonis' (vegan R package, Oksanen et al. 2018). A perMANOVA first applies an analysis of variance (ANOVA) test to compare within and between group variance, resulting in a pseudo F-statistic that is calculated as the ratio of among-group sum of squares and within-group sum of squares (Anderson 2001). The observed pseudo F-statistic was then compared to a permutated F-statistic expected under the null hypothesis.

Though perMANOVA tests are a useful tool that can partition observed variability across different groups using any distance measure, it only indicates the presence of group-level differences and does not reveal whether these differences are due to their positioning in ordination space, variance, or both. Therefore, to examine the variance within groups, homogeneity of group dispersion was tested using 'betadisper,' which performs an ANOVA on average distances between group objects and group centroids or medians in ordination space (Anderson 2006) against a null hypothesis assuming uniform variance across groups. Separate perMANOVA and group homogeneity tests were also conducted on counts within each region to examine changes over time, though changes in homogeneity across years could be a product of the number of sites surveyed rather than true ecological variation.

To examine whether some of the variation in age class composition is correlated with oceanographic conditions, PC regressions were conducted with PC scores from the first PC axis as the response variable and annual PDO index and upwelling as predictor variables separately for each region. To further tease apart the relationship between age classes with significant loadings on the first PC axis and multiple categorical and continuous response variables, classification and regression tree (CART) models were examined using 'rpart' (rpart R package, Milborrow 2016). In this approach, age group proportions per site are successively partitioned into mutually exclusive groups by minimizing a goodness-of-fit measure for each child node with respect to the explanatory variables (site type, region, PDO, upwelling). Regression tree analyses include predicted age class proportions based on combinations of categorical response variables. Tree pruning was not necessary due to the smaller number of explanatory variables. All analyses were conducted using the statistical software R (version 3.5.1; R Development Core Team 2009).

Results

Across regions, sites were generally dominated by higher proportions of juveniles compared with other age classes, though this varies by site type and region. Sites in the western Aleutians had higher proportions of pups and females and a lower proportion of juveniles compared to any other region (Figure 2), though this could be partly due to the higher proportion of rookery versus haul-out sites surveyed in the region (Table 1). Overall, females and pups have the highest maximum and mean counts, though pups have a low median count due to the large proportion of sites that are haul-outs where pups are not present (Table 2).

Approximately 53% of variability in age class composition was explained by the first principal component (PC) axis and an additional 25% by the second PC, both of which were significant according to the randomization test ($p < 0.001$) (Table 3). The presence of bulls, females, and pups was strongly positively correlated with PC1 while the presence of juveniles was negatively correlated with PC1 (Figure 3, Table 3). Object PC scores for rookery sites were dominated by pups, females, and bulls and positively correlated with PC1 while haul-out sites were dominated by juveniles and negatively correlated with PC1 (Figure 3a). Grouping PC scores by region showed sites to be relatively dispersed in ordination space, though the western Aleutian Islands had more sites with higher PC1 scores, representing a stronger dominance of pups, females, and bulls (Figure 3b). Approximately 64 and 78% of variability in the counts of females and pups was explained by PC1 and 80% of variability in sub-adult male counts was

explained by PC2 (squared structure coefficients, Table 3). Visual inspection of region-specific PCA biplots (not shown) indicated some regions with less inter-annual variability in age class composition compared with others.

Results of perMANOVA and group dispersion heterogeneity tests indicated that the age composition was significantly different between rookeries and haul-outs in ordination space (pseudo-F = 836.0, $p < 0.01$) and in the degree of dispersion around the centroid (F = 59.6, $p < 0.01$), with heterogeneity being greater at haul-out compared to rookery sites (Table 4). Similarly, age composition also varied in both ordination space (pseudo-F = 6.6, $p < 0.01$) and dispersion across regions (F = 6.8, $p < 0.01$), with the greatest variability around the centroid in southeast Alaska and the least in the western Aleutians. Pairwise comparisons of dispersion indicated that the western Aleutians are different than the other Aleutian regions and that regions in the Gulf of Alaska are different from the central and eastern Aleutians (Appendix Table S1). At the regional level, variation in ordination space over time was significant only in the western Aleutians (pseudo-F = 3.17, $p < 0.1$). However, dispersion or group homogeneity was significantly different across years in the central (F = 1.7, $p < 0.1$) and eastern (F = 1.96, $p < 0.1$) Aleutians (Table 3).

Regression analysis of PC1 scores and environmental variables showed a significant negative correlation between higher PC1 scores (sites characterized by the prevalence of pups, females, and bulls compared to sites dominated by juveniles) and annual PDO index values, though the effect size is small ($y = -0.18x$, $p < 0.001$, $R^2 = 0.02$). However, the nature of this relationship varied across the Steller sea lion range, with neighboring regions exhibiting similar patterns (Figure 4). In contrast to the significant negative correlation between PC1 scores and PDO values in the eastern ($y = -0.20x$, $p < 0.05$, $R^2 = 0.02$) and central ($y = -0.17x$, $p < 0.1$, $R^2 = 0.01$) Aleutians, PC1 scores for sites in the western Aleutians exhibited a positive (albeit non-significant) relationship with PDO values. Upwelling values were not correlated with PC1 scores except in southeast Alaska ($y = -0.02$, $p < 0.05$).

CART model analyses examining age class composition predicted by explanatory variables indicated that different sets of predictor variables were important for reproductively active versus non-breeding age classes. All age classes with significant positive or negative loadings on PC1 (pups, females, bulls, and juveniles) had site type as the primary predictor of relative abundance (proportion of a given age class at a given site). For pups, site type was the sole predictor, with 30% pups expected for rookery sites and 1.3% predicted at haul-outs (Figure 5). For bulls, site type and region were predictors, with the highest expected proportion at rookeries in southeast Alaska and the lowest at haul-outs in all Aleutian regions (Figure 5). For females, PDO was the second most distinguishing predictor followed by region, with the highest proportion of females at haul-out sites expected under cool PDO phase years in many regions. For juveniles, which correlated negatively with the presence of the other age classes, environmental variables were predictors but not region, with the highest proportion of juveniles at haul-out sites expected in warm PDO phases and greater upwelling (68% and 71%, respectively) (Figure 5).

Figure 1. *Map of Steller sea lion haul-outs (green) and rookery (purple) sites throughout the range of the western DPS (excluding Russia) and the southeast Alaska portion of the eastern DPS range that extends along the U.S. West Coast.*

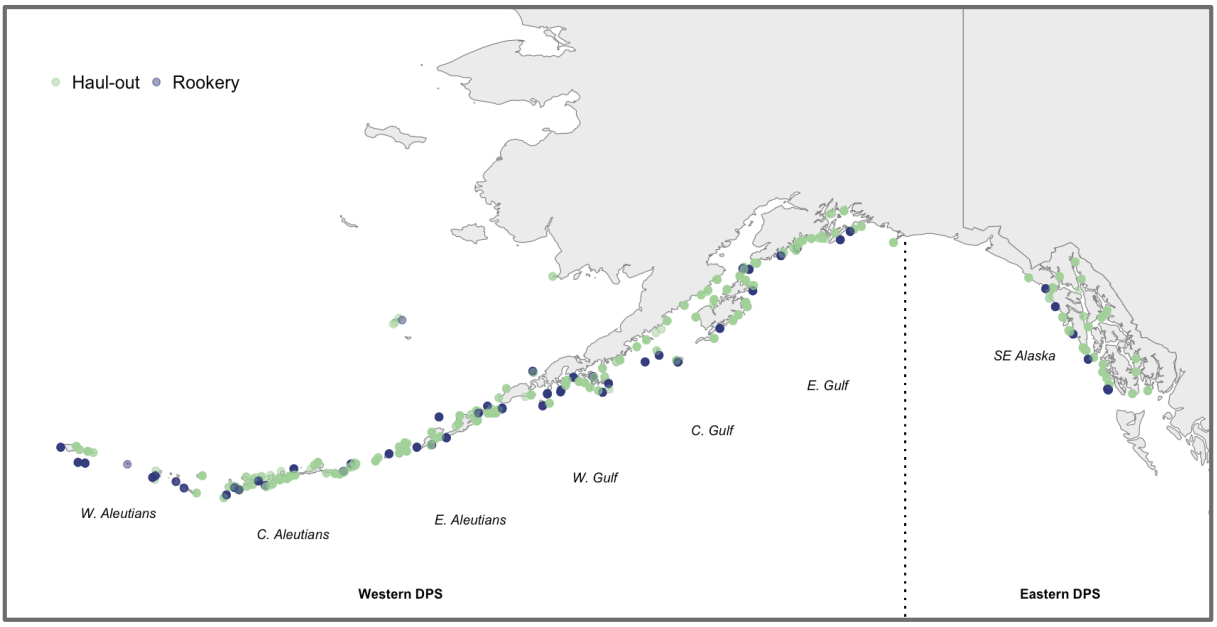

Figure 2. *Mean proportion of age classes counted at rookeries and haul-outs by region. Horizontal line indicates mean across all years and sites, dots indicate outliers. Large range of proportions is due in part to averaging across rookeries and haul-out site types.*

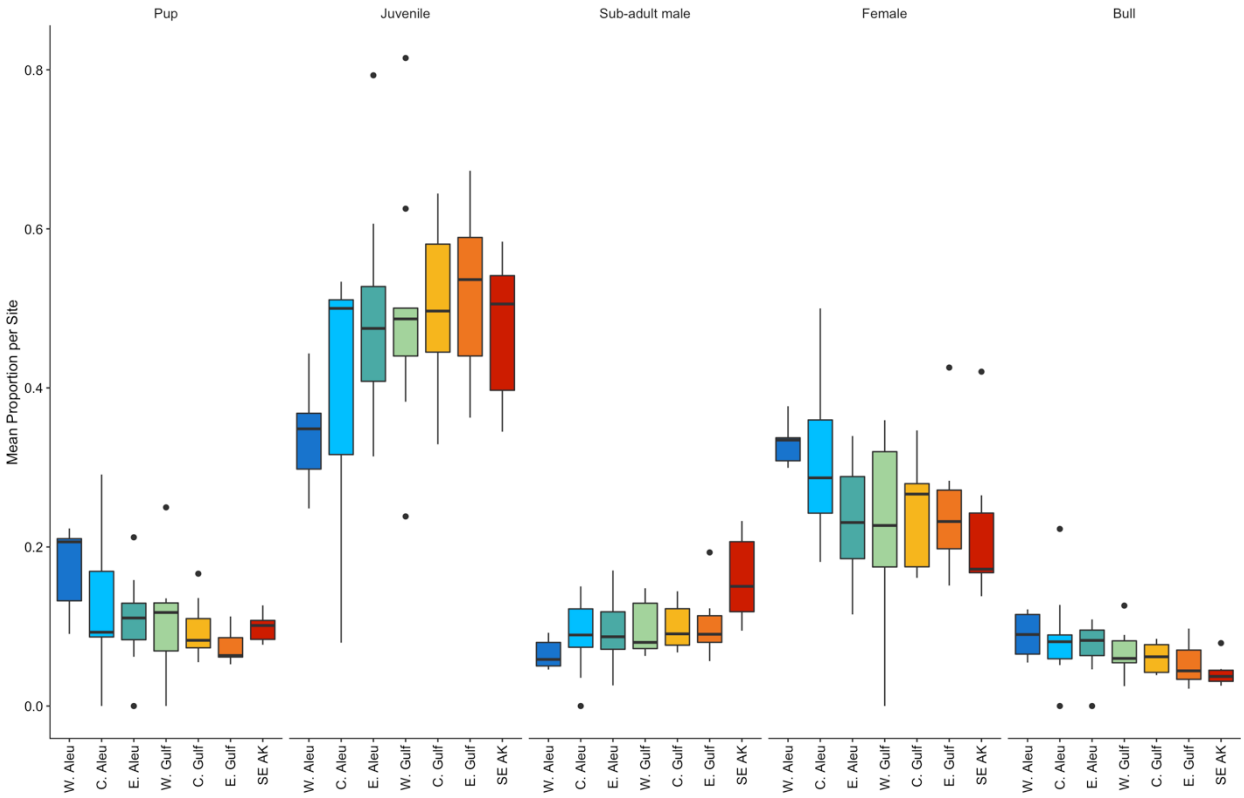

Figure 3. *Principal component analysis scores of site-level counts per year grouped by (a) site type and (b) regions listed from west to east, with loading vectors representing correlations between age classes and their relative influence on principal component axes.*

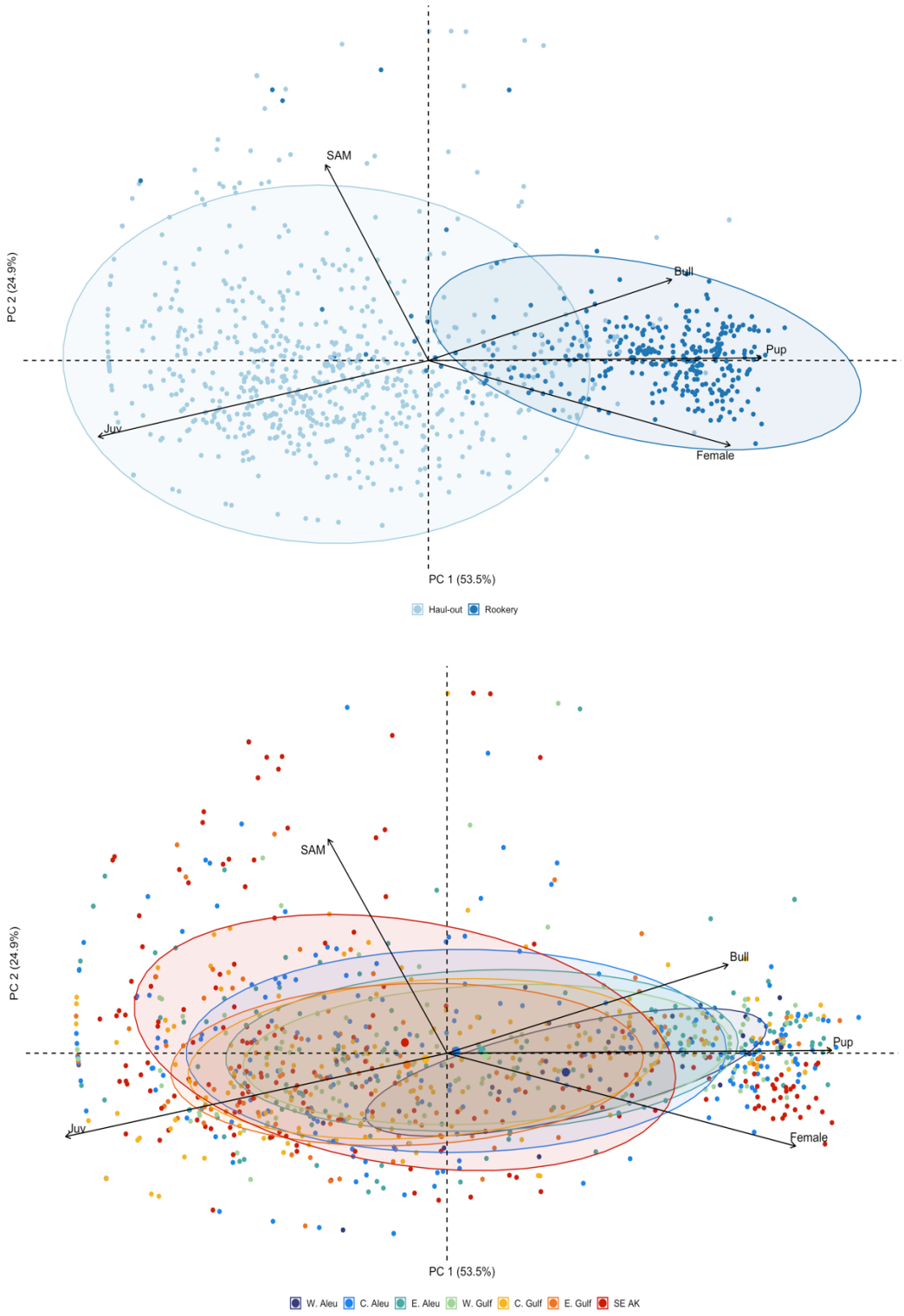

Figure 4. *Principal component regression of PC1 scores against annual PDO index values represented by loess lines for each region (colors) and all combined regions (black dashed) with 95% confidence interval depicted in grey.*

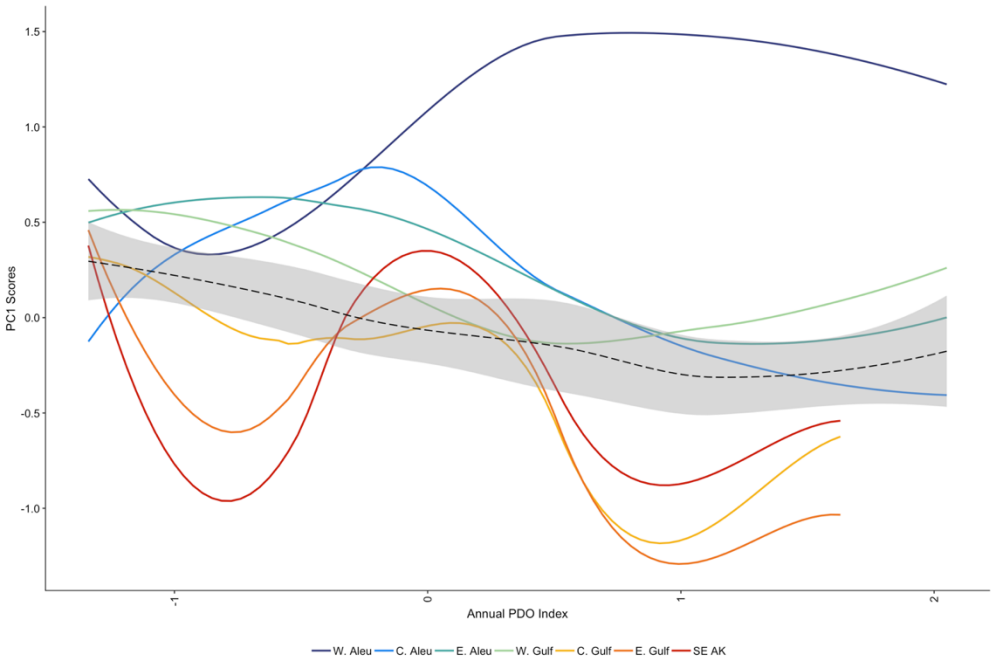

Figure 5. *Classification and regression trees for the proportion of bulls, females, pups, and juveniles according to site type, region, PDO, and upwelling as explanatory predictor variables.*

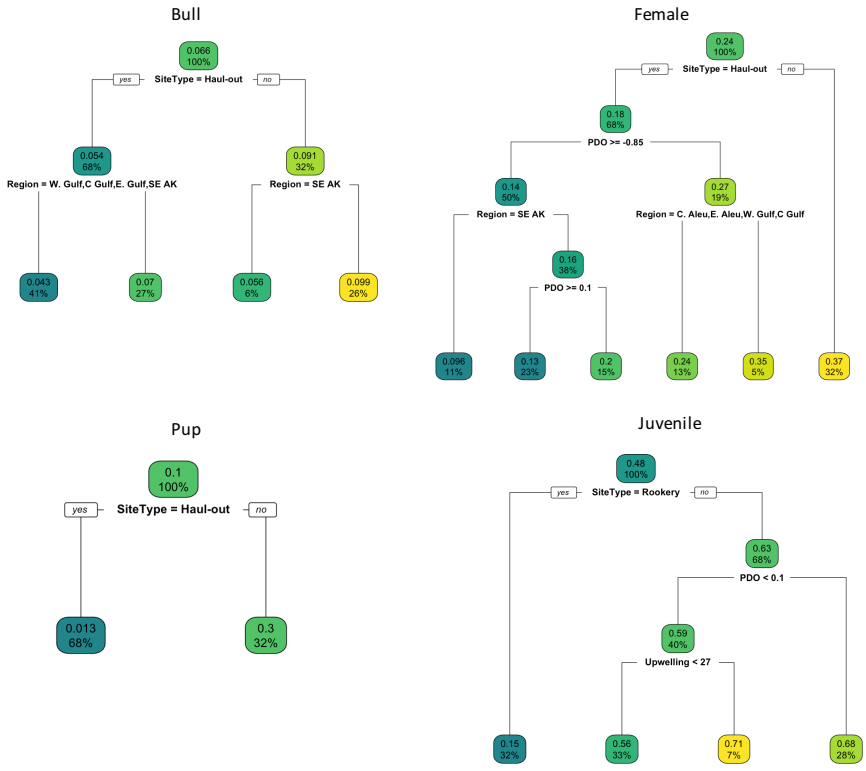

Table 1. *Regions included in annual aerial surveys from 2008-2017 listed from east to west and the proportions of each site type per region.*

	Rookery	Haul-out	2008	2009	2010	2011	2012	2013	2014	2015	2016	2017
W. Aleu	0.50	0.50	✓			✓	✓		✓		✓	✓
C. Aleu	0.19	0.81	✓	✓	✓	✓	✓		✓	✓	✓	✓
E. Aleu	0.26	0.74	✓	✓	✓	✓			✓	✓	✓	✓
W. Gulf	0.38	0.62	✓	✓	✓	✓		✓	✓	✓	✓	✓
C. Gulf	0.20	0.80	✓	✓	✓	✓		✓		✓		✓
E. Gulf	0.12	0.88	✓	✓	✓	✓		✓		✓		✓
SE AK	0.25	0.75	✓	✓	✓			✓		✓		✓

Table 2. *Summary statistics for age class count data per site per year for all regions, including mean proportion and maximum, median, mean, and standard error of the mean number of animals counted.*

	Bull	Sub-adult male	Female	Juvenile	Pup
Max count	379	399	2,108	1,561	1,999
Median	8.0	12.5	31.0	63.0	1.0
Mean	26.1	29.1	136.8	112.7	99.3
Standard error	1.3	1.33	7.94	4.94	7.47
Mean Proportion	0.07	0.11	0.24	0.48	0.10

Table 3. *Principal component analysis results for the two significant PC axes including loadings and squared structure coefficients that represent the proportion of variance in each age class explained by the first and second principal components. Significant loadings (bold) were considered those greater than 0.6.*

	PC1 (53.5%, $p < 0.001$)		PC2 (24.9%, $p < 0.001$)	
	Loadings	*(Structure Coef.)²*	*Loadings*	*(Structure Coef.)²*
Bull	**0.645**	0.416	-0.376	0.141
Sub-adult male	-0.273	0.075	**-0.908**	0.824
Female	**0.8**	0.640	0.394	0.155
Juvenile	**-0.875**	0.766	0.354	0.125
Pup	**0.883**	0.780	-0.012	0.000

Table 4. Summary results of perMANOVA (left) and group dispersion homogeneity (right) tests with significant p-values indicated in bold ($\alpha < 0.1$). Variation in age class composition is compared across all regions, site type, and over time in each region.

	perMANOVA			Dispersion	
	F Statistic	R-sq	p-value	F Statistic	p-value
Region	6.606	0.021	**0.001**	6.865	**0.000**

Site type	836.003	0.446	**0.001**	59.615	**0.000**
Year : W. Aleutians	3.171	0.099	**0.059**	0.269	0.926
Year : C. Aleutians	1.584	0.007	0.193	1.703	**0.099**
Year : E. Aleutians	0.140	0.001	0.953	1.960	**0.065**
Year : W. Gulf	1.216	0.009	0.286	1.096	0.371
Year : C. Gulf	0.629	0.004	0.531	1.797	0.103
Year : E. Gulf	0.663	0.006	0.547	1.211	0.307
Year : SE Alaska	0.561	0.003	0.608	1.066	0.380

Discussion

This study used multivariate approaches to collectively examine Steller sea lion age class composition with the aim of ascertaining environmental or endogenous factors that might contribute to or inform our understanding of the divergent population trends observed across Alaska. While it may not be practical or meaningful to compare each of the seven regions, differing patterns are evident in the western Aleutians compared to other regions, particularly relative to the eastern DPS sites in southeast Alaska. Researchers have hypothesized that the continued decline of populations in the western Aleutians may be due to different age structure, lower demographic rates, or poor foraging conditions. While definitively answering that question is outside the scope of this study, exploring the variation in population structure and the explanatory variables driving that variability can provide insight for future inferential studies. Taken together, these multivariate analyses can give a holistic representation of how population structure might change over time and vary over space relative to environmental conditions.

The relative abundance of age classes is the backbone of population structure, which in turn governs reproductive output and other demographic parameters. Mean proportions of pups, bulls, and females generally decrease from west to east while that of juveniles and sub-adult males increase. Higher mean proportions of reproductively active age classes in the western Aleutians over the last decade could theoretically signal that there is the capacity for population growth at least equal to that observed in other regions where the proportions are lower. However, population dynamics are complex and it is likely that many factors such as density-dependence, emigration, survival, and environmental conditions all interact to influence observed abundance trends. With additional data on demographic rates such as age-specific survival and natality, a Fourth Corner Analysis (Legendre et al. 1997) could be used to elucidate these coinciding variables. And similarly, another caveat to be mindful of is that this analysis was conducted on raw counts, which does not fully include unsurveyed areas nor does it account for the unknown proportion of non-pup age classes that are hauled out, though presumably this proportion remains at least somewhat constant over time and space.

Regardless of the caveats, this study is a novel approach to examining these data that reveal areas for further exploration. Bulls, females, and pups comprise the breeding population at a given time and drive the variability in age class composition, particularly at rookeries (Figure 3). The stark contrast between population structure at the two site types is consistent with the expectation that individuals at rookeries during the breeding season would most generally be breeding age groups, particularly for a territorial polygynous species. Homogeneity was also different between site types and regions, indicating that sites in the western Aleutians and particularly rookeries had the least dispersion or variability. The heterogeneity observed in southeast Alaska compared with more homogenous age class composition in the western Aleutians could provide stability or resilience to stressors, which might help explain divergent recovery rates in the two populations. Though the differences could also be a product of the different number of survey years in each of the regions, the fact that age composition has not significantly changed over the study period in most regions indicates that the existing observed patterns are likely relatively stable.

In addition to the inherent variability in population structure, environmental conditions likely also have a strong influence on

population dynamics through the quantity and quality of available foraging resources. Researchers have postulated that Steller sea lion abundance is influenced by oceanographic oscillations and consequent changes in diet (Pascual and Adkison 1994; Merrick et al. 1997; Sinclair et al. 2013), though the mechanisms underlying this connection for a long-lived species have been unclear or inadequately tested (Conn et al. 2014). More likely is that oceanographic conditions and prey availability have age- and region-specific effects on juvenile survival, body condition, mating probability, and/or natality. Though specifically testing that hypothesis would require different data than what was analyzed here, changes in demographic rates are moderated through age class population structure, so these results do allude to a connection between the environment and observed population counts. Moving along the PC1 gradient from sites dominated by juveniles to an increasing prevalence of pups, bulls, and females correlated with cool phase PDO values, though this relationship appeared non-linear in the Gulf of Alaska and was not evident in the western Aleutians. This correlation between the prominence of breeding age classes during cool PDO phases could indicate that the persistence of these conditions over multiple years in some way supports reproductive activities and/or synchronous presence at rookeries during the breeding season.

Numerous interacting mechanisms could explain this connection between age class composition and oceanographic conditions. Identifying which demographic rate(s) are most impacted remains challenging, particularly due to oceanographic regimes affecting individuals and populations at varying spatial scales (Francis et al. 1998; Mannocci et al. 2017). Oceanographic regime shifts do not necessarily have predictable ecosystem-level changes over time and space, where a change to a warm PDO phase might have disparate impacts in different regions depending on local physical and ecological landscape features (Benson and Trites 2002). The apparent absence of this relationship between PDO and age class composition in the western Aleutians could indicate that those local breeding populations are less adaptable to prevailing conditions or that those areas are less influenced by the same physical forcing patterns and foodweb interactions as areas closer to the coastline. Further examining the effect size, significance, and spatial extent of this relationship would provide insight into spatio-temporal population dynamics but would require disentangling seasonal versus inter-annual variability in abundance, survival, and reproduction.

The interaction of regional and environmental effects was apparent in CART models that delineate factors driving the prevalence of breeding age groups. The site-level proportion of pups was predicted solely by site type for all regions whereas the prevalence of bulls was also dependent on region. Having PDO appear as a predictor of female prevalence across regions (Figure 5) could reflect the importance of oceanographic conditions for nursing females that have very high energetic demands. Oceanographic conditions are thought to influence the timing or date of weaning, whereby females can continue nursing and forego breeding in a given year (York et al. 2008; Maniscalco et al. 2014). Or, it could reflect differences in prevailing prey species aggregation patterns, as Steller sea lion haul-out distribution has been found to change seasonally to minimize distance to dense spawning aggregations (Womble et al. 2005). At an observational level, oceanographic conditions in a given year could influence not only foraging success but also the amount of time spent foraging or the seasonal arrival at rookeries, which would directly effect detection probability during aerial surveys. This examination of CART models showed similar results to that of the principal component regression because PC1 was so highly loaded by variability in breeding age classes, but CART models provide additional information about factors important for the prevalence of each age class individually rather than collectively.

In addition to examining oceanographic conditions against age group traits such as survival in a Fourth Corner Analysis, future research could be enhanced by adding region- or site-specific environmental covariates such as sea surface temperature, bathymetry, or local prey density rather than just using basin-wide annual indices. Additionally, examining the predictive strength of seasonal index values (i.e., winter PDO rather than annual) would further refine our understanding of when oceanographic conditions might have the greatest impact on behavior. This study provides insight into spatio-temporal differences in population structure that may help explain some aspect of the divergent

recovery rates in the western and eastern DPS. Population dynamics are just that - *dynamic*. Multivariate approaches enable improved understanding of how populations change as a whole in response to their environment. This work can guide future inferential studies aiming to estimate demographic rates and abundance with respect to oceanographic conditions and climate change, which can ultimately inform ongoing conservation and management options for this depleted species.

Acknowledgements
This work would not have been possible without the dedication of NOAA staff at the Alaska Fisheries Science Center's Marine Mammal Laboratory who collect and analyze annual aerial survey data. This project was supported by the University of Washington School of Aquatic and Fishery Sciences, the National Science Foundation, and the ARCS Foundation.

References

Anderson, M.J. 2001. A new method for non-parametric multivariate analysis of variance. *Austral Ecology* 26: 32–46.

Anderson, M.J. 2006. Distance-based tests for homogeneity of multivariate dispersion. *Biometrics* 62: 245–253.

Atkinson, S., D.P. Demaster, and D.G. Calkins. 2008. Anthropogenic Causes of the Western Steller Sea Lion Eumetopias Jubatus Population Decline and Their Threat to Recovery. *Mammal Review* 38 (1): 1–18. doi:10.1111/j.1365-2907.2008.00128.x.

Benson, A.J., and A.W. Trites. 2002. Ecological Effects of Regime Shifts in the Bering Sea and Eastern North Pacific Ocean. *Fish and Fisheries* 3 (2): 95–113. doi:10.1046/j.1467-2979.2002.00078.x.

Chavez, F.P., J.R., Salvador, E. Lluch-Cota, and M. Ñiquen. 2003. From Anchovies to Sardines and Back: Multidecadal Change in the Pacific Ocean. *Science* 299 (5604): 217–21. doi:10.1126/science.1075880.

Conn, P.B., D.S. Johnson, L.W. Fritz, and B.S. Fadely. 2014. Examining the Utility of Fishery and Survey Data to Detect Prey Removal Effects on Steller Sea Lions (*Eumetopias Jubatus*). *Canadian Journal of Fisheries and Aquatic Sciences* 71 (8): 1229–42. doi:10.1139/cjfas-2013-0602.

Francis, R.C., S.R. Hare, A.B. Hollowed, and W.S. Wooster. 1998. Effects of Interdecadal Climate Variability on the Oceanic Ecosystems of the NE Pacific. *Fisheries Oceanography* 7 (1): 1–21. doi:10.1046/j.1365-2419.1998.00052.x.

Fritz, L. W., and C. Stinchcomb. 2005. Aerial, ship, and land-based surveys of Steller sea lions (Eumetopias jubatus) in the western stock in Alaska, June and July 2003 and 2004. U.S. Dep. Commer., NOAA Tech. Memo. NMFS-AFSC-153, 56 p.

Fritz, L., K. Sweeney, D. Johnson, M. Lynn, T. Gelatt, and J. Gilpatrick. 2013. Aerial and ship- based surveys of Steller sea lions (*Eumetopias jubatus*) conducted in Alaska in June-July 2008 through 2012, and an update on the status and trend of the western distinct population segment in Alaska. U.S. Dep. Commer., NOAA Tech. Memo. NMFS-AFSC- 251, 92 p.

Fritz L., R. Towell, T. Gelatt, D. Johnson, and T. Loughlin. 2014. Recent increases in survival of western Steller sea lions in Alaska and implications for recovery. Endang. Spec. Res. 26(1):13–24. doi: 10.3354/esr00634.

Fritz, L., K. Sweeney, R. Towell, and T. Gelatt. 2016. Aerial and ship- based surveys of Steller sea lions (*Eumetopias jubatus*) conducted in Alaska in June-July 2013 through 2015, and an update on the status and trend of the western distinct population segment in Alaska. U.S. Dep. Commer., NOAA Tech. Memo. NMFS-AFSC-321, 72 p. doi:10.7289/V5/TM-AFSC-321.

Hare, S.R., and N.J. Mantua. 2000. Empirical Evidence for North Pacific Regime Shifts in 1977 and 1989. *Progress in Oceanography* 47 (2): 103–45. doi:10.1016/S0079-6611(00)00033-1.

Holmes, E.E., L.W. Fritz, A.E. York, and K. Sweeney. 2007. Age-Structured Modeling Reveals Long-Term Declines in the Natality of Western Steller Sea Lions. *Ecological Applications* 17 (8): 2214–32. doi:10.1890/07-0508.1.

Kuhn, C.E., K.C., L. Fritz, and D. Johnson. 2017. Estimating Dispersal Rates of Steller Sea Lion (Eumetopias Jubatus) Mother-Pup Pairs from a Natal Rookery Using Mark-Resight Data. *PLOS ONE* 12 (12): e0189061. doi:10.1371/journal.pone.0189061.

Kuhn, C.E., K.C., D. Johnson, and L. Fritz. 2017. A Re-Examination of the Timing of Pupping for Steller Sea Lions Eumetopias Jubatus Breeding on Two Islands in Alaska.

Endangered Species Research 32: 213–22. doi:10.3354/esr00796.

Lander, M., T. Loughlin, M. Logsdon, G. VanBlaricom, and B. Fadely. 2010. Foraging Effort of Juvenile Steller Sea Lions *Eumetopias Jubatus* with Respect to Heterogeneity of Sea Surface Temperature. *Endangered Species Research* 10 (March): 145–58. doi:10.3354/esr00260.

Lander, M.E., M.L. Logsdon, T.R. Loughlin, and G. Van Blaricom. 2011. Spatial Patterns and Scaling Behaviors of Steller Sea Lion (Eumetopias Jubatus) Distributions and Their Environment. *Journal of Theoretical Biology* 274 (1): 74–83. doi:10.1016/j.jtbi.2011.01.015.

Legendre, P., Galzin, R. and M. L. Harmelin-Vivien. 1997. Relating behavior to habitat: solutions to the fourth-corner problem. *Ecology* 78: 547–562.

Legendre, P. and E.D. Gallagher. 2001. Ecologically meaningful transformations for ordination of species data. *Oecologia* 129:271-280.

Loughlin, T.R. 1997. Using the phylogeographic method to identify Steller sea lion stocks. *Molecular Genetics of Marine Mammals* 3:159-171.

Loughlin, T.R, and A.E. York. 2000. An Accounting of the Sources of Steller Sea Lion, *Eumetopias jubatus*, Mortality. *Marine Fisheries Review*, 6.

Lusseau, D., R. Williams, B. Wilson, K. Grellier, T.R. Barton, P.S. Hammond, and P.M. Thompson. 2004. Parallel Influence of Climate on the Behaviour of Pacific Killer Whales and Atlantic Bottlenose Dolphins. *Ecology Letters* 7 (11): 1068–76. doi:10.1111/j.1461-0248.2004.00669.x.

Maniscalco, J.M., A.M., Springer, P. Parker, M.D. Adkinson. 2014. A longitudinal study of Steller sea lion natality rates in the Gulf of Alaska with comparisons to census data. PLOS One 9:e111523.

Mannocci, L., A.M. Boustany, J.J. Roberts, D.M. Palacios, D.C. Dunn, P.N. Halpin, S. Viehman, et al. 2017. Temporal Resolutions in Species Distribution Models of Highly Mobile Marine Animals: Recommendations for Ecologists and Managers. *Diversity and Distributions* 23 (10): 1098–1109. doi:10.1111/ddi.12609.

Merrick, R.L., M.K. Chumbley, and G.V Byrd. 1997. Diet Diversity of Steller Sea Lions (*Eumetopias Jubatus*) and Their Population Decline in Alaska: A Potential Relationship. *Canadian Journal of Fisheries and Aquatic Sciences* 54 (6): 1342–8. doi:10.1139/f97-037.

Moore, S.E. 2008. Marine Mammals as Ecosystem Sentinels. *Journal of Mammalogy* 89 (3): 534–40. doi:10.1644/07-MAMM-S-312R1.1.

Pascual, M.A., and M.D. Adkison. 1994. The Decline of the Steller Sea Lion in the Northeast Pacific: Demography, Harvest or Environment? *Ecological Applications* 4 (2): 393–403. doi:10.2307/1941942.

Pitcher, K.W., and D.G. Calkins. 1981. Reproductive Biology of Steller Sea Lions in the Gulf of Alaska. *Journal of Mammalogy* 62 (3): 599–605. doi:10.2307/1380406.

Pitcher, K.W., V.N. Burkanov, D.G. Calkins, B.J. Le Boeuf, E.G. Mamaev, R.L. Merrick, and G.W. Pendleton. 2001. Spatial and Temporal Variation in the Timing of Births of Steller Sea Lions. *Journal of Mammalogy* 82 (4): 1047–53. doi:10.1644/1545-1542(2001)082<1047:SATVIT>2.0.CO;2.

R Core Team. 2009. R: a language and environment for statistical computing. R Foundation for Statistical Computing, Vienna, Austria. http://www.R-project.org/.

Raum-Suryan, K.L., K.W. Pitcher, D.G. Calkins, J.L. Sease, and T.R. Loughlin. 2002. Dispersal, Rookery Fidelity, and Metapopulation Structure of Steller Sea Lions (*Eumetopias Jubatus*) in an Increasing and a Decreasing Population in Alaska. *Marine Mammal Science* 18 (3): 746–64. doi:10.1111/j.1748-7692.2002.tb01071.x.

Sease, J., and T. R. Loughlin. 1999. Aerial and land-based surveys of Steller sea lions (*Eumetopias jubatus*) in Alaska, June and July 1997 and 1998. U.S. Dep. Commer., NOAA Tech. Memo. NMFS-AFSC-100, 61 p.

Sease, J. L., W. P. Taylor, T. R. Loughlin, and K. W. Pitcher. 2001. Aerial and land-based surveys of Steller sea lions (*Eumetopias jubatus*) in Alaska, June and July 1999 and 2000. U.S. Dep. Commer., NOAA Tech. Memo. NMFS-AFSC-122, 52 p.

Simmonds, M.P., and S.J. Isaac. 2007. The Impacts of Climate Change on Marine Mammals: Early Signs of Significant Problems. *Oryx* 41 (1): 19–26. doi:10.1017/S0030605307001524.

Sinclair, E. H., D. S. Johnson, T. K. Zeppelin, and T. S. Gelatt. 2013. Decadal variation in

the diet of Western Stock Steller sea lions (*Eumetopias jubatus*). U.S. Dep. Commer., NOAA Tech. Memo. NMFS-AFSC-248, 67 p.

Snyder, G.M., K.W. Pitcher, W.L. Perryman, and M.A. Lynn. 2001. Counting Steller sea lion pups in Alaska: an Evaluation of medium format, color aerial photography. *Marine Mammal Science* 17(1) 136-146.

Sweeney, K.L., V.T. Helker, W.L. Perryman, D.J. LeRoi, L.W. Fritz, T.S. Gelatt, and R.P. Angliss. 2015. Flying beneath the clouds at the edge of the world: using a hexacopter to supplement abundance surveys of Steller sea lions (*Eumetopias jubatus*) in Alaska. J. Unmanned Vehicle Syst. 4(1): 1-12. doi.org/10.1139/juvs-2015-0010.

York, A.E. 1994. The Population Dynamics of Northern Sea Lions, 1975-1985. *Marine Mammal Science* 10 (1): 38–51. doi:10.1111/j.1748-7692.1994.tb00388.x.

York, A. E., R. L. Merrick, and T. R. Loughlin. 1996. An analysis of the Steller sea lion metapopulation in Alaska, p. 259-292. *In* D. McCullough (editor) Metapopulations and Wildlife Conservation and Management. Island Press, Covelo, California.

York, A. E., J. R. Thomason, E. H. Sinclair, and K.A. Hobson. 2008. Stable carbon and nitrogen isotope values in teeth of Steller sea lions: Age of weaning and the impact of the 1975- 1976 regime shift in the North Pacific Ocean. Can. J. Zool. 86: 33-44.

Womble, J. N., M. F. Willson, M. F. Sigler, B. P. Kelly, and G. R. VanBlaricom. 2005. Distribution of Steller sea lions *Eumetopias jubatus* in relation to spring-spawning fish in SE Alaska. Mar. Ecol. Progr. Ser. 294: 271-282

Appendix

Table S1. Observed p-values from permutations of pairwise comparisons of group dispersion tests indicating that homogeneity varies across regions.

	W. Aleu	*C. Aleu*	*E. Aleu*	*W. Gulf*	*C. Gulf*	*E. Gulf*	*SE AK*
W. Aleu		**0.003**	**0.009**	0.151	0.235	0.286	**0.004**
C. Aleu	**0.001**		0.434	**0.001**	**0.001**	**0.001**	0.323
E. Aleu	**0.007**	0.426		**0.014**	**0.013**	**0.017**	0.138
W. Gulf	0.144	**0.005**	**0.015**		0.875	0.786	**0.001**
C. Gulf	0.235	**0.001**	**0.011**	0.88		0.892	**0.001**
E. Gulf	0.283	**0.001**	**0.016**	0.782	0.892		**0.002**
SE AK	**0.003**	0.318	0.135	**0.001**	**0.001**	**0.001**	